Signaling events modulated by the exosome-FPR2 axis in early *L. major* infections

Nada Al-Emadi

Master of Science

Department of Microbiology & Immunology

McGill University, Montreal

March2022

A thesis submitted to McGill University in partial fulfillment of the requirements of the degree of Master of Science

Contents

1 Figures

Tables:

2 Abstract

Leishmania is a protozoan parasite that causes leishmaniasis, infecting millions of individuals every year. The parasites utilize different virulence factors to camouflage their presence from macrophages and promote their survival. In recent years, evidence has emerged for the role of exosomes as virulence factors. Co-inoculating mice and macrophages with *L. major* exosomes exacerbate infections and increase parasite load. Our lab recently identified a potential role of Formyl Peptide Receptor 2 (FPR2) in exosome-mediated exacerbation of *L. major* infections. Hence, in this thesis, we investigate the interaction between FPR2 and *L. major* exosomes, and we evaluate downstream signaling pathways activated by the exosome-FPR2 axis.

Using *L. major*-LUC parasites, we report a significant increase in infectivity in Lm-1 macrophages treated with exosomes or FPR2 agonist, WKYMVm. However, the effect of exosomes was attenuated using the FPR2 antagonist WRW4. We observed similar results in intraperitoneal infections in mice. Next, we explored the role of FPR2 in *L. major* infections by analyzing cytokine gene expression and concentration. We observed suppression of TNF-α production by the agonist, while the antagonist slightly enhanced the production of this cytokine. We also observed an increase in IL-6 production in infected macrophages stimulated with the antagonist. These results were not significant. Due to the role of nitric oxide (NO) in parasite clearance, we analyzed NO levels following co-infections with FPR2 agonist and antagonist. We conclude that FPR2 doesn't modulate NO production during *L. major* infections.

To have a global snapshot of the signaling events activated by the exosome-FPR2 axis, we infected mice intraperitoneally for 6-hours at different conditions and analyzed the proteomic and phosphoproteomic profiles of inflammatory cells lysates. Our results indicate that exosomes differentially regulate proteins in *L. major* infections. We report uniquely shared proteins between EXL and AGO enriched in neutrophils activation and degranulation terms. We also report that upregulated phosphopeptides in EXL and AGO were specifically enriched in cytoskeletal organization and regulation of hemopoiesis terms. Kinase enrichment analysis of the upregulated phosphopeptides revealed a potential role of ERK1/2 in the phosphorylation events orchestrated by the exosome-FPR2 axis. Our data show that exosomes enhance *L. major* internalization by interacting with FPR2, altering cellular signaling in myeloid cells to favor parasite survival.

3 Résumé

Les protozoaires du genre *Leishmania* sont la cause de la leishmaniose, une maladie parasitaire affectant des milliers d'individus mondialement à chaque année. Afin de camoufler leur présence dans les macrophages et permettre leur survie, ces parasites emploient de divers facteurs de virulence, dont les exosomes. En effet, la co-inoculation d'exosomes de *L. major* avec le parasite dans des macrophages et dans un modèle murin mène à une exacerbation significative de l'infection et de la charge parasitaire. Notre laboratoire a récemment identifié une fonction potentielle du récepteur *Formyl Peptide Receptor 2* (FPR2) dans l'exacerbation des infections de *L. major* arbitrées par les exosomes. C'est ainsi que, dans ce mémoire, nous investiguons l'interaction entre FPR2 et les exosomes dérivées de *L. major*, et les événements signalétiques engendrés par l'axe exosome-FPR2. D'abord, nous avons rapporté une augmentation significative de l'infection par des parasites *L. major*—LUC dans des macrophages traités avec des exosomes ou un agoniste de FPR2, WKYMVm. Cependant, l'effet des exosomes peut être atténué par l'utilisation d'un antagoniste de FPR2, WRW4. Des résultats similaires peuvent être observés lors d'infections intrapéritonéaux dans un modèle murin. Ensuite, nous avons exploré le rôle de FPR2 dans l'infection par *L. major* en analysant l'expression différentielle des cytokines par les macrophages. Nous avons observé une suppression de la production de TNF-α par l'agoniste, tandis que l'antagoniste a induit une légère augmentation dans la production de cette cytokine. De plus, l'antagoniste mène à une augmentation de IL-6. Toutefois, ces résultats ne sont pas significatifs. Par la suite, nous avons analysé les niveaux d'oxyde nitrique après co-infections avec l'agoniste et l'antagoniste, compte-tenu du rôle du composé dans l'élimination des parasites. Nous avons pu conclure que le récepteur FPR2 ne module pas la production d'oxyde nitrique pendant l'infection par *L. major*. Pour obtenir une image globale des événements signalétiques engendrés par l'axe exosome-FPR2, nous avons infecté des souris par voie intrapéritonéale pour 6 heures à de différentes conditions, pour ensuite étudier les lysats de cellules inflammatoires par analyses protéomique et phosphoprotéomique. Nos résultats indiquent que les exosomes régulent les protéines de manière différentielle lors des infections par *L. major*. Nous rapportons que les protéines exprimées uniquement dans EXL et AGO sont enrichies dans les fonctions d'activation de neutrophiles et de dégranulation. Nous rapportons également une régulation positive de phosphopeptides en EXL et AGO qui ont pour fonction l'organisation du cytosquelette et de la régulation de l'hématopoïèse. Une analyse d'enrichissement de kinases de ces phosphopeptides montre un rôle potentiel de ERK1/2 dans les événements de phosphorylation qui sont engendrés par l'interaction exosome-FPR2. Nos données révèlent que les exosomes renforcent l'infectivité de *L. major* par l'interaction avec FPR2, qui altère la signalisation cellulaire dans les cellules myéloïdes afin de favoriser la survie des parasites.

4 Acknowledgments

First and foremost, I wish to thank my dearest friend Duha Al Awad for being my companion on this journey. I am forever grateful for your unwavering love and support, for listening to me talk about my lab work, and for the long discussions and ideas that followed.

This thesis would not have been possible without the support of my supervisor Dr. Martin Olivier. Thank you for offering me the opportunity to join your lab and providing continuous guidance. I extend my thanks to my advisory committee, Dr. Stéphane A. Laporte, Dr. Jorg Fritz, and Dr. Christopher Fernandez-Prada, for their valuable insight and advice. I thank Qatar University for the scholarship that funded my studies at McGill University. I especially thank Dr. Maha Al-Asmakh for her role as my advisor and her support.

To all the members of the MOL lab past and present, thank you for welcoming me to the lab and for your continuous help. To Caroline Martel, thank you for introducing me to the lab and guiding me on my first days as a member of the MOL lab. To George Dong, thank you for helping me learn new techniques and run the TEM experiments. To Alonso Filho, thank you for passing the knowledge of your project and always answering my questions. To Dr. Emmanuella Fajardo & Andrea Lafleur, thank you for helping me start with bioinformatics and for the good time together. To Fio Vialard, Laura Paez, and Carlos Villalba, thank you for being great friends and lab mates and sharing our journeys. I want to extend my thanks to Aretha Chan, Selena Yu, and Mohammed Daoudi for their warm welcome. I must also thank Khlood Alsulami from our neighboring lab for her continuous advice and support.

I thank my parents, Ali Al-Emadi and Ameena Al-Emadi, for supporting me and encouraging me to pursue my dreams. I extend my deepest gratitude to Dr. Susu Zughaier and Dr. Asma Al-Thani for believing in me, supporting me, and being great role models; I look up to both of you. I want to thank my friends from Qatar Sara Al-Qahoumi, Yasmin El-Ali, Hend Al-Qahtani, Alaa Elsayed, Kamilia Ahmed, and Asma Ahmed, Maha, Dina, and Almayaaa Al-Emadi for their unconditional support and for making me feel like I never left home by sharing their stories with me, playing video games, and having long video calls despite living in different time zones. Finally, I thank my cats Griffin, Bahlool, and Fluffy, who were always present by my side, especially since the pandemic started and for entertaining me while I wrote my thesis.

5 Preface

This thesis was written in accordance with McGill University's The candidate has chosen to present her thesis as a "manuscript-based thesis": "as an alternative to the traditional format, the thesis may be presented as a collection of scholarly papers of which the student is the first author or co-first author; that is, a manuscript based Master's thesis must include the text of one or more manuscripts published, submitted, or to be submitted for publication and re-formatted according to the described requirements. The thesis must contain additional text that will connect the manuscript in a logical progression, producing a cohesive, unitary focus, and documenting a single program of research."

All work towards this thesis was performed under the supervision of Dr. Martin Olivier. The candidate Nada Al-Emadi is the first author of the manuscript presented in Section 8 which will be submitted for publication.

Author contributions are as described: The project was designed and envisioned by Dr. Martin Olivier. In vitro experiments, RT-qPCR, NO assay, and luciferase assay were performed by N. Al-Emadi. In vivo experiments were designed and performed by N. Al-Emadi and M. Olivier with aid from Fiorella Vialard and George Dong. TEM imaging was performed by G. Dong. NTA measurements, preparation of samples for LC-MS/MS and was performed by N Al-Emadi with guidance from G. Dong.

Proteomic and phosphoproteomics analysis was performed by N Al-Emadi with guidance from Emanuella Fajardo, G. Dong, and Alonso Lira. Statistical analysis was performed by N. Al-Emadi. N. Al-Emadi wrote the manuscript with editorial guidance and direction from M. Olivier.

6 List of Abbreviation

Akt Protein Kinase B

ANXA Annexin A1

BCL-2 B-cell Lymphoma 2

BMDM Bone Marrow Derived Macrophages

CL Cutaneous Leishmaniasis

DC Dendritic Cells

DCL Diffuse Cutaneous Leishmaniasis

ECM Extracellular Matrix

EVs Extracellular Vesicles

FPR Formyl Peptide Receptor

GIPL Glycosylinositol Phospholipids

GPCR G-Protein Coupled Receptor

GPI Glycophosphatidylinositol

IAV Influenza A Virus

IFNγ Interferon Gamma

iNOS Inducible Nitric Oxide Synthase

LFA-1 Lymphocyte Function-associated Antigen 1

LPG Lipophosphoglycan

LUC Luciferase

Lundep Endonuclease Lutzomyia NET destroying protein

LXA4 Lipoxin A4

MAPK Mitogen Activated Protein Kinase

MCL Mucocutaneous Leishmaniasis

MHC Major Histocompatibility Complex

NETs Neutrophil Extracellular Traps

NO Nitric Oxide

NTA Nanoparticle tracking analysis

PI3K Phosphoinositide-3-Kinase

PKC Protein Kinase C

PKR Protein Kinase RNA-activated

PPG Proteophosphoglycans

PRR Pathogen Recognition Receptor

PTP Protein Tyrosine Phosphatase

RLU Relative Light Units

ROS Reactive Oxygen Species

RT-qPCR Real Time Reverse Transcriptase Quantitative Polymerase Chain Reaction

SAA Serum Amyloid A

SAP Secreted Acid Phosphatase

SPM Specialized Pro-resolving mediators

TEM Transmission electron microscopy

TGFβ Tumor Growth Factor Beta

TNFα Tumor Necrosis Factor Alpha

VL Visceral Leishman7

7 Literature Review and Research Objectives

7.1 Introduction to Leishmaniasis

Leishmaniases are a group of diseases caused by different species of the intracellular protozoan parasite *Leishmania.* It is considered one of the most prevalent vector-borne diseases globally and is distributed over 98 countries globally [1]. It is endemic in Africa, Asia, the Americas, and the Mediterranean region leaving 350 million people at risk [2]. More than 1.5 million new cases and 20,000 – 40,000 deaths are reported annually [3]. The disease is becoming a public health priority due to leishmaniasis's mortality, morbidity, and geographical distribution.

There are over 20 species of *Leishmania* that are transmitted to humans by phlebotomine sandflies during their blood meal. Depending on the infecting species, the disease manifests itself in three forms: cutaneous leishmaniasis, mucocutaneous leishmaniasis, and visceral leishmaniasis (Kala-azar) [4, 5]. Despite the high prevalence of the disease, there is a lack of safe and effective treatment options. Drugs face increasing parasite resistance in combination with adverse side effects and potential toxicity [6]. Hence, research on leishmaniasis disease onset and progression is necessary to develop new therapeutic strategies.

7.1.1 Classification of *Leishmania*

Leishmania parasites are of *Leishmania* genus, Subfamily Leishmaniinae, Family Trypanosomatidae, Order Trypanosomatida, Subclass Metakinetoplastina, Class Kinetoplastea, and Kingdom Protista [7]. All kinetoplastids have a kinetoplast containing a large mitochondrion with a DNA-containing region in it. To date, there are more than 50 species of *Leishmania* recognized to infect reptiles and mammals and are transmitted by sandflies [8]. Twenty of these species are known to be human pathogens [9]. The human pathogens are in the section (clade) Euleishmania and subgenuses *Leishmania* and *Viannia* [10]. *L. (Leishmania)* is found in both New and Old World while *L. (Viannia)* is only found in the Neotropics (North, Middle, and South America) [11].

7.1.2 Disease manifestation

The manifestation of leishmaniasis depends on the parasite species and the host immune response. Cutaneous leishmaniasis (CL) is the most common form of the disease. It starts as a small red papule on the skin that can progress to more prominent papules, nodules, or ulcerative skin lesions [12]. Although cutaneous leishmaniasis is not life-threatening and can heal spontaneously, scars left by healed lesions can lead to significant disfiguration and self-and social stigma [13]. In the Americas, CL is commonly caused by *Leishmania mexicana, Leishmania panamensis, and Leishmania (Viannia) braziliensis,* while *Leishmania major, Leishmania tropica,* and *Leishmania aethiopica* are the causative agents of CL in the rest of the world [12, 14].

Unlike CL, mucocutaneous leishmaniasis (MCL) could potentially be life-threatening and usually requires treatment. MCL is typically found in the Americas and is linked to *Leishmania* species of the subgenus *Viannia,* primarily *L. V. braziliensis, L. V. guyanesis, L. V. panamensis, and L. V. amazonensis* [12]. Years after the initial CL infection, a small percentage of previously infected individuals develop MCL characterized by inflammation and destructive lesions, mainly in the nasal and pharyngeal mucosa [12].

Visceral leishmaniasis (VL) is the most lethal form of leishmaniasis (also known as Kala-zar). Like the other disease manifestations, it could range from subclinical to a more aggressive form, causing a disseminated infection that could affect the spleen, liver, blood cells, and the lymphatic system [15]. VL is mainly caused by *L. donovani* and *L. infantum* [16]. When *L. infantum* was imported to South America it was given the name *L. chagasi,* which is currently considered a synonym to *L. infantum* [14].

7.1.3 *Leishmania* life cycle in sandflies

Leishmania is a digenetic protozoan parasite alternating its life cycle between a mammalian host and an insect vector. Phlebotomine sandflies are the sole vectors of *Leishmania* and are found in the tropics, sub-tropics, and temperate regions. *Phlebotomus* female*s* in the Old World and *Lutzomyia* in the New World are the only human vectors of the pathogenic *Leishmania* species [17].

Leishmania life cycle in sandflies is restricted to the digestive tract. The exact location varies depending on the *Leishmania* subgenera. *Leishmania (Viannia)* is identified as a peripylarian parasite because it enters the hindgut of the sandfly before it migrates forward to the midgut. In contrast, most *Leishmania (Leishmania)* species development is limited to the midgut classifying it as a suprapylarian parasite [18]. Since most parasite-vector interaction studies are on suprapylarian parasites, the cell cycle discussed will mainly describe this subgenus.

Parasites enter the vector's body when a female sandfly ingests a blood meal containing macrophages infected with amastigotes, which are small (3-5 um), non-motile, and round forms of the parasite [19]. The change in the parasite environment between the sandfly midgut and the mammalian host induces differentiation of the amastigotes into replicative procyclic promastigotes with a short flagellum and weak motility (Figure 1). After 48-72 hours of entry, procyclic promastigotes slow down their replication and transform into long nectomonad promastigotes that are highly motile [19, 20]. At this stage, the parasites will escape from the type 1 peritrophic matrix the blood meal was encased in and move to the anterior midgut, where they develop into leptomonad promastigotes, which are replicative forms [20, 21]. Eventually, the parasites detach and migrate to the stomodeal valve and transform into infective metacyclic promastigotes [22].

The parasites form a block to the sandfly midgut and alter its feeding behavior. This is done by secreting filamentous proteophosphoglycan (fPPG), secreted by leptomonad promastigotes that condenses to form promastigote secretory gel, which forces the sandfly to regurgitate some parasites while taking a blood meal [19]. Serafim *et al*. recently identified that the metacyclic promastigote, considered a terminally differentiated stage, reverses its form in the sandfly midgut after the blood meal into a leptomonad-like stage, named the retroleptomonad promastigote. This reverse stage can rapidly divide and differentiate into metacyclic promastigotes amplifying the number of parasites in the sandfly midgut by around 125 times, making the next blood meal more infectious [23].

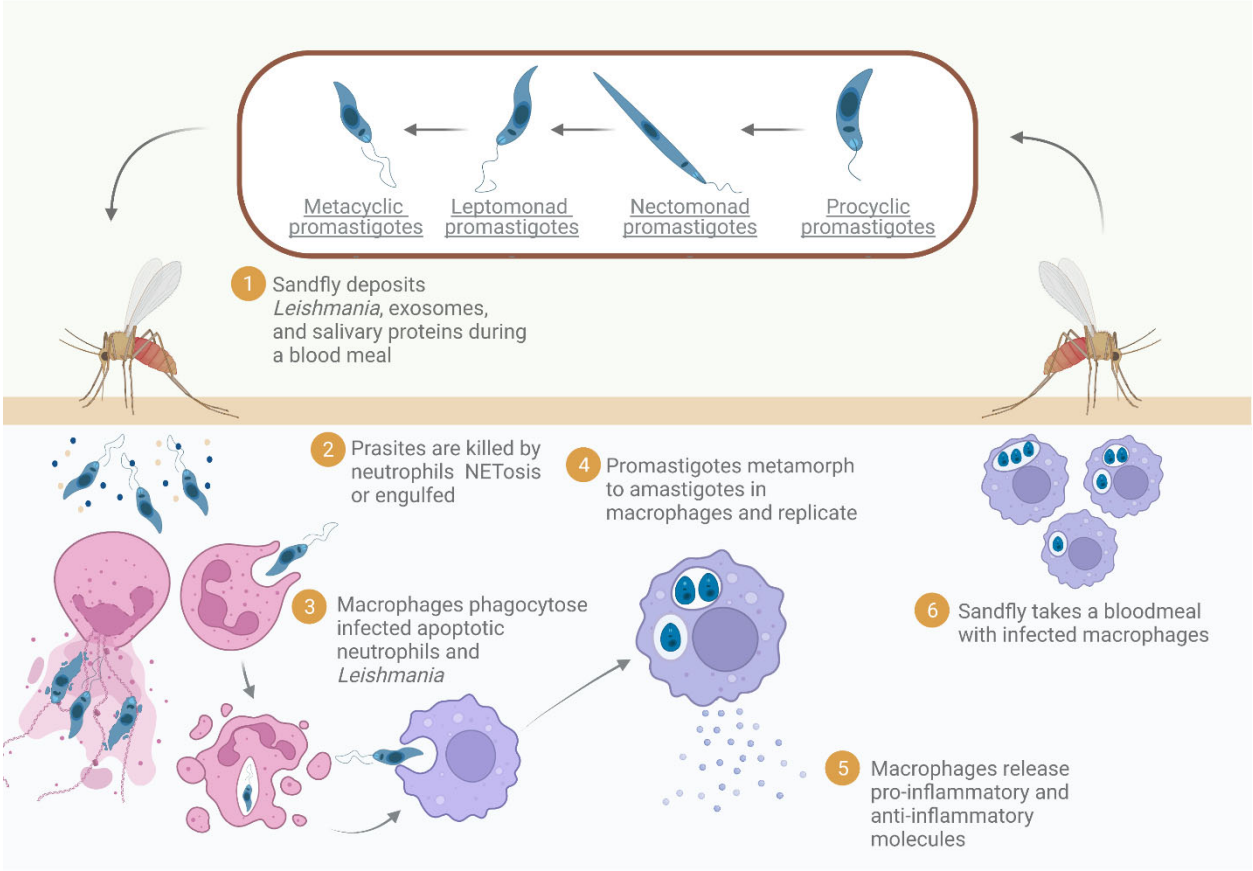

Figure 1: Leishmania's life cycle
The life cycle of Leishmania starts with depositing parasites by infected sandflies into the host dermis. Followed by the interaction between promastigotes and neutrophils and/or macrophages. The lifecycle restarts when a sandfly takes a blood meal with infected macrophages. The figure is created using Adobe Illustrator and BioRender.com

7.1.4 *Leishmania* life cycle in mammalian hosts

The first interaction between *Leishmania* and its new host happens when a female sandfly injects metacyclic parasites into the dermis of the host. The success of infection is determined by the proportion of metacyclic promastigotes injected [24]. Infected sandfly first bite provides a hefty dose of parasites with low purity, containing higher proportions of parasites at different stages and less of metacyclic promastigotes [24]. However, as the sandfly takes more blood meals, parasite doses are enhanced to be smaller but contain a high proportion of metacyclic promastigotes. Interestingly, infections with lower purity result in an exacerbated immune response identified by neutrophil accumulation and IL-1β release, while infections with higher purity, containing more metacyclic promastigotes, exhibit smaller lesions and less macrophage accumulation [24].

The contact of proboscides of a sandfly with the skin ruptures the dermis and its capillaries, leading to endothelial activation and neutrophil infiltration [25, 26]. The inflammatory infiltrates create a toxic environment for promastigotes that need to escape by entering host cells. For *Leishmania* promastigotes to infect cells, they need to escape the complex ECM structure and interact with basement membrane proteins. Studies displayed the ability of parasites to attach to and move through collagen I, which is one of the major components present in the ECM during early infection [27-29]. Fibronectin, a basement membrane protein, is also predominantly expressed during *Leishmania* infections in murine models [28]. Surface proteins found in both promastigote and amastigote forms can directly bind fibronectin to promote their uptake by monocytes or degrade fibronectin [30, 31]. *Leishmania* GP63 surface metalloproteinase or cysteine protease degrade fibronectin, releasing fragments capable of inhibiting the formation of reactive oxygen species by macrophages [30, 31]. Similarly, promastigotes interact dynamically with other molecules present in the ECM to promote their infectivity and persistence.

The first cells to interact with the parasites upon entry are infiltrating neutrophils and resident macrophages. Neutrophils release NETs and enzymes to kill the parasites at the site of infection (Figure 1). However, some parasites survive neutrophil killing [32, 33]. The survival of these parasites could be mediated by their expression of 3'-nucleotidase/nuclease, which cleaves NET-DNA allowing parasites to escape [34]. Another facilitator of NET-DNA mesh deterioration are endonucleases delivered with the parasites in the sandfly saliva. For example, *Lutzomyia longipalpis* saliva contains endonuclease *Lutzomyia* NET destroying protein (Lundep), a powerful endonuclease enabling the parasites to escape [34]. However, recent evidence by Guimarães-Costa *et al.* shows that NETs could have pro-parasitic activity [35]. NETs interaction with monocytes decreases their differentiation into dendritic cells and disables their microbicidal activity, making them more susceptible to parasite entry [35].

Likewise, surviving promastigotes are engulfed by neutrophils at the site of infection [36]. These parasitized neutrophils act as "Trojan horses" and are readily engulfed by phagocytic cells. This mode of entry to mononuclear phagocytic cells gives parasites easy access to their primary host cells while evading immune activation. Promastigotes alter neutrophils' function to promote their uptake by macrophages. For example, neutrophils infected with *L. major* exhibit a

delay in their programmed cell death and secret MIP-1β, a known macrophage chemoattractant [37]. Parasites that survive neutrophil killing and phagocytosis are ultimately phagocytosed by neighboring phagocytic cells [37, 38]. Overall, neutrophils play a dual role in *Leishmania* infection, which is protective in some instances and permissive in others.

While neutrophils predominantly contain parasites during early infection, *Leishmania* does not differentiate in neutrophils [25]. Instead, the main hosts for the final development of the parasite are phagocytic mononuclear cells [25, 39]. The parasites are internalized by macrophages, monocytes, and dendritic cells (DCs) [40]. The initiation of phagocytosis occurs when phagocytic cells recognize *Leishmania* surface molecules. Macrophages internalize the parasites directly or by engulfing apoptotic parasitized neutrophils. Internalization of promastigotes in phagolysosomes triggers their transformation into a non-flagellate replicative amastigote form [41]. Amastigotes start replicating in macrophages until they eventually rupture and infect neighboring cells. The life cycle is completed when a sandfly takes a blood meal containing infected amastigotes that transform to procyclic promastigotes in the sandfly midgut [20].

Leishmania employs virulence factors to modify host cell signaling and facilitate its persistence. These alterations could affect the activation and recruitment of immune cells and cytokine/chemokine production [42]. The resolution of infection depends on host and parasite-related factors, e.g., *Leishmania* species or host immune response. For example, the resolution of cutaneous leishmaniasis caused by *Leishmania major* in murine models relies on the balance between activating cytokines, mainly produced by Th1 cells, and deactivating cytokines produced by Th2 cells and some regulatory T cells [43].

7.1.5 Modulation of macrophage signaling by *Leishmania*

As described above, when *Leishmania* enters the host, it encounters cells of the innate immune system that can activate a cascade of pro-inflammatory signaling pathways endangering its survival. Hence, parasites need to manipulate the host immune response to favor their survival, evade the immune system, and establish a successful infection within macrophages.

Macrophage phagocytosis traps *Leishmania* within phagosomes that mature to phagolysosomes to degrade parasites. To survive, *Leishmania* halts phagosome maturation to

phagolysosomes through the effect of lipophosphoglycan (LPG) that prevents the recruitment of acidifying vesicular proton-ATPase and PKCα [44]. PKC is an essential regulator of reactive oxygen species production (ROS), a molecule recruited to the phagolysosome to kill parasites. PKC activity is also inhibited by *Leishmania* GP63 [45].

Within macrophages, *Leishmania* dampens the immune response to prevent its elimination. For example, the suppression of PKCδ by the parasite is associated with suppressing IL-12 release, a cytokine that promotes the anti-Th-1 immune response [46]. Similarly, the phosphorylation of mitogen-activated protein kinases (MAPKs) leads to a potent inflammatory response, which is also inhibited in *Leishmania* infection. Studies have shown that following infection with *Leishmania* promastigotes and amastigotes, MAPKs are not activated [47]. *Leishmania* also suppresses the activation of other members of the MAPK family ERK1/2 and p38, which impairs the ability of interferon-gamma (IFNγ) to induce the production of the pro-inflammatory cytokine tumor necrosis factor (TNF) [47]. The dephosphorylation of ERK1/2 is suggested to result from the activation of protein tyrosine phosphatases (PTPs) during *Leishmania* infection [48].

PTPs negatively regulate cell signaling, and their cleavage and activation by *Leishmania* GP63 have been reported [49, 50]. PTPs activation plays an essential role in evading host immune response and establishing infection. When mice infected with *Leishmania* were treated with PTP inhibitors, they showed an improved immune response and resolution of inflammation marked by controlled parasite survival mediated by NO production [51, 52].

In addition to the inhibition of PKCδ, *Leishmania* also inhibits the production of IL-12 by activating phosphoinositide 3-kinase (PI3K). *L. major* infected PI3K deficient mice have an enhanced anti-leishmanial Th1 response compared to wild-type mice [53]. Likewise, protein kinase RNA-activated (PKR) activation plays a role in the growth of *L. amazonesis* by promoting the expression of the anti-inflammatory cytokine IL-10, which deactivates macrophages [54]. However, in *L. major,* the activation of PKR was suppressed by serine peptidase inhibitor ISP2 of the parasite [55].

The Janus kinase (JAK)-signal transducer and activator of transcription (STAT) play an essential role in the immune response to invading pathogens. Different cytokine receptors

activate the JAK/STAT pathway. Its activation results in the transcription of pro-inflammatory genes like IL-12, MHC II, and inducible nitric oxide synthase (iNOS) [56]. Pro-inflammatory molecules released due to JAK/STAT activation could limit *Leishmania* infection. Hence, the parasites inhibit this pathway either by degrading STAT-1 or dephosphorylating JAK-2 [57]. In patients exhibiting diffuse cutaneous leishmaniasis (DCL) caused by *L. meixcana*, genes involved in JAK/STAT signaling pathways are downregulated [58]. Another mechanism of JAK/STAT inhibition observed in *L. donovani* is to inhibit STAT-1α translocation to the nucleus preventing downstream activation of pro-inflammatory molecules [59].

To survive within macrophages, *Leishmania* utilizes virulence factors that generate a sequence of complex adjustments to cellular signaling to silence the immune response. The modifications aim to increase the production of anti-inflammatory signals while simultaneously suppressing the production of pro-inflammatory molecules.

7.1.6 *Leishmania* Virulence Factors

Leishmania evades the host immune response by utilizing virulence factors. The parasite's surface is densely coated with molecules that act as a barrier between the parasite and the extracellular milieu. Many of these surface molecules are virulence factors like lipophosphoglycans (LPGs), proteophosphoglycans (PPGs), Glycosylinositol phospholipids (GIPLs), and GP63 glycoprotein [60, 61]. These molecules are anchored to the plasma membrane via glycophosphatidylinositol (GPI) anchor.

LPG is the most abundant glycoconjugate in *Leishmania,* and it plays a vital role in parasite survival within a host cell. It is highly expressed in promastigotes but downregulated in amastigotes [62]. Because LPG spans the parasite cell surface, it acts as a barrier that prevents the attachment of host complement proteins to the parasite [60-62]. It also plays a role in parasite phagocytosis by facilitating their attachment to macrophages by directly binding to macrophage surface receptors or indirectly by interacting with proteins that promote parasite internalization [63]. LPG also provide other immune evasion mechanisms to *Leishmania,* such as preventing complement lysis and promoting their survival within macrophages [60]

PPGs are mucin-like glycoproteins that have a similar structure to LPG. They are present on the surface of promastigotes and amastigotes but could also be released by the parasites directly while inside the parasitophorous vacuole [64]. PPGs play a role in parasite binding to macrophages, internalization, and modulation of the host immune response. They can impair the synthesis of cytokines like TNF-α when macrophages are activated by cytokines and prevent the opsonization of *Leishmania.*

Little is known about the role of GIPL as a virulence factor. It is found on both forms of the parasite, and it inhibits the synthesis of nitric oxide by macrophages and impairs the PKC pathway [60, 65]. Both mechanisms lead to enhancing parasite survival within macrophages.

Another important virulence factor is the zinc-dependent metalloendopeptidase GP63 attached to the parasite membrane by GPI anchor but could also be secreted by the parasite. It is one of the main virulence factors identified in *Leishmania* due to its versatile functions in promoting parasite survival [66]. The activity of GP63 spans from inhibiting C3b factor, which inhibits the complement cascade, facilitating parasite binding to macrophages via fibronectin receptors, cleaving proteins of the extracellular matrix of the host, suppressing the production of TNF-α and IL-12 as well as NO, and the inhibition of mTOR kinase [67-70]. The diverse cellular effects caused by GP63 contribute to parasite survival and the persistence of infection by suppressing/modifying the host immune response.

Leishmania has many virulence factors in addition to those described above, like KMP-11, secreted acid phosphatases (SAPs), proteinases, nucleotidases, heat-shock proteins, and transporters [71] (Figure 2). These molecules contribute to the parasite virulence by modifying the host immune response or protecting the parasite against host defenses. Extracellular vesicles released by *Leishmania* have been identified, and evidence of their role in exacerbating infections is recognized [72].

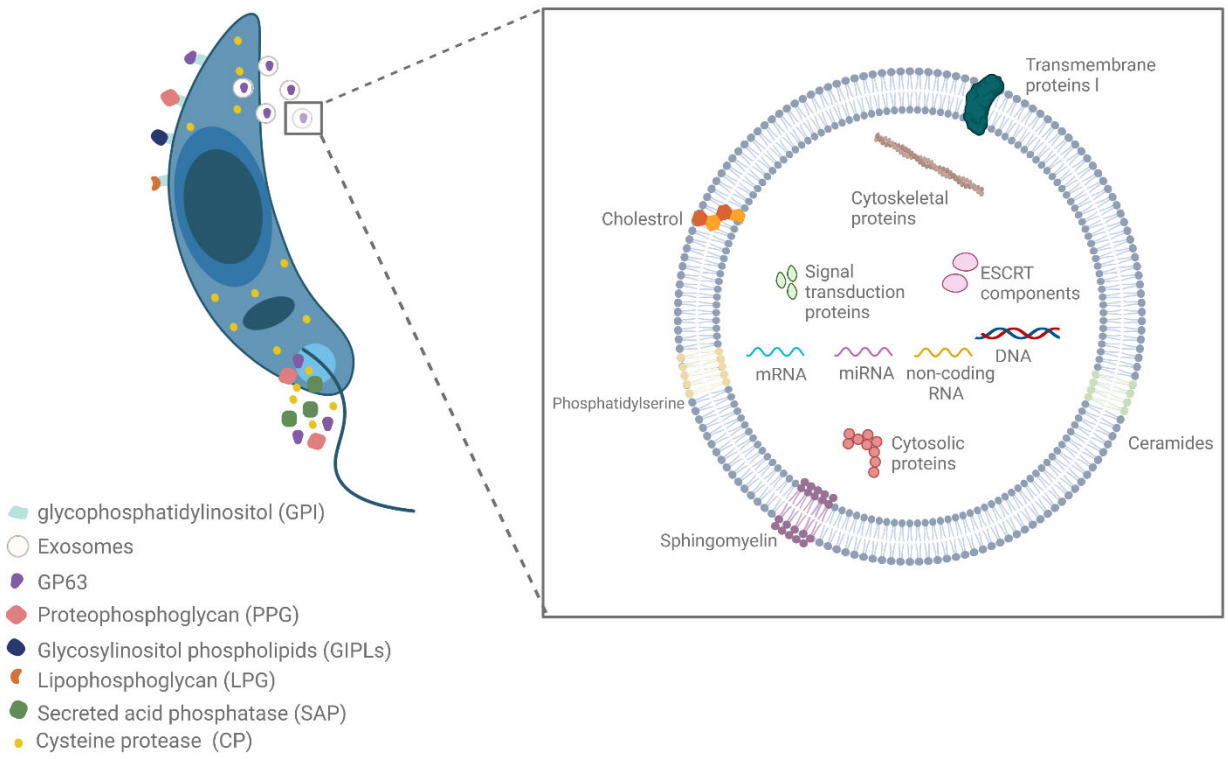

Figure 2: Schematic presentation of Leishmania virulence factors.
Leishmania virulence factors can be anchored to the plasma membrane via GPI anchor or secreted. A zoomed view of a general eukaryotic exosome and its potential components are illustrated. The figure is created using Adobe Illustrator and BioRender.

7.2 Extracellular Vesicles

In 1946 extracellular vesicles (EV) were observed in the blood by Charagaff and West [73]. Later, they were classified as "platelet dust" by Wolf in 1967 [74]. Then, EVs were observed in rectal adenoma microvillus cells and identified as plasma membrane fragments [75]. During the same period, membrane fragments from cancer cells were identified to be strongly immunoreactive [76]. In 1983 two papers reported the association of small vesicles around 50 nM in size with reticulocytes' transferrin receptors [77, 78]. Vesicles were observed to bud from reticulocytes into the extracellular environment when multivesicular bodies (MVBs) fuse with the plasma membrane [79]. The term exosome was coined to refer to these EVs. Exosomes were found to have antigen-presenting capabilities and can induce T-cell response [80]. Valadi *et al.* in

2007 identified the presence of RNA in EVs, which reignited the interest in exosomes as mediators of cell-to-cell communication [81].

7.2.1 Characterization of Extracellular Vesicles

All eukaryotic cells produce EVs, which explains their heterogeneity [82]. Contrary to the first classification of all EVs as exosomes, EVs are now classified based on the size and assumed biological pathways into exosomes, microvesicles, and apoptotic bodies [83]. Exosomes are the smallest of EVs with a size of 50-150 nm. They are generated by the inward budding of early endosomes forming multivesicular bodies released to the extracellular environment [84].

Microvesicles range between 100-1000 nm in diameter and are produced directly from the plasma membrane. On the other hand, apoptotic bodies are 50-5000 nm in diameter and are released by apoptotic cells due to plasma membrane blebbing [85]. Despite the different biogenesis of these groups, they all share overlapping chemical and physical properties. Using current methods, it has been virtually impossible to isolate and characterize homogenous sub-groups of vesicles due to the similarities between them, especially exosomes and microvesicles [82]. Thus, the current recommendation is to use the term small extracellular vesicles for vesicles obtained by ultracentrifugation at high speeds (100,000g), a solution usually enriched with exosomes. Medium/large extracellular vesicles are obtained by centrifuging at lower speeds (10,000 g), and these preparations are enriched with microvesicles [86].

7.2.2 Cellular effects of extracellular vesicles

The composition of EVs is derived from the parental cells. They could contain proteins, lipids, and nucleic acids [87, 88]. EVs act as a medium for information transport between cells by releasing cargo altering cellular function and activity [89]. Health cells release EVs that could prevent cancers by preventing DNA accumulation in the cytoplasm; however, EVs from cancerous cells alter the microenvironment to enhance tumor growth [90, 91].

Similarly, microorganisms utilize EVs capacity to modify cell function to establish infections. For instance, during viral infections, components of EVs obtained from infected cells are modified to contain viral genetic material and proteins [92]. EVs deliver these viral particles

to influence host response during viral infections [93]. The role of EVs in bacterial infections is not clear. However, EVs from the intracellular bacterium *Mycobacterium tuberculosis*-infected cells activate macrophages and T-cells and increase TNFα and IL-12 production [94]. Obligate intracellular parasites like the malaria-causing agent *Plasmodium* promote the release of EVs in their host cells. EVs obtained from RBCs infected with *P. falciparum* can activate macrophages and neutrophils to release cytokines, contributing to the cytokine storm seen in malaria infections [95]. Interestingly, kinetoplastid parasites from the genus *Leishmania* and *Trypanosoma* produce EVs in their hosts and vectors, eliciting immunomodulatory effects [72, 96]. All in all, EVs play an essential role in cellular communication and can be utilized by different pathogens and cells to modulate cellular activity.

7.2.3 *Leishmania* extracellular vesicles

Microvesicles produced by protozoan parasites were reported before the discovery of exosomes. However, in 2008 Silverman *et al.* analyzed the secretome of *Leishmania donovani* and found that only 14% of the proteins had an N-terminal classical secretion signal peptide [97]. All the proteins in *L. donovani* secretome with a *Leishmania* ortholog resembled the proteins found in exosomes secreted by B lymphocytes and dendritic cells [97]. The group also identified 50 nm vesicles budding from the flagellar pocket of the parasites using scanning electron microscopy [97]. Silverman *et al.* reported the release of microvesicles by *L. Mexicana, L. major*, and *L. donovani,* which possessed characteristics identical to mammalian exosomes [98]. *Leishmania* labeled with GFP produced GFP labeled exosomes that were taken by naive macrophages. These exosomes also induced the secretion of IL-8 in macrophages indicating their ability to modify host behavior [98].

Hassani *et al.* demonstrated that *Leishmania mexicana* parasites show augmented protein release and vesicle secretion within 4-6 hours of exposure to temperature shift which mimics parasite entry to its mammalian host [99]. Inducing macrophages with the exoproteome of these parasites resulted in PTP cleavage. Activated PTPs inhibit various kinases, namely JAK2, IRAK 1, and MAP kinases that are necessary for macrophage activation. To add, the exoproteome of *L. mexicana* also inhibited LPS induced nitric oxide (NO) release in macrophages. Inhibition of NO is a crucial factor for parasites survival within macrophages [99]. Recently, Castelli *et al.* reported that promastigotes and amastigotes of *L. infantum* can produce EVs capable of

increasing macrophages motility, increasing IL-10 production, and suppressing IL-18 release [100].

The components of exosomes are derived from parental cells, and in the case of *Leishmania* different virulence factors and molecules that enhance infection are packaged into exosomes. Specifically, in addition to being secreted by *Leishmania,* the virulence factor GP63 is also packaged into exosomes [49, 101]. Furthermore, LmPRL-1, a novel phosphatase identified in *L. major* is excreted via the exosome pathway [102]. Using ectopic secretion analysis LmPRL-1 was found to be important in promoting parasite survival within macrophages [102]. The exosome secretion pathway is also utilized by *Leishmania* RNA Virus 1 (LRV1), a virus known to cause a hyperinflammatory response in mammalian hosts leading to an exacerbation of mucocutaneous leishmaniasis. The virus is packaged within exosomes and is subsequently released to the extracellular environment. Mice induced with LRV-1 exosomes and *Leishmania* showed an exacerbation of lesion size, which was not observed upon infection of *Leishmania* with LRV1 alone [103].

Previous studies have shown the production of *Leishmania* vesicles *in vitro* but capturing vesicle production *in vivo* proved challenging. Through TEM studies, Atayde *et al*. showed that *Leishmania* parasites release vesicles within the sandfly midgut [72]. The group used a system that allows *Leishmania* infected sandflies to feed through a chicken membrane to study the egested material. Exosomes were found to be egested with *Leishmania* during the sandfly meal. These exosomes had similar structure and constituents as *in vitro* produced exosomes. Co-inoculation of these exosomes with parasites resulted in an exacerbated inflammatory response marked by an increase in IL-17 [72]. All in all, exosomes secreted by different species of *Leishmania* contain factors modulating host cellular behavior in favor of parasite survival and persistence.

7.3 Formyl peptide receptors family

The immune system is equipped with an arsenal of molecules that could sense cellular damage or the presence of pathogens. Pathogen Recognition Receptors (PRRs) are proteins that can recognize molecules found on pathogens or released during cellular damage. PRRs are found in many cell types, however, they are mainly expressed in antigen-presenting cells. Formyl peptide receptors (FPRs) are members of the G-protein coupled receptors (GPCRs) family and

are considered PRRs [104]. They are predominantly expressed on leukocytes and are also found in different cell types, including glial, endothelial, neuronal, and epithelial cells [105]. However, their role in these cells is not fully understood. FPRs are unique in their ability to interact with a wide range of molecules like endogenous proteins and peptides, small molecular ligands, lipids, and eicosanoids [106, 107]. They are involved in many physiological and pathological processes in the body due to their distinctive binding properties and the diversity of their ligands.

FPRs are extensively studied for their role in regulating innate immunity, inflammation, cellular migration, proliferation, and superoxide production [108]. They modulate intracellular signaling cascades and regulate different kinases and phosphatases such as PKC, phosphoinositide-3-kinase (PI3K), mitogen-activated protein kinase (MAPK), protein kinase B (Akt), p38MAPK, PTEN, DUSP3/VHR, and PTP-PEST [106, 109]. They also regulate NADPH ROS generation by phosphorylating and translocating $p47^{phox}$ and $p67^{phox}$ across the cell membrane [110]. FPR1 and FPR2 also activate ROS-dependent TKR transactivation and translocate and phosphorylate transcription factors [106].

Humans have three FPR genes on chromosome 19 coding for FPR1, FPR2, and FPR3 proteins [111]. All proteins in the FPR family have an extracellular N-terminus, seven transmembrane domains, and an intracellular C-terminus [112]. The term FPR1 was coined due to the protein's high binding affinity to bacterial and mitochondrial N-formylated peptides; the only ligand shared between the three receptors [111]. Unlike FPR1, FPR2 binds formylated peptides with low affinity. However, it has a broader range of ligands, including non-formylated peptides, small molecules, and lipid mediators, making it the most promiscuous peptide in the GPCR family [111]. Names used to describe FPR2 in the literature are formyl peptide receptor-like 1 (FPRL1), and FPR2/ALX, LX4R, or ALX due to its ability to bind lipoxin A4 (LXA4) and aspirin-triggered lipoxin [107, 111]. In this paper, the term FPR2 will be used to describe this protein. Unlike other members of the FPR family, FPR3 function and ligands are poorly investigated [113]. Even so, FPR3 is highly phosphorylated, indicating that it is rapidly internalized after binding to its ligands. It is speculated that it acts as a decoy receptor to prevent ligand binding to other receptors [114].

The gene family is more complex in mice as it consists of 8 different genes (mFpr1, mFpr2, mFpr-rs1, mFpr-rs3, mFpr-rs4 *mFpr-rs6, mFpr-rs7, and mFpr-rs8*) on chromosome 17A3.2. Three genes (*mfpr1, mfpr2, and mfpr-rs1*) code for receptors found in leukocytes coding

for mFpr1, mFpr2, and mFpr-rs1proteins [111]. Research has been focused on studying *m*Fpr1 and *m*Fpr2 as the orthologs of human FPR1 and FPR2, respectively [114].

7.3.1 FPR2 and its agonists

Acute inflammation is a protective mechanism to tissue injury or infection. Once the homeostasis and function of the injured/infected tissue are restored, the inflammatory process is followed by resolution [115]. Resolution of inflammation is an active process involving specialized pro-resolving mediators (SPMs) like LXA4.

Due to its high expression in neutrophils and monocytes, FPR2 plays a pivotal role in regulating inflammation. Amongst the family of FPRs, FPR2 has an extensive range of ligands. Most of its agonists are peptides like annexin A1 (ANXA1), except for LXA4 and the synthetic small-molecular weight ligands. FPR2 has a dual role in the inflammatory process depending on the ligand it binds. It can mediate the pro-resolving effects of LXA4 and the pro-inflammatory responses to serum amyloid A (SAA). For example, the expression of NF-κB is increased by SAA binding to FPR2 and suppressed by LXA4 [116]. The ability of FPR2 to elicit both pro-inflammatory and pro-resolving responses could be due to the differential binding of agonists to different domains on the receptor.

7.3.2 Annexin A1 and FPR2 axis

ANXA1 (previously termed lipocortin 1) is a 37 kDa peptide and a member of the annexin superfamily of calcium-dependent phospholipid-binding proteins [117]. It was first described in the 1800s as a secondary messenger downstream of glucocorticoids. ANXA1 is expressed in most immune cells like neutrophils, monocytes, and T-cells [118]. When cells are activated, ANXA1 translocates to the cell membrane and is secreted by different pathways depending on the cell type [119].

The anti-inflammatory effects of ANXA1 are mediated through its primary receptor, FPR2, but it also binds FPR1 and FPR3 at a lower affinity [120]. The cleaved N-terminal product of ANXA1, Ac2-26, has been reported to induce the activation of both FPR1 and FPR2 [121].

7.3.3 ANXA1 in regulating neutrophil function

ANXA1 plays a pivotal role in the resolution of inflammation. ANXA-/- mice exhibit prolonged inflammation exacerbating the adverse effects of the inflammatory process [122, 123]. An essential step in the resolution of inflammation is the apoptosis and phagocytosis of neutrophils by macrophages, which are modulated by ANXA1 [124, 125].

The inflammatory process leads to the rapid recruitment of neutrophils to the affected site. Neutrophils release many inflammatory molecules, resulting in tissue damage if not strictly regulated [126]. To contain the damage, neutrophils undergo apoptosis once their biological roles are fulfilled. Thus, the resolution of inflammation requires tight control of neutrophil infiltration and the removal of apoptotic neutrophils to prevent excessive neutrophil accumulation [127]. The process of neutrophil trafficking to the inflamed site requires neutrophils to adhere to blood vessels and transmigrate through them [128]. As a pro-resolution inflammatory regulator, ANXA1 inhibits the migration and recruitment of neutrophils and promotes the detachment of adherent cells [129, 130].

It also induces apoptosis in neutrophils by promoting calcium flux and inhibiting B-cell lymphoma 2 (BCL-2) antagonist. ANXA1 regulates the removal of apoptotic neutrophils by localizing to the surface of apoptotic cells with the ‘eat me’ signal phosphatidylserine [124, 131, 132]. The role of ANXA1 extends to promoting monocyte recruitment, the polarization of macrophages, and efferocytosis of apoptotic neutrophils

7.3.4 ANXA1 in regulating macrophage function

Phagocytic clearance of apoptotic neutrophils by macrophages plays an essential role in the resolution of inflammation. It prevents the accumulation of toxins released by neutrophils and uncontrolled neutrophil activation [133, 134].

The proteins released by neutrophils at the site of inflammation play an essential role in the recruitment of monocytes [135]. ANXA1 is one of those proteins released extensively by apoptotic neutrophils, making them the primary source of ANXA1 at the inflammatory site [136]. The presence of ANXA1 triggers the chemotaxis of monocytes via the ANXA1/FPR2 axis

[136]. This process leads to the activation of p38 MAPK and subsequent induction of chemotaxis by lysophosphatidic acid receptor 2 and actin cytoskeleton mobilization [136].

The release of ANXA1 by apoptotic neutrophils also promotes efferocytosis [136]. Macrophages contain and release ANXA1, which can modulate their function and the function of neighboring cells to promote efferocytosis [137]. The role of ANXA1 in regulating efferocytosis is evident by the defective phagocytosis seen in bone marrow-derived macrophages (BMDMs) obtained from ANXA (-/-) mice [137]. Another function of ANXA1 pro-resolution activity modulates macrophages to a pro-resolution phenotype. ANXA1 leads to increased transforming growth factor β (TGFβ) and decreases the pro-inflammatory cytokine 1L-6 [125, 137]. Parallel to this observation, macrophages deficient in ANXA1 exhibit an increased tumor necrosis factor-alpha (TNFα) and IL-6 production [138]. ANXA1/FPR2 axis activates the p38 MAPK pathway and the production of IL-10 in human monocytes and *in vivo* following an intraperitoneal ANXA1 injection [139].

7.3.5 The role of ANXA1/FPR2 axis in infectious disease

Due to the role of the ANXA1/FPR2 axis in the resolution of inflammation, it has been extensively studied in the context of inflammatory and autoimmune diseases. However, the role of the ANXA1/FPR2 axis in infectious disease is not widely studied.

7.3.5.1 AXA1/FPR2 in Bacterial Infection

ANXA1 knockout mice are more susceptible to *M. tuberculosis* infection. When infected with the bacterium, these mice exhibit an increase in bacterial burden and exacerbation of inflammation due to their inability to activate naïve T cells [140]. Macrophages infected with *M. tuberculosis* eventually become apoptotic and release apoptotic vesicles containing *M. tuberculosis* parasites [141]. These vesicles also contain ANXA1 on their surface, a ligand recognized by bystander macrophages and dendritic cells facilitating the phagocytosis of bacteria-carrying vesicles [141]. Hence, the ANXA1 pro-resolution effect is vital in controlling the immune response against *M. tuberculosis.*

Consistent with *M. tuberculosis* infections, mice lacking ANXA1 are more susceptible to *Streptococcus pneumoniae* infections due to uncontrolled inflammation, increased bacterial

proliferation, increased neutrophil activation, and cytokine production in the lungs [142]. On the other hand, treating ANXA1(-/-) mice with Ac2-26 peptide (AXA1 peptide) in *S. pneumoniae* infection reduced the severity of inflammation and bacterial burden by promoting phagocytosis [142].

Similarly, in an endotoxemia model induced by LPS, the absence of ANXA1 leads to hyperinflammation and an increase in pro-inflammatory cytokines like IL-6 and TNFα. Incidentally, ANXA1(-/-) mice were rescued when given human recombinant ANXA1 [143].

7.3.5.2 ANXA1/FPR2 in viral infections

A few studies explored the role of ANXA1 in modulating the immune response in viral infections. Hiramoto *et al.* reported a role of ANXA1 in hepatitis C virus infection, particularly in the case of viral-induced chronic hepatitis [144]. When ANXA1 is exogenously expressed by human hepatoma cells infected with hepatitis C virus, viral replication was suppressed due to ANXA1 Regulation of viral replication rather than by regulating viral entry [144].

Downregulation of ANXA1 is also associated with arboviral infections, whereas women infected by the Zika virus had lower ANXA1 expression than control groups (65). Similarly, levels of ANXA1 in the serum of individuals infected by the chikungunya virus are lower than in control groups (66).

Recently, the role of the ANXA1/FPR2 axis in Influenza A virus (IAV) replication and propagation has emerged. In 2016 Arora *et al.* reported that the expression of ANXA1 is increased during IAV infection and that ANXA (-/-) mice challenged with IAV infection had lower viral titers and improved inflammatory cell infiltration. ANXA1 enhances IAV replication, binding, endosomal trafficking to the nucleus, and IAV mediated apoptosis [145]. Later reports showed that IAV promotes increased FPR2 expression by IFNγ mediated signal transducer and activator of transcription 3 (STAT3) activation. Repression of FPR2 by inhibiting the phosphorylation of STAT3 led to decreased viral load [146]. Indicating the role played by ANXA1 in increasing viral expression is mediated by the ANXA1/FPR2 axis. Blocking FPR2 using an antagonist (WRW4) leads to an accumulation of viral RNA in endosomes and a decrease in viral replication [147].

7.3.5.3 ANXA1/FPR2 in parasitic infections

ANXA1 seems to have a role in parasitic disease development and persistence; however, a limited number of studies have investigated this role. *Toxoplasma gondii* is a parasite that causes toxoplasmosis, characterized by a potentially life-threatening disease in immunocompromised individuals. When human placental explants infected with *T. gondii* were treated with Ac2-26, they exhibited an increase in endogenous ANXA1 coupled with a decrease in parasite load [148].

Furthermore, levels of ANXA1 are higher in *Leishmania braziliensis* infected mice and in the sera of patients with mucosal leishmaniasis compared to control groups. ANXA1 deficiency in *L. braziliensis* infection results in a higher accumulation of inflammatory infiltrates and large lesion size. BMDMs from ANXA (-/-) also have lower parasite intake compared to WT-BMDMs despite a similar parasite burden. This effect was associated with an early increase in TNF-α and later IL-10 levels after infection.

Recently our lab identified that the exacerbation of parasite load observed during *L. major* infections with co-inoculation with exosomes is mediated by the ANXA1/FPR2 axis (Not Published). Mice footpads inoculated with both parasites and FPR2 agonist (WKYMVm) showed a significant increase in footpad thickness comparable to that seen in parasite and exosomes infections. Using an antagonist (WRW4) to FPR2 in parasite-exosomes infections attenuated the exacerbated increase in footpad thickness. When ANXA (-/-) mice were infected with parasite-exosomes, the increase in infection compared to parasite-only infected cells was also attenuated; however, this effect is bypassed by using the FPR2 agonist. Similar results were observed using BMDMs where parasite loads were increased using leishmania-exosomes and FPR2 agonist. These results suggest that exosomes of *L. major* activate the ANXA1/FPR2 axis leading to an increase in parasite internalization in the initial stages of infection.

7.4 Objectives of Research and Rationale

Extensive research on *Leishmania* exosomes led to establishing these vesicles as virulence factors. The inoculation of parasites by the vector under the host's skin leads to a temperature shift that induces exosome production. Co-inoculation of *L. major* and exosomes in mice exacerbates infection and lesion size, accompanied by a significant increase in parasites within myeloid cells during early infection. Although the role of exosomes in promoting *Leishmania* infections is clear, little is known about the mechanisms employed by these vesicles to modify host cellular functions. Recently, we were able to demonstrate a potential interaction between FPR2 and *L. major* exosomes. However, the downstream signaling pathways activated upon FPR2-exosome interaction are unknown, and the role played by FPR2 in *L. major* infections is not clear. Expanding the research in this avenue would provide insight into novel pathogenic pathways employed by exosomes to favor infection persistence and aid in developing new tools to control disease progression and transmission.

This prompted us to the research question, "How does the exosome-FPR2 axis influence the early innate immune response and promote *L. major* infections?"

We hypothesized that the exosome-FPR2 axis enhances phagocytosis of *L. major* parasites by neutrophils and macrophages

To test our hypothesis, we developed the following objectives:

1) Perform *in vitro* experiments to investigate the role of the exosome-FPR2 axis on *L. major* infection in macrophages.
2) Determine the differential proteomic and phosphoproteomic regulation by *L. major* exosomes via FPR2 using an *in vivo* intraperitoneal infection model.

8 Methods, Results, and Discussion

8.1 Preface

The results of this project will be submitted in the form of a manuscript for publication. The paper focuses on the research objective as laid out in section 7.4 that is to perform *in vitro* experiments to investigate the role of the exosome-FPR2 axis on *L. major* infection in macrophages and to determine the differential proteomic and phosphoproteomic regulation by *L. major* exosomes via FPR2 using an *in vivo* intraperitoneal model. The methods and results in this paper discuss the role of macrophage FPR2 in early *L. major* infection and the differential regulation of the proteome and phosphoproteome of innate inflammatory cells recruited to the peritoneum during the early immune response by the exosome-FPR2 axis.

8.2 Author contribution

The project was designed by Dr. Martin Olivier. In vitro experiments were performed by Nada Al-Emadi. In vivo experiments were designed and executed by M Olivier and N Al-Emadi. TEM imaging was performed by George Dong. NTA measurements, sample preparation for LC-MS/MS, bioinformatic analysis of proteomics and phosphoproteomics data, and statistical analysis were done by N Al-Emadi.

Cellular Mechanisms Driving Increased *L. major* internalization via its Exosomes involve Macrophage FPR2 receptor

Nada Al-Emadi[1,2], Martin Olivier[1,2]

1 Department of Microbiology and Immunology, McGill University
2 Infectious Diseases and Immunology in Global Health, Research Institute of McGill University Health Centre.

Abstract

Leishmaniasis is a group of diseases caused by the protozoan parasite *Leishmania*. The innate immune response to *Leishmania* infections involves neutrophils and macrophages, the latter being the ultimate host cells of the parasite. *Leishmania* utilizes different virulence factors to evade the activity of the professional phagocytic cells and promote their survival. Extracellular vesicles, namely exosomes, are nano-sized vesicles released by the parasites that are shown to enhance *Leishmania* infections and promote their survival in myeloid cells. Recently, our lab identified a possible interaction between exosomes and Formyl Peptide Receptor 2 (FPR2).

This paper investigates the exosome-FPR2 axis and analyzes the downstream signaling pathways activated by this axis using molecular, proteomic, and phosphoproteomic approaches. We report that FPR2 agonist WKYMVm mimics the enhanced infectivity seen with exosomes, and blocking the receptor using WRW4 co-infection with exosomes, inhibits their effect. These observations were made in vitro using LM-1 macrophages and in vivo using an intraperitoneal infection model. Next, we show that FPR2 activation does not alter the gene expression of IL-6, IL-1β, MCP-1, MIP-1α, or MIP-1β. However, we observed a reduction in TNF-α gene expression and release into the supernatants using the agonist. Similarly, blocking FPR2 did not influence these cytokines, yet, a slight increase in TNF-α and IL-6 production were observed. We investigated the role of FPR2 in nitric oxide production during *L. major* infections and our data showed that FPR2 is not involved in nitric oxide release.

To have a snapshot of the signaling events activated by the exosome-FPR2 axis, we used LC-MS-MS for proteomic and phosphoproteomic analysis of samples obtained from peritoneal *L. major* infections in mice. Our data shows that *L. major* exosomes differentially regulate proteins in infections. We report that exosomes and FPR2 agonists promote the expression of shared unique proteins that are enriched in neutrophils activation and degranulation terms. Phosphoproteomic analysis showed commonly upregulated proteins between exosome and agonist co-infected groups, these were enriched in cytoskeletal organization and regulation of hemopoiesis terms. Using X2K platform kinase enrichment analysis, we reveal a potential role of MAPK and ERK in the phosphorylation events leading to enhanced internalization of *L. major*. Overall, our data show that the effect of exosomes is FPR2 dependent, and the exosomes-FPR2 interaction alters cellular signaling in myeloid cells to favor parasite survival.

8.3 Introduction

Leishmania is a protozoan parasite causing a group of diseases termed leishmaniasis. It is a highly prevalent diseasee with more than 1.5 million new cases reported annually [3]. Due to the mortality, morbidity, and geographical distribution of leishmaniasis, it is becoming a public health priority. Depending on the infecting species and the host immune response, the disease manifests as cutaneous, mucocutaneous, or visceral leishmaniasis [4, 5]. *L. major* is causes cutaneous leishmaniasis, the most common form of the disease that manifests as skin lesions ranging from small red papules to ulcerative lesions [12]. Although this form of the disease is not lethal, healed lesions can lead to significant disfiguration and self-and social stigma [13].

The life cycle of the parasite alternative between an insect vector and a mammalian host [17]. The sole vectors of *Leishmania* are female phlebotomine sandflies. *Leishmania* enters the mammalian host body when an infected sandfly takes a blood meal and injects metacyclic parasites into the dermis [17, 19]. Rupturing of the dermis and its capillaries by the sandfly proboscides results in endothelial activation and neutrophil recruitment [25, 26]. To evade the immune response initiated by the sandfly bite in addition to the immune recognition and subsequent destruction of *Leishmania* promastigotes, the parasites utilize a host of virulence factors. For instance, promastigotes release 3'-nucleotidase/nuclease that cleaves neutrophil extracellular traps (NETs)-DNA allowing them to escape NET killing [32-34]. Similarly, the zinc-dependent metalloendopeptidase gp63 is one of the main virulence factors utilized by the parasites owing to its diverse functions in promoting *Leishmania* survival [66].

Extracellular vesicles are vesicles produced by all eukaryotic cells and are classified by on the size and assumed biological pathways into apoptotic bodies, microvesicles, and exosomes [82, 83]. Exosomes are the smallest extracellular vesicles with a size of 50-150 nm and are generated by the inward budding of early endosomes that form multivesicular bodies released to the extracellular environment [84].

Over the past decade, multiple studies reported that *Leishmania* secretes extracellular vesicles, namely exosomes in cultures [97, 98]. They were also found to be secreted in the sandfly midgut and following temperature shift from 25 C to 37 C, which mimics the parasite environment as it moves between the vector and the mammalian host [99]. The composition of exosomes is derived from the parental cells and could contain diverse molecules like proteins,

lipids, and nucleic acids [87, 88]. Hence, *Leishmania* exosomes are found to contain a myriad of parasite-derived molecules such as the virulence factor GP63 [49, 101].

Exosomes of *L. mexicana* result in modulating macrophage function by PTP cleavage, which is essential for inhibiting various kinases like JAK2, IRAK1, and MAPK which are important for macrophages activation [99]. The exosomes also inhibited LPS induced nitric oxide release in macrophages [99]. Similarly, exosomes obtained from *L. infantum* enhance macrophage motility and IL-10 production while suppressing IL-18 release [100]. To add, *Leishmania* RNA Virus 1 (LRV1), a virus that causes hyperinflammatory response exacerbating cutaneous leishmaniasis is packaged within *Leishmania* exosomes [103]. Mice co-infected with *Leishmania* and LRV1 packed exosomes led to sever lesions compared to mice infected with *Leishmania* only [103]. To add, *L. major* exosomes co-inoculation in mice results in a significantly larger lesion size compared to *L. major* only infections accompanied with a marked increase in IL-17 production [72].

Although the role of exosomes in modulating *Leishmania* infection is well studied, the mechanisms and signaling pathways activated by exosomes are less understood. Recently, our lab was able to show that exosomes potentially elicit their immune-modulatory effects by interacting with formyl peptide receptor 2 (FPR2) via ANXA1 (Olivier & Lira, Not Published). FPR2 is a member of the G-protein coupled receptors (GPCRs) family that are known pathogen recognition receptors mainly expressed on the surface of leukocytes [104, 105]. The unique ability of FPR2 to bind a wide range of ligands allows them to be involved in many physiological and pathological processes in the body. They are extensively studied for their role in inflammation and innate immunity [108]. They modulate multiple intracellular cascades by regulating kinases and phosphatases such as PKC, PI3K, MAPKs, and Akt [106, 109].

In this study, we provide an insight into the role of the exosome-FPR2 axis in *L. major* infections using both *in vitro* and *in vivo* studies. We also highlight select potential novel signaling pathways activated by the exosome-FPR2 axis leading to enhanced parasite phagocytosis and survival within neutrophils and macrophages.

8.4 Materials and Methods

8.4.1 Cell Culture

Immortalized murine bone marrow-derived litter mate 1 (LM-1) cell (generated in Olivier's lab [149] were grown at 37 °C in 5% CO_2 in Dulbecco's Modified Eagle Medium (DMEM) (Wisent Inc., St-Bruno, QC, Canada) supplemented with 10% heat-inactivated FBS (Invitrogen, Burlington, ON, Canada), 2 mM L-glutamine, 100 U/mL penicillin and 100 µL/mL streptomycin (Wisent Inc, St-Bruno, QC, Canada).

8.4.2 Leishmania culture

L. major strain NIH S (MHOM/SN/74/Seidman) clone A2 and luciferase-expressing *L. major* strain LV39 [150] were cultured at 25 °C in Schneider's Drosophila Medium (Gibco-BRL, Grand Island, NY) that is supplemented with 10% heat-inactivated FBS (Wisent, St. Bruno, QC, Canada), 5 mg/mL Hemin, 2 mM L-glutamine, 100 U/mL penicillin, and 100 µL/mL streptomycin. *L. major*-LUC parasites were grown in the presence of G418 selection (Wisent, St-Bruno, QC, Canada). Logarithmic phase promastigotes (day 3-4 after passage) were passaged bi-weekly to maintain the parasite culture and were grown to stationary phase (day 6-8 after passage) for use in macrophage and mice infections [151].

8.4.3 FPR2 Agonist and Antagonist

To study the interaction between L. major exosomes and FPR2, we obtained an agonist WKYMVm and antagonist WRW4 of FPR2 (Tocris, Canmotor Ave, ON, Canada). The agonist (WKYMVm) and antagonist (WRW4) were diluted with sterile H2O to 2 mg/mL and 1 mg/mL, respectively.

For use in cell culture experiments with LM-1 macrophages, the concentration of agonist and antagonist used ranged between 5-20 µM. The volume of agonist used for peritoneal infections was 200 µL from a 2 mg/ml stock.

8.4.4 Extracellular Vesicles Extraction

Extracellular vesicles were extracted from *L. major* A2 stationary phase parasites (7-8 days of growth) in 800 mL of SDM media. The density and condition of cells were confirmed using light microscopy. Parasite culture was transferred to 50 mL tubes, centrifuged at 300 x g at 25 °C for 5 minutes, and washed twice with 50 mL PBS at 300 x g at 25 °C for 5 minutes. The pellet was then resuspended in 60 mL of RPMI 1640 at a concentration around 1-4 x 10^8

parasites/mL. The tubes were then placed horizontally and incubated for 4 hours at 37 °C with low agitation at 40 rpm.

Afterwards, the tubes were centrifuged at 1000 x g at 25 °C for 5 minutes. The supernatant containing exosomes was transferred to clean centrifuge tubes. This process was repeated twice. The final volume of exosomes in RPMI obtained is around 60 mL.

The supernatant was then passed through a 0.45 µM filter followed by a 0.22 µM filter. The filtered supernatants were then transferred to ultracentrifuge tubes (Beckman Coulter, Brea, CA, USA), balanced, and loaded to SW32.1 Ti swinging bucket rotor (Beckman Coulter). The tubes were centrifuged at 100,000 x g at 4 °C for 80 minutes, supernatants were removed leaving around 500 µL in each tube, and 12 mL of exosome buffer (137mM NaCl, 20mM HEPES) was added for a second centrifugation cycle at 100,000 x g at 4 °C for 80 minutes. The supernatant was then aspirated, leaving around 200-300 µL of concentrated exosomes in exosome buffer and stored at -80 °C. Aliquots were prepared and stored at -80 °C for Nano Tracking Assay (NTA), Transmission Electron Microscopy (TEM), and MicroBCA analysis.

The MicroBCA assay (Fisher Scientific, Waltham, MA, USA). was used to determine the protein concentration in extracellular vesicle extract following the manufacturer's protocol.

8.4.5 Nanoparticle Tracking Analysis

Extracted EVs were analyzed using nanoparticle tracking analysis (NTA). Aliquots of 80 µL were diluted in 1000 µL of exosome buffer and placed in the sample chamber. The size distribution of EVs was determined by taking three videos that are 30 seconds each for each sample using NanoSight NS300 Instrument (Malvern Panalytical, Malvern, Worcestershire, UK). The samples were maintained at 37 °C for the duration of the videos, and camera settings were optimized and kept consistent for all samples. The concentration of particles, median, mean, and mode size of particles were calculated and graphed using NTA 3.4 Build 3.4.4 software [152].

8.4.6 Transmission Electron Microscopy

Aliquots of extracted EVs suspended in exosome buffer were deposited on Fomvar carbon grids (Mecalab, Montreal, QC, Canada) and fixed with 1% glutaraldehyde in 0.1 M sodium cacodylate buffer. The EVs were washed 3 times with autoclaved Milli-Q water and stained with 1% uranyl acetate. Each step was performed for the duration of 1 minute.

The FEI Technai-12 120 kV Transmission Electron Microscope (TEM) and AMT XR80C CCD camera were used to visualize the samples (Facility for Electron Microscopy Research, McGill University, Montreal, Canada).

8.4.7 Luciferase Assay

To verify that *L. major* luciferase activity measured corresponds to the number of parasites, a serial dilution of 10^7 to 10^3 stationary phase LUC-parasites was prepared and washed 2x in PBS (Wisent, St-Bruno, QC, Canada) at 3000 rpm at room temperature. Pellets were lysed in 60 µL of lysis reagent (1X Tris-NaCl-EDTA, 20% Glycerol, and 1% Igepal in ddH2O). The lysates were vortexed, centrifuged at 13,000 rpm for 5 minutes, and transferred to new tubes. Twenty microliters of lysates were added to 100 µL of Luciferase Assay Working Reagent (Biotum, Inc, Fremont, CA, USA) in white 96-well plates. The luminescence intensity was measured using Synergy H4 luminescence reader.

To determine the survival of *L. major* within LM-1 macrophages, macrophages were plated in 24-well plates (2.5 x 10^5 cells/well). The following day, cells were infected with stationary phase *L. major*-LUC promastigotes (at 5:1, 10:1, or 20:1 ratio) and exosomes (10-40 µg/mL), WRW4 (antagonist, 5-20 µM), or WKYMVm (agonist, 5-20 µM) for 3 hours. After the set incubation time, the cells were washed 3x with sterile PBS to remove non-phagocytosed parasites. 80 µL of lysis reagent (1X Tris-NaCl-EDTA, 20% Glycerol, and 1% Igepal in ddH2O) was added, and the lysate was collected and centrifuged at 13,000 rpm for 5 minutes. Then, 20 µL of the lysate was mixed with 100 uL of Luciferase Assay Working Reagent in white 96-well plates. The luminescence intensity was measured using Synergy H4 luminescence reader.

8.4.8 Nitric Oxide Assay

The Griess reaction was used to quantify the amount of nitric oxide (NO) released from LM-1 macrophages infected with *L. major* under different conditions [153].

Briefly, 0.125 x 10^6 macrophages/well were seeded in 24-well plates and incubated overnight. The next day, fresh media was added to the cells, and they were stimulated/infected with *L. major* (20:1 ratio), 20 µM agonist, 20 µM antagonist, or 100 ng/mL LPS. After overnight incubation, supernatants were collected, and the assay was performed using a NO assay kit (Invitrogen). The Griess reaction was performed by adding 10 µL of 0.1% N-(1-napthyl)-ethylenediamine dihydrochloride and 10 µL of 1% Sulfanilic acid in 5% phosphoric acid to 150

µL of cell culture supernatant and 130 µL of deionized water. After 30 minutes of incubation at room temperature, the absorbance was read at 548 nm using Infinite 200 Pro plate reader (Tecan Trading AG, Switzerland).

8.4.9 Real-Time Reverse Transcriptase Quantitative Polymerase Chain Reaction

LM-1 macrophages were seeded at a density of 0.5 x 10^6 cells/mL in 6-well plates overnight. The next day, the cells were stimulated/infected with PBS, 20 µM agonist, 20 µM antagonist, *L. major* A2 (20:1 ratio), *L. major* A2 with either 20 µM agonist or antagonist, and 100 ng/mL of LPS. All samples were run in duplicates. After 6 hours, the supernatants were collected for multiplex cytokine/chemokine quantification and stored at – 80 °C.

The cells were then washed with PBS, and RNA was extracted using TRIzol reagent (Life Technologies, Rockville, MD, USA) according to the manufacturer's protocol. RQ1 DNAse (Promega, Madison, WI, USA) was used to clear possible genomic DNA contamination. The RNA in samples was purified using the phenol/chloroform extraction method. One microgram of purified RNA was used to prepare cDNA using Protoscript II Reverse Transcriptase (New England Biolabs, Whitby, ON, Canada) and random primers oligo-hexamers (Carlsbad, CA, USA). The samples were then treated with *Escherichia coli* RNase H (New England Biolabs) to clear RNA-DNA helices. All samples were dosed to a standard concentration for quantitative Real-Time Reverse Transcriptase Polymerase Chain Reaction (qRT-PCR). SYBR Green Supermix (Bio-rad, Mississauga, ON, Canada) and qRT-PCR primers for targeted genes (Integrated DNA Technologies, Coralville, IO, USA) were added to the cDNA templates, and qRT-PCR reactions were run in CFX96 Touch Real-Time PCR Detection System (Bio-Rad). Results were analyzed by the ΔΔCt method.

8.4.10 Multiplex Cytokine/Chemokine Quantification Assay

A hundred microliters from supernatants were collected from the experiment described above. They were used to determine the levels of cytokines and chemokines using multiplex mouse cytokine array/chemokine array 10-plex assay (Eve Technologies, Calgary, AB, Canada) that detects the levels of IFNγ, IL-1β, GM-CSF, IL-2, IL-3, IL-4, IL-6, IL-10, IL-12 (p70), MCP-1 and TNF-α in a sample.

8.4.11 Animals and Ethics

Animal experiments were carried out in pathogen-free housing according to CACC Guidelines and approved by the McGill University Animal Care Committee (UACC) under the Animal Use Protocol number 7791 at McGill University

The experiments were performed in the McGill University Health Center Research Institute (MUHC-RI) in a containment level 2 housing facility. Female C57BL/6 wild-type adult mice (6-8 weeks) from our in-house colony were used for intraperitoneal infections with *L. major.*

8.4.12 Intraperitoneal Infection

Intraperitoneal infections in mice were performed to evaluate proteomic and phosphoproteomic profiles of innate inflammatory cells and to confirm the observations seen *in vitro.* Groups of 2 mice stimulated with PBS, infected with 10^8 *L. major* A2 strain only, 10^8 *L. major* A2 and 20 µg of exosomes, and 10^8 *L. major* A2 and 200 µL of agonist. The preparations were injected into the intraperitoneal cavity accordingly. After 6 hours of infection, the intraperitoneal lavage was performed using 5 mL of ice-cold endotoxin-free PBS. The workflow of this section is illustrated in (Figure 3).

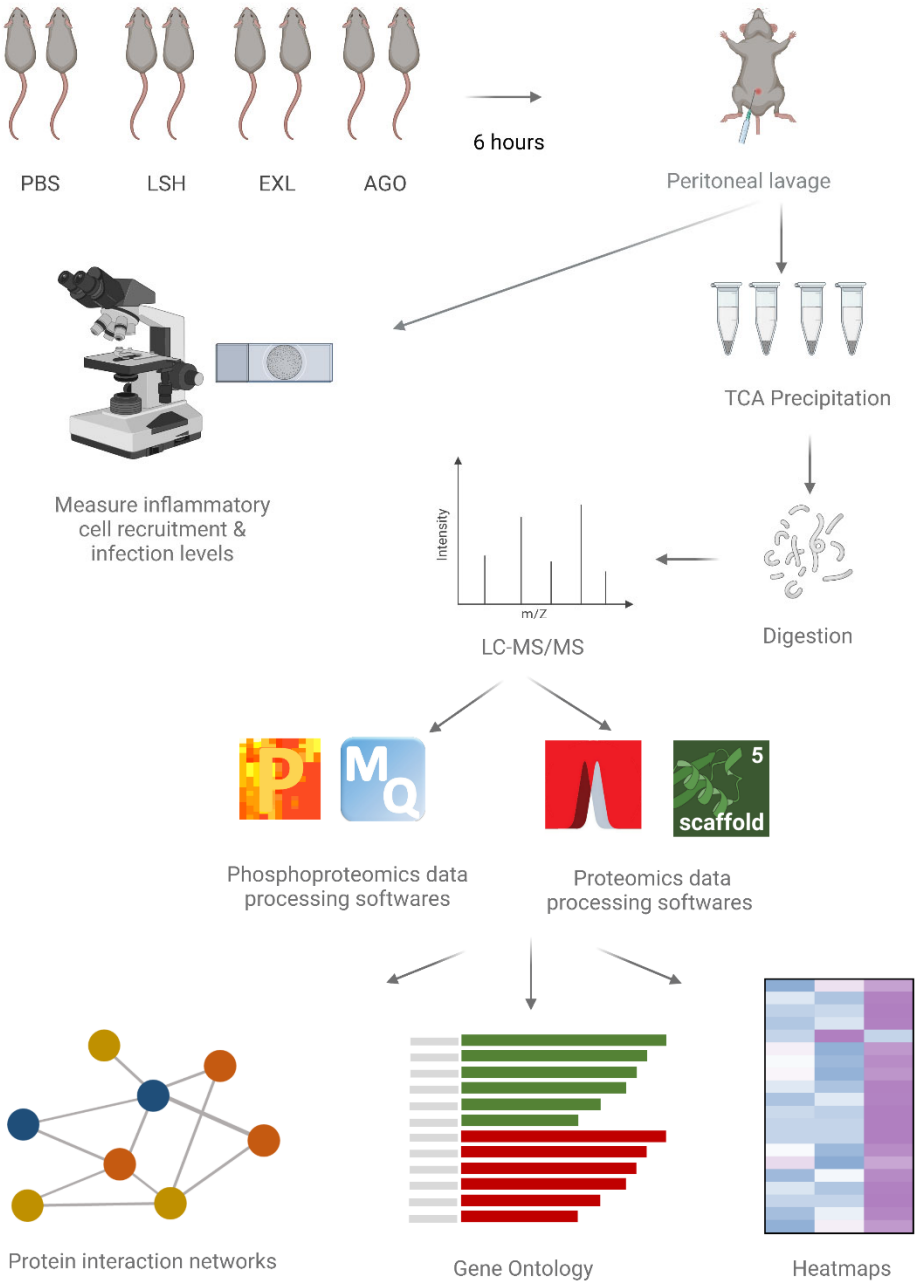

Figure 3: Proteomics and Phosphoproteomics experimental workflow.
In vivo peritoneal infections of mice at different experimental conditions for 6-hours were followed with intraperitoneal lavage. A portion of cells was deposited on microscopic slides to measure inflammatory cell recruitment and infection levels. The rest of the cells were lysed, and the proteins were precipitated using TCA precipitation. Proteins were digested and analyzed by LC-MS/MS. Phosphoproteomic data was processed using MaxQuant followed by Perseus, while proteomic data was analyzed using Mascot followed by Scaffold software. Bioinformatic analysis for both phosphoproteomics and proteomics included protein-protein interaction networks, Gene Ontology analysis and heatmaps.The figure is created *using* Adobe Illustrator and Biorender.com

Cells were concentrated and deposited on microscopic glass slides using a Cytofunnel (ThermoFisher, Waltham, MA, USA). A 150 µL of cell suspension was aliquoted and centrifuged at 300 rpm for 5 minutes to deposit the cells on the slides. The dried slides were stained using a Diff-Quick kit (RAL Diagnostics, Martillac, France). Differential count of cells and the number of infected cells was counted using a standard light microscope at 100x magnification with oil immersion.

The remaining lavage samples were centrifuged at 1800 RPM for 10 minutes. The supernatants were dispensed, and the pellets were used in TCA precipitation assay for LC-MS/MS analysis.

8.4.13 TCA Precipitation Assay

The number of proteins in the pellets extracted from intraperitoneal infection was measured using Bradford assay (Bio-Rad, Mississauga, ON, Canada).

For proteomics, 10 µg of proteins were aliquoted, and the volume was completed to 100 µL with ddH_2O. Then,100 µL 10X Tri-HCL-EDTA, 100 µL 0.3% sodium deoxycholate, and 100 µ L of 72% TCA were added to the 100 µL protein suspension.

For phosphoproteomics, 50 µg of proteins were aliquoted, and the volume was completed to 200 µL with ddH_2O. Accordingly, 200 µL of 10X Tris-HCL-EDTA, 200 µL 0.3% sodium deoxycholate and 200 µL of 72% TCA were added to the suspension.

All tubes were incubated on ice for 1 hour and centrifuged at 14,000 rpm at 4 $^{\circ}$C for 20 minutes. The supernatant was discarded, and the pellet was resuspended in 100 µL of 90% acetone (room temperature). The tubes were incubated at – 20 $^{\circ}$C overnight and centrifuged the next day at 14,000 rpm at 4 $^{\circ}$C for 20 minutes. The supernatant was discarded, and the pellet was air-dried at room temperature and then stored at -20 $^{\circ}$C.

8.4.14 Liquid Chromatography-Mass Spectrometry (LC-MS/MS)

Proteins precipitated with 15% trichloroacetic acid/acetone were sent to the Institute de Recherches Clinique de Montreal (Universite de Montreal, Montreal, QC, Canada) for Liquid Chromatography-Tandem Mass Spectrometry (LC-MS/MS) analysis. At the institute 200 ng/µL of sequencing grade trypsin (Promega) and 50 mM ammonium bicarbonate was used to reduce,

alkylate, and digest the proteins. The digestions were carried out at 37 °C for 18 hours and it stopped with 5 µL of 5% formic acid.

The digests of samples sent for proteomic analysis were cleaned with C18 ZipTip pipette tips (Millipore, Burlington, MA, USA). Then, the peptides were desalted using Zorbax Extended-C18 desalting column (Agilent) and separated on Biobasic 18 Integrafrit capillary column (Thermo Scientific, USA) by Nano high-performance liquid chromatography (HPLC). Eluted peptides were electrosprayed and analyzed using QTRAP 4000 linear ion trap mass spectrometer (SCIEX/ABI).

Digested proteins from samples sent for phosphoproteomics were desalted using Oasis HLB extraction plate (Waters UK), lyophilized, and treated for phosphopeptide enrichment with MagReSyn® TiO2 beads (ReSyn Biosciences). The phosphopeptides were then desalted with Oasis HLB and lyophilized. HPLC was performed on the samples using Easy-nLC 1200 (Proxeon Biosystems). The system was coupled with Orbitrap Fusion mass spectrometer (Thermo Scientific) by Nanospray Flex Ion Source. A full scan MS survey spectra (m/z 360-1560) with a resolution of 120,000 and target value at 4e5 were obtained in the Orbitrap. This was followed by fragmenting the 15 most intense peptide ions in the HCD collision cells and analyzing them in the linear ion trap with a normalized collision at a 30 V target value of 1e4. When a neutral loss of phosphoric acid is detected (48.99, 32.66 or 24.5 Th) in MS2 scans, a MS3 scanning was executed. After two MS2 events, ions selected for fragmentation were excluded for 25 seconds.

8.4.15 Proteomics data processing

Mascot 2.6 (Matrix Science) was used for searching protein databases against the Refseq Mus Musculus protein database. Proteome discoverer version 2.3 was used to create peak list files using a minimum mass of 500 Da, maximum mass of 6000 Da, no grouping of MS/MS spectra, precursor charge auto, the minimum number of fragment ions set to 5. Mass tolerance for precursor ions was set at 10 ppm and for fragment ions at 0.02 Da. Trypsin was used as the enzyme which allows for up to 2 missed cleavage. Modification of Cysteine carbamidomethylation was set as fixed modification, while modifications in methionine oxidation, serine, threonine, and tyrosine phosphorylation were set as variable modifications.

Scaffold software version 4.8.9 (Proteome Software Inc., Portland, OR, USA) was used for MS/MS peptide and protein identification. The inclusion criteria for identified peptides had greater than 95% probability by the Peptide Prophet algorithm with Scaffold delta-mass correction. Protein identification criteria required higher than 80% probability and having at least two identified peptides in at least one biological replicate.

8.4.16 Phosphoproteomics data processing

Phosphoproteomic data were analyzed using MaxQuant software. The database search for phosphopeptide identification was executed against the Refseq *Mus Musculus* protein database. The selected enzyme is trypsin which allows for two missed cleavages. Cysteine carbamidomethylation was set as a fixed modification, while methionine oxidation, serine, threonine, and tyrosine phosphorylation were variable modifications. The mass tolerance for precursor ions was set to 10 ppm and for fragment ions to 0.5 Da, with the minimum required peptide length at seven amino acids. The maximum false discovery rates (FDR) for protein and peptide identification were 0.01. The initial maximum allowed mass deviation was set to 7 ppm and 0.5 Da for MS/MS peaks. Data obtained from MaxQuant was processed in Perseus version **1.6.5.0**. Processing included removing reverse and contaminants, filtering columns based on localization probability of $x > 0.75$, and valid values of 70%. Intensity values were log2 transformed.

8.4.17 Bioinformatic Analysis

Data were normalized and quantified using Scaffold software and Perseus for proteomics and phosphoproteomics, respectively. Microsoft Excel was used to create unique and common proteins tables for downstream analysis. Gene Ontology was performed using Panther (www.pantherdb.org) and Enrichr (https://maayanlab.cloud/Enrichr/) [154, 155]. String analysis was done using String version 11.5 (https://string-db.org/) [156]. Heatmaps were created using R Studio version 3.0.1 with pHeatmap package. Kinase enrichment analysis (KEA) was done using X2K platform [157].

8.4.18 Statistical Analysis

Statistical analysis was executed using GraphPad Prism version 9.3.0 (La Jolla California, USA). Unless stated otherwise, p-values were determined using one way ANOVA followed by Dunett's multiple comparisons test.

8.5 Results

8.5.1 *L. major* exosomes significantly enhance infections in macrophages

To perform infection assays with exosomes, we extracted exosomes from L. major parasites by inducing their release via temperature shift from 25 °C to 37 °C followed by ultracentrifugation to concentrate the yield. We used a Nanoparticle tracking assay (NTA) and transmission electron microscopy (TEM) to confirm the purity of extracted exosomes. NTA analysis consistently showed results within the expected range for exosome diameter. NTA analysis for a representative sample (Figure 4-A) shows the diameter of vesicles was mainly distributed around 170 nm, indicated by the peak in the figure. It is important to note that the machine used in this analysis has a known overestimation of vesicle size. Confirming NTA results, images obtained by TEM also showed most vesicles to be around 120 nm in size (Figure 4-B) At 30,000x and 49,000x magnification, the round cup shape of exosomes can be visualized along with the lipid bilayer.

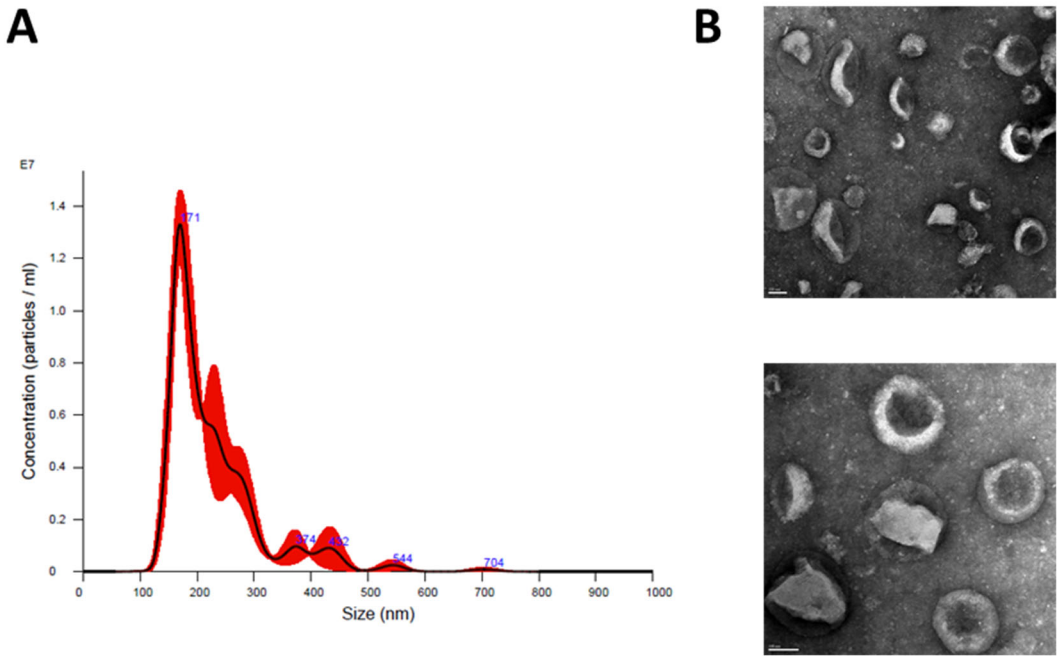

Figure 4: Nanosight Tracking Analysis (NTA) and Transmission Electron Microscopy (TEM) of L. major exosomes. A) Representative NTA analysis showing the average nanoparticle distribution and concentration calculated from three videos per sample. B) TEM negative staining of exosomes derived from *L. major* promastigotes. The top image was taken at 30000x; bottom image at 49000x. Scale bars represent 100 nm.

Next, we performed infection assays using *L. major*-LUC parasites labeled with luciferase for *in vitro* infections with exosomes [150]. This assay provides an easy and reliable method to quantify parasites within macrophages, wherein luminescence measured in Relative Light Units (RLU) is proportional to parasite count. To confirm the proportional relationship between parasite count and RLU, we performed a serial dilution of parasites and measured luminescence activity (Figure 5). RLU measured was proportional to *L. major*-LUC counts at different dilutions. However, below 10^3 parasites, the method's sensitivity was reduced (not shown). In our experimental setup, we infect macrophages with 10^5-10^6 parasites, hence the level of infections measured is above 10^3 parasites cut-off.

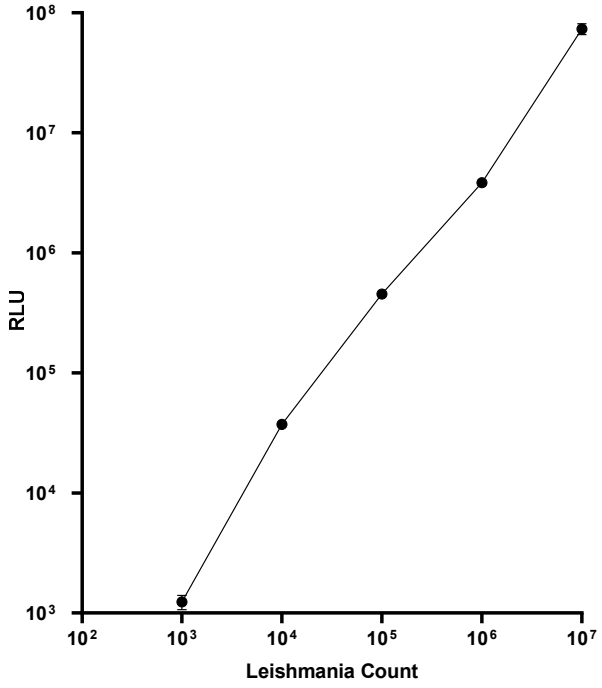

Figure 5: Correlation between luciferase activity in L. major-LUC and parasite count. L. major parasites were diluted by 10-fold serial dilution and subsequently counted using a hemacytometer. Luciferase activity is expressed as RLU (Relative Light Units) and is measured using a luminometer. Bars show ± SEM of two duplicates.

To optimize the system and choose an optimal infection time and parasite to macrophage ratio, we infected macrophages at 5:1, 10:1, and 20:1 ratio for either one or three hours (Figure 6). We decided to conduct the rest of our experiments at a 5:1 ratio for 3 hours based on the number of washes required to eliminate non-attached parasites.

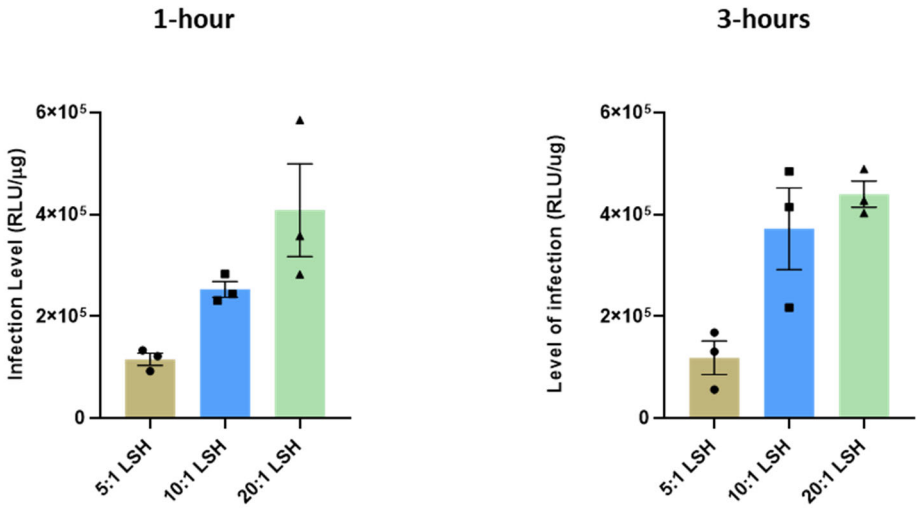

Figure 6: Determination of macrophage L. major infection using luciferase assay. LM-1 macrophages were infected at different ratios of *L. major-LUC* (5:1, 10:1 and 20:1) over 1-hour (left) and 3-hours (right) time periods. The results are representative of one out of three experiments performed independently, n=3, Bars show ± SEM.

Then, we infected macrophages with a 5:1 ratio of *L.major*-LUC to macrophages, and with an increasing concentration of *L. major* exosomes. At all concentrations, exosomes significantly increased parasite load in macrophages compared to cells infected with *L.major*-LUC and PBS (Figure 7).

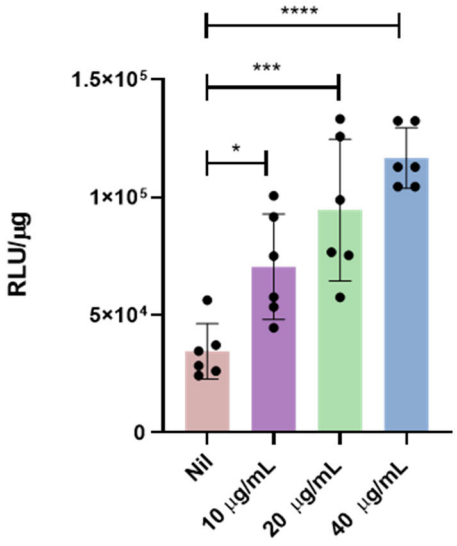

Figure 7: Exosomes significantly increase the level of L. major infection in macrophages. Macrophages were infected with *L. major* and an increasing concentration of exosomes (10 µg/mL, 20 µg/mL, and 40 µg/mL) at a 5:1 parasite to macrophage ratio for 3 hours. The results are represent the mean of two independent experiments with n=6. Statistical significance was determined using ordinary one way ANOVA followed by Dunett's multiple comparisons test. Bars show ± SEM. * $p<0.05$, *** $p<0.001$, **** $p<0.0001$.

8.5.2 FPR2 enhances *L. major* internalization in macrophages

To confirm the interaction between *L. major* exosomes and FPR2, we primed macrophages with increasing FPR2 antagonist (WRW4) concentrations for 10 minutes. Then, We infected macrophages with *L. major*-LUC and 20 µg/mL of exosomes. *L. major* only treated cells and *L. major*-exosomes co-induced cells were used as controls. We observed a significant decrease in the level of infection at all concentrations between exosome only and antagonist-exosome treated cells (Figure 8A).

To determine if FPR2 activation using an agonist would increase the level of *L. major* infection in macrophages, we co-induced *L. major* infected macrophages with an increasing concentration of FPR2 agonist (WKYMVm). We saw an increase in infection levels at all concentrations compared to infected macrophages treated with *L. major* only (Figure 8B). This increase was significant at a concentration of 20 µM of agonist but not at 5 or 10 µM. To add, at 20 µM, the level of infection increased similarly to exosomes co-induced cells. This data shows that exosome-mediated exacerbation of infection occurs mainly via FPR2, and activation of FPR2 alone could mimic the effect seen with exosomes.

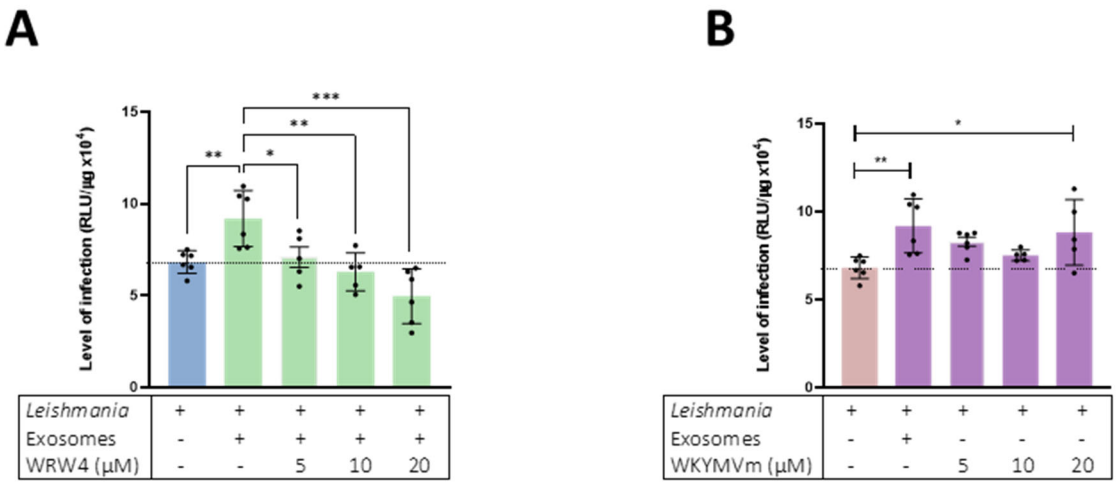

*Figure 8: Impact of FPR2 agonist and antagonist on L. major infections.*macrophages infected with a 5:1 ratio of *L. major* to macrophages and 20 µg/mL of exosomes were induced with different concentrations of the antagonist, 5 µM, 10 µM, and 20 µM for 3 hours. B) Macrophages were infected with a 5:1 ratio of *L. major* and an increasing concentration of agonist 5 µM, 10 µM, and 20 µM for 3 hours. Results are the mean of two independent experiments (n=6). Statistical significance was determined using ordinary one way ANOVA followed by Dunett's multiple comparisons test. Bars show ± SEM. * $p<0.05$,** $P<0.01$, *** $p<0.001$.

8.5.3 Modulation of cytokine and chemokine levels in early *L. major* infections by FPR2

As a first step in deciphering signaling pathways activated by the FPR2-exosome axis, we analyzed expression levels of chemokines/cytokines involved in *Leishmania* infections and the inflammatory process in macrophages using RT-qPCR. To confirm whether FPR2 agonist and antagonist alone could influence gene expression of LM-1 macrophages, we quantified gene expression of MIP-1β, MCP-1, or IL-6 after 6-hours of stimulation with FPR2 agonist or antagonist at different concentrations ranging from 5 µM to 40 µM (Figure 9). As expected, the agonist and antagonist did not modify gene expression levels of selected cytokines at all tested concentrations.

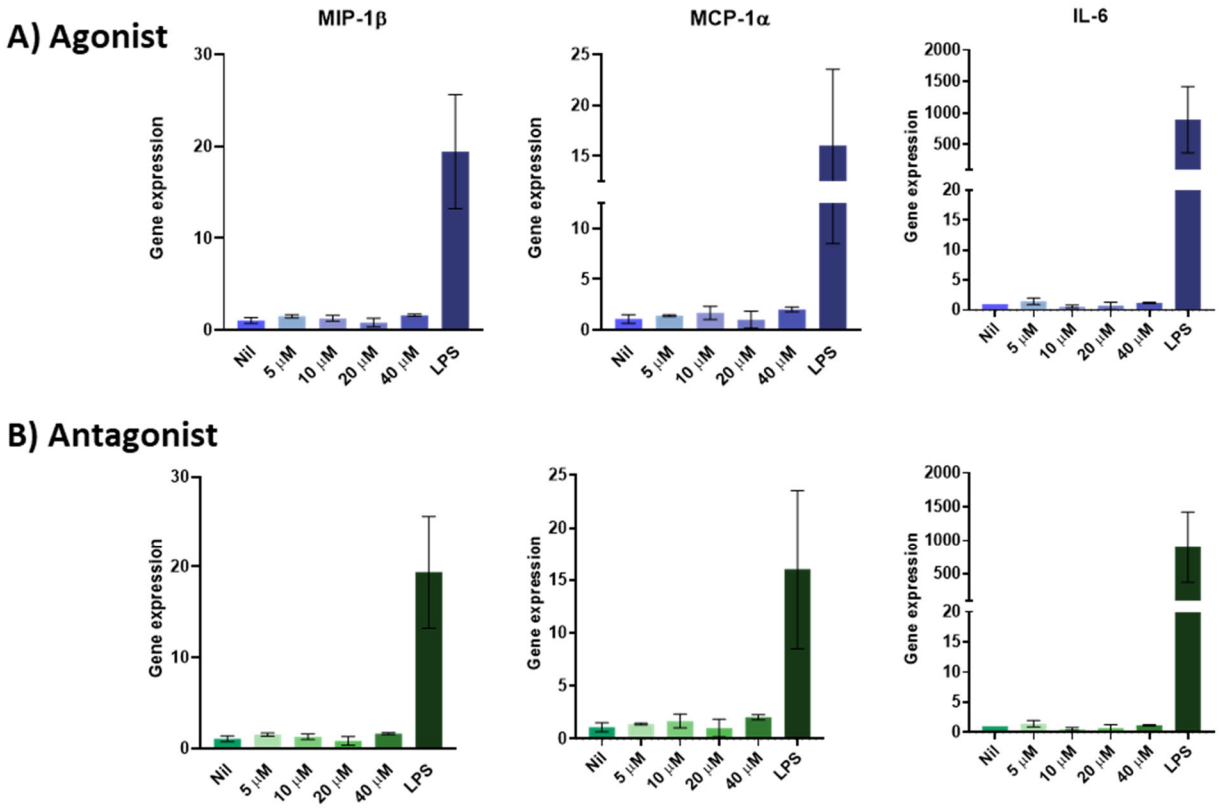

Figure 9: Gene expression analysis of macrophages induced with FPR2 agonist and antagonist. Impact of FPR2 on MIP-1B, MCP-1, and IL-6 gene expression in macrophages was assessed by stimulating macrophages for 6 hours with increasing concentrations of A) agonist or B) antagonist followed by collecting cell lysates for RT-qPCR analysis. The results show representative figures of normalized gene expression levels of MIP-1B, MCP-1a, and IL-6 in macrophages, Bars represent ± SEM, n=2.

Furthermore, to determine whether FPR2 plays a role in inducing cytokine and chemokine expression in macrophages during early *Leishmania* infection, we infected macrophages and co-stimulated them with 20 μM of FPR2 agonist and antagonist for 6 hours. When the antagonist was used, it was added to the cell culture for 10 minutes to prime cells. Like our previous observation, gene expression levels of MIP-1α, MIP-1β, MCP-1, IL-6, and IL-1β were not modified during *L. major* infection following both agonist and antagonist co-induction (Figure 10-A). However, we observed a decrease in TNFα gene expression in agonist-treated infected macrophages compared to macrophages infected with *L. major* only. Yet, This reduction was not significant.

We also measured the levels of selected cytokines: IL-6, TNFα, and MCP-1 in cell culture supernatants using a multiplex assay (Figure 10-B). The agonist and antagonist did not modify MCP-1 concentration in supernatants compared to *Leishmania* infected macrophages. However, we observed a trend of higher TNF-α levels in supernatants of cells co-inoculated with the antagonist and *L. major* compared to cells infected with *L. major* only. When used alone, the antagonist induces higher levels of TNFα compared to control cells. However, this increase is not significant.

Interestingly, we observed a trend of an increase in IL-6 concentration in supernatants of cells co-induced with the antagonist compared to cells infected with *L. major* only. Overall, the agonist and antagonist did not significantly alter the levels of chemokines and cytokines expression. However, FPR2 activation during *L. major* infection using the agonist WKYMVm seems to suppress TNF-α gene expressions. On the other hand, using the antagonist of FPR2 results in higher levels of TNF-α measured in the cell culture supernatants. We also observed an increase in IL-6 concentration with FPR2 antagonist.

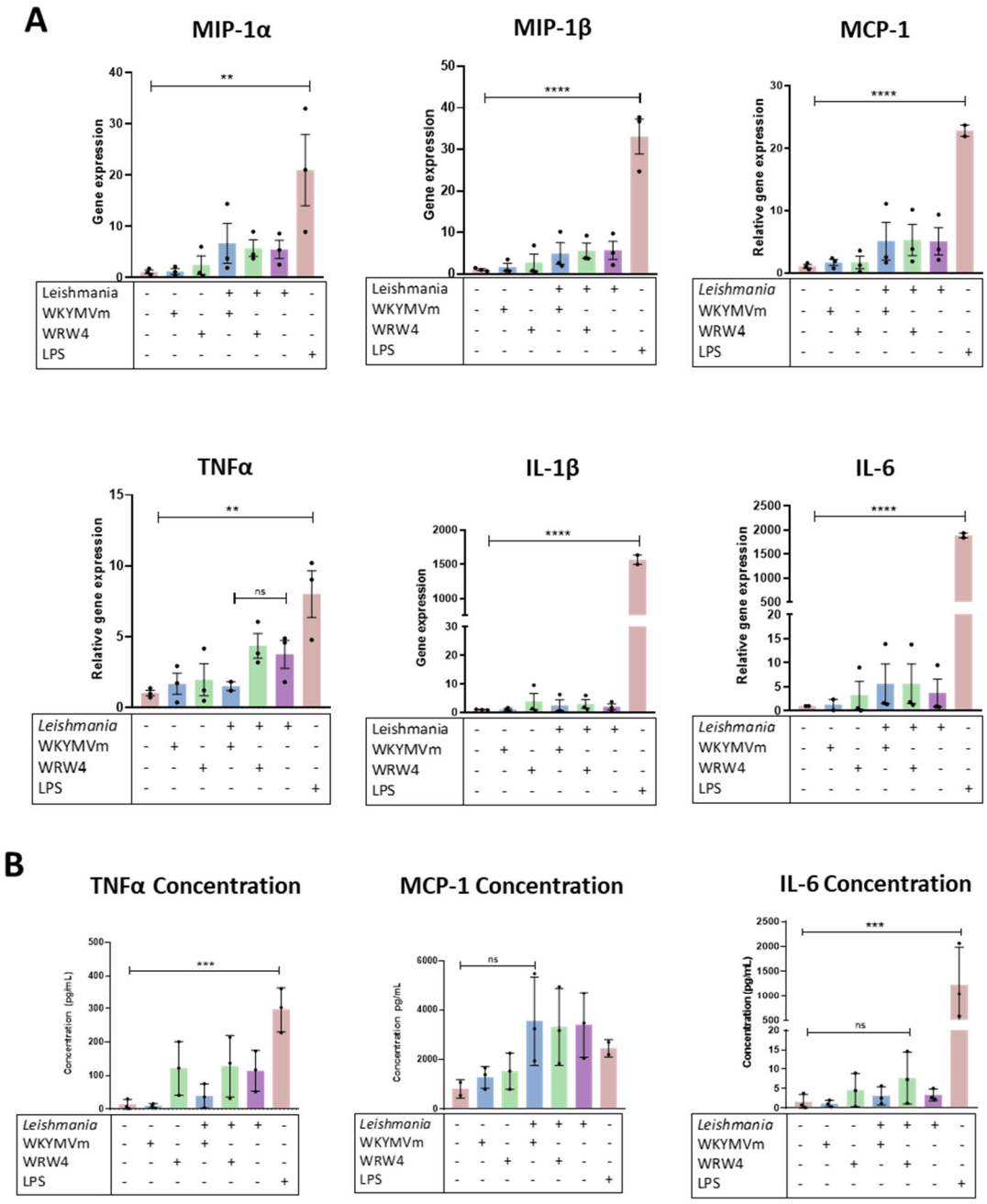

Figure 10: Impact of FPR2 on macrophage cytokine gene expression and concentration during L. major infection. Representative figure of the measurement of selected cytokines and chemokines in LM-1 macrophages induced/infected with different conditions A) gene expression and B) concentration in macrophages stimulated with *L. major* and FPR2 agonist or antagonist, agonist alone, antagonist alone, and LPS for 6 hours, n=3. Bars represent ± SEM. Statistical significance was determined using ordinary one way ANOVA followed by Dunett's multiple comparisons test. ns $p>0.05$, ** $p<0.01$, *** $p<0.001$, **** $p<0.0001$.***FPR2 does not influence nitric oxide release during Leishmania infection*** Nitric oxide is a crucial molecule in the

control of Leishmania infection. Parasites use different virulence factors to suppress nitric oxide release to promote their survival [158]. To establish the role of FPR2 in nitric oxide release during L.major infection, we infected macrophages under different stimulation conditions for 24 hours and measured nitric oxide levels in supernatants. The agonist and antagonist alone did not induce nitric oxide release, nor did they influence nitric oxide release in L. major infection (Figure 11).

To further confirm the role of FPR2 in nitric oxide release, we induced cells with both LPS, a potent inducer of nitric oxide release, and the agonist and antagonist (Figure 11). Like our previous findings, the agonist and antagonist did not influence nitric oxide levels during LPS stimulation. Hence, these findings suggest that FPR2 does not modify nitric oxide production in macrophages in early infection.

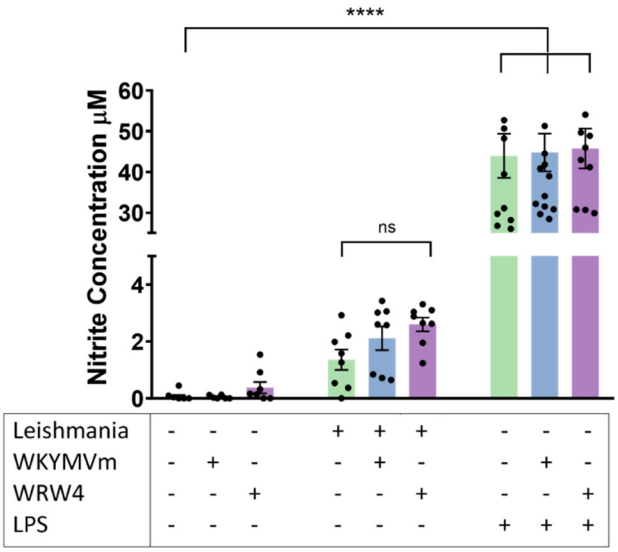

Figure 11: FPR2 agonist and antagonist influence on macrophages nitric oxide production during L. major infection. Nitrite concentration (µM) was measured using Griess assay in LM-1 macrophages supernatants after 24 hours of infection with agonist (WKYMVm) and antagonist (WRW4) alone, with *L. major* or with 100 ng/mL of LPS. Results represent the mean of two independent experiments (n=8), and three independent experiments (n=14) for data points with LPS stimulation. Bars represent ± SEM. Statistical significance was determined using ordinary one-way ANOVA followed by Dunnett's multiple comparisons test., ns $p>0.05$, **** $p<0.0001$.

8.5.4 *Leishmania* exosomes alter proteomic profiles of macrophages

Next, we proposed that phenotypes observed with exosomes and FPR2 agonist would be associated with a change in protein composition and differential phosphorylation patterns. We used an intraperitoneal infection model to define proteomic and phosphoproteomic profiles during early innate immune response in *L. major* co-infections. The peritoneal cavity is an ideal model for studying early innate immune response and retrieving large volumes of inflammatory cells required for proteomic/phosphoproteomic studies. We injected mice with *PBS, L. major* (LSH)*, L. major* with exosomes (EXL), *L. major* with agonist (AGO), and *L. major* with antagonist and exosomes (ANTA-EXL). The experiment was done with n=2. According to previous studies in our lab, maximum leukocyte recruitment in *L. major* infection occurs at 6 hours [159]. Hence, we collected peritoneal cavity lavages 6 hours following infection.

We measured the percentage of inflammatory cells recruited using cytospin Diff-Quick slides. Compared to PBS control, all *L. major* infected groups showed a significantly higher number of neutrophils recruited and a proportionally lower number of macrophages in comparison (Figure 12-A). Lower percentages of lymphocytes, eosinophils, and basophils were also recruited.

We also calculated the percentage of infected neutrophils and macrophages amongst all infection groups. We found an increase in the percentage of infected neutrophils in EXL and AGO-infected mice compared to LSH. However, ANTA-EXL groups showed a similar infection percentage to LSH groups (Figure 12-B). Similarly, we observed a significant increase in infected macrophages in AGO and EXL compared to LSH. Yet, ANTA-EXL attenuated the effect of exosomes and presented a similar infection rate as LSH infected groups (Figure 12-C). These findings are parallel to our results from *L. major-LUC* experiments.

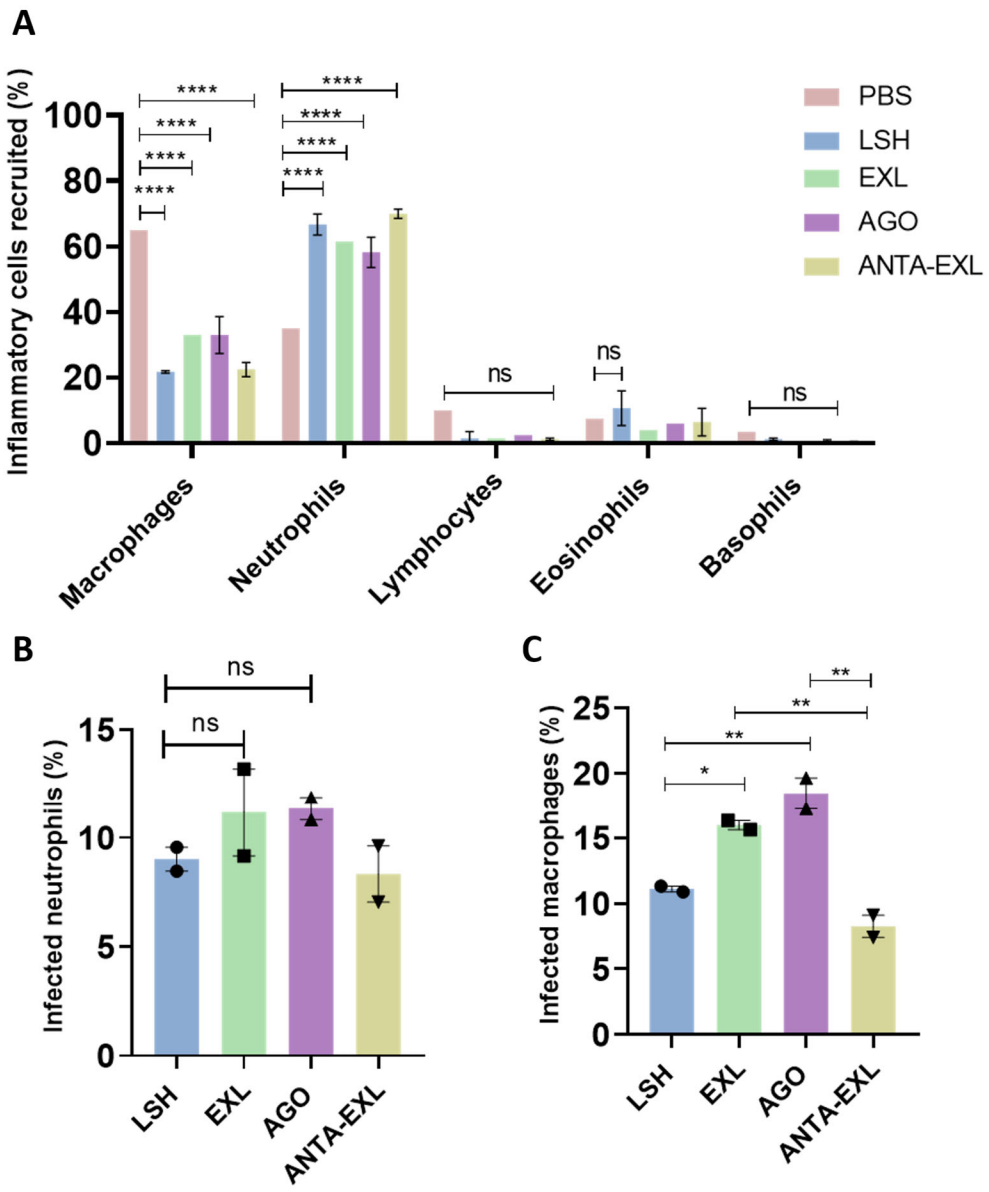

Figure 12: Exosomes increase the percentage of infected myeloid cells in peritoneal infections via FPR2 activation. Mice were infected with *L. major* (LSH), *L. major* with exosome co-inoculation (EXL), *L. major* with FPR2 agonist WKYMVm (AGO), *L. major* with FPR2 antagonist WRW4 (ANTA-EXL) in the peritoneal cavity for 6-hours. Endotoxin-free PBS was used as a control. Following infection, peritoneal lavage was performed, and inflammatory cells recruited were counted. A) Distribution of inflammatory cells following 6-hours peritoneal infection in mice at different conditions. Statistical significance was determined using 2Way ANOVA analysis. B) Percentage of infected neutrophils in each condition, and C) Percentage of infected macrophages. Statistical analysis was done using one-way ordinary ANOVA analysis followed by Dunnett's multiple comparisons test. Bars represent ± SEM. ns $p>0.05$, * $P<0.05$, ** $p<0.01$, **** $p<0.0001$.

Following peritoneal infections, we selected PBS, LSH, EXL, and AGO samples for proteomic analysis, and for phosphoproteomics, we analyzed LSH, EXL, and AGO only. Due to blood contamination in one of the PBS and EXL samples, these samples were eliminated from bioinformatics analysis to prevent skewing the results with high levels of erythrocytic proteins. Hence, PBS and EXL conditions represent n=1, while results from LSH and AGO represent an average of n=2.

The first set of samples we analyzed were PBS, LSH, and EXL infected mice which had had a total of 631, 517, and 604 proteins identified, respectively (Figure 13A). PBS group had the highest number of unique proteins, 186, while EXL group had 76 unique proteins, and LSH had 15 unique proteins.

We assessed total proteins' biological and molecular function in all groups using gene ontology terms biological process and molecular function (Figure 13B-C). Global characterization of these proteins based on gene ontology did not differ between the three groups, except for a slight increase in the terms Binding and Catalytic Activity in the Molecular Function GO terms for EXL and LSH compared to PBS. Furthermore, protein interaction networks of total proteins in each group using STRING analysis showed a difference in the sizes of main clusters and a differential clustering pattern for smaller clusters (Figure 14).

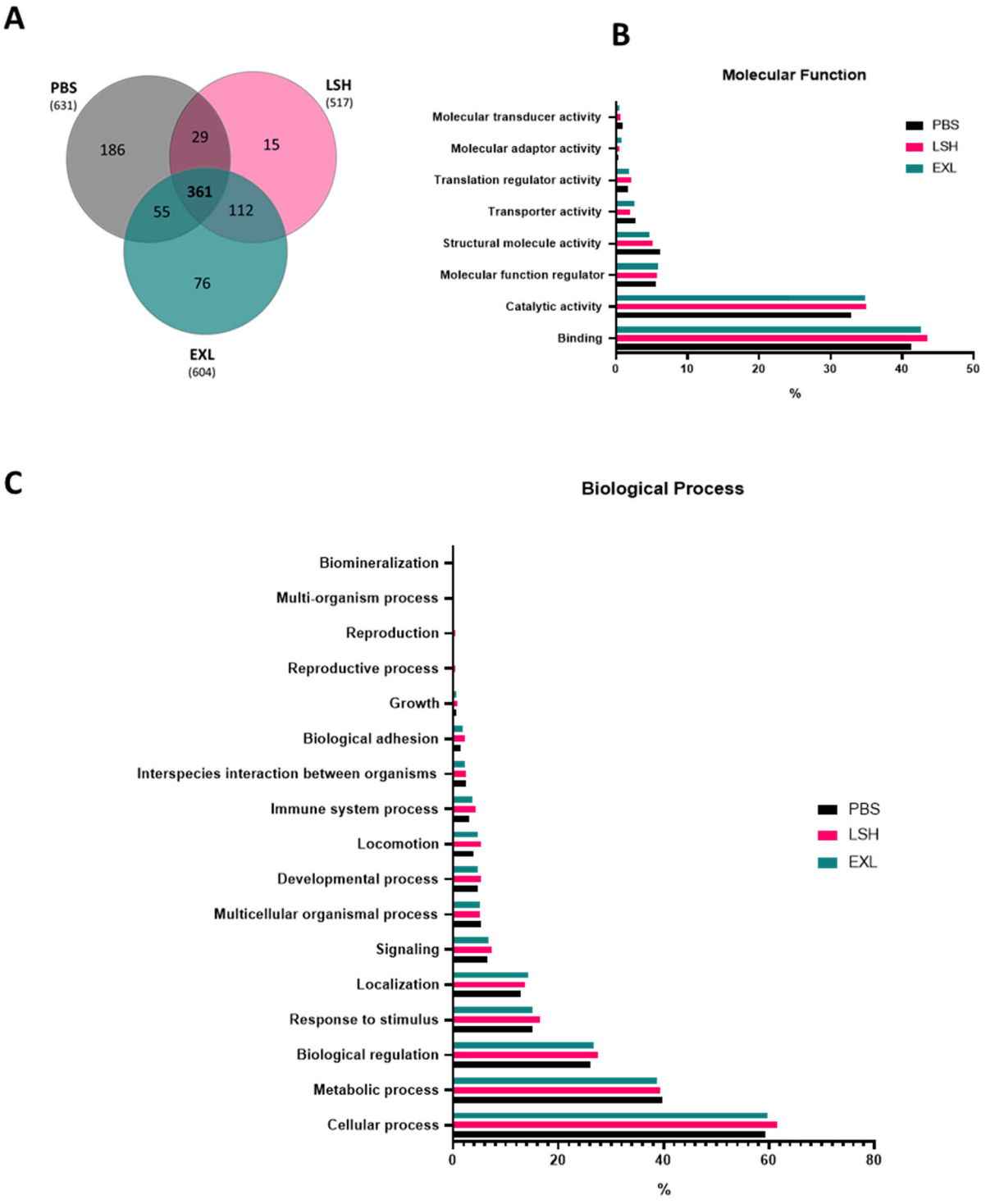

Figure 13: Bioinformatic analysis of proteomics data obtained from Leishmania (LSH) infected macrophages, Leishmania plus exosome co-inoculation (EXL) and PBS groups. A) Venn diagram of total proteins identified in PBS, LSH, and EXL. B) Top GO Molecular Function terms and C) top GO Biological process terms for proteins identified in the three groups.

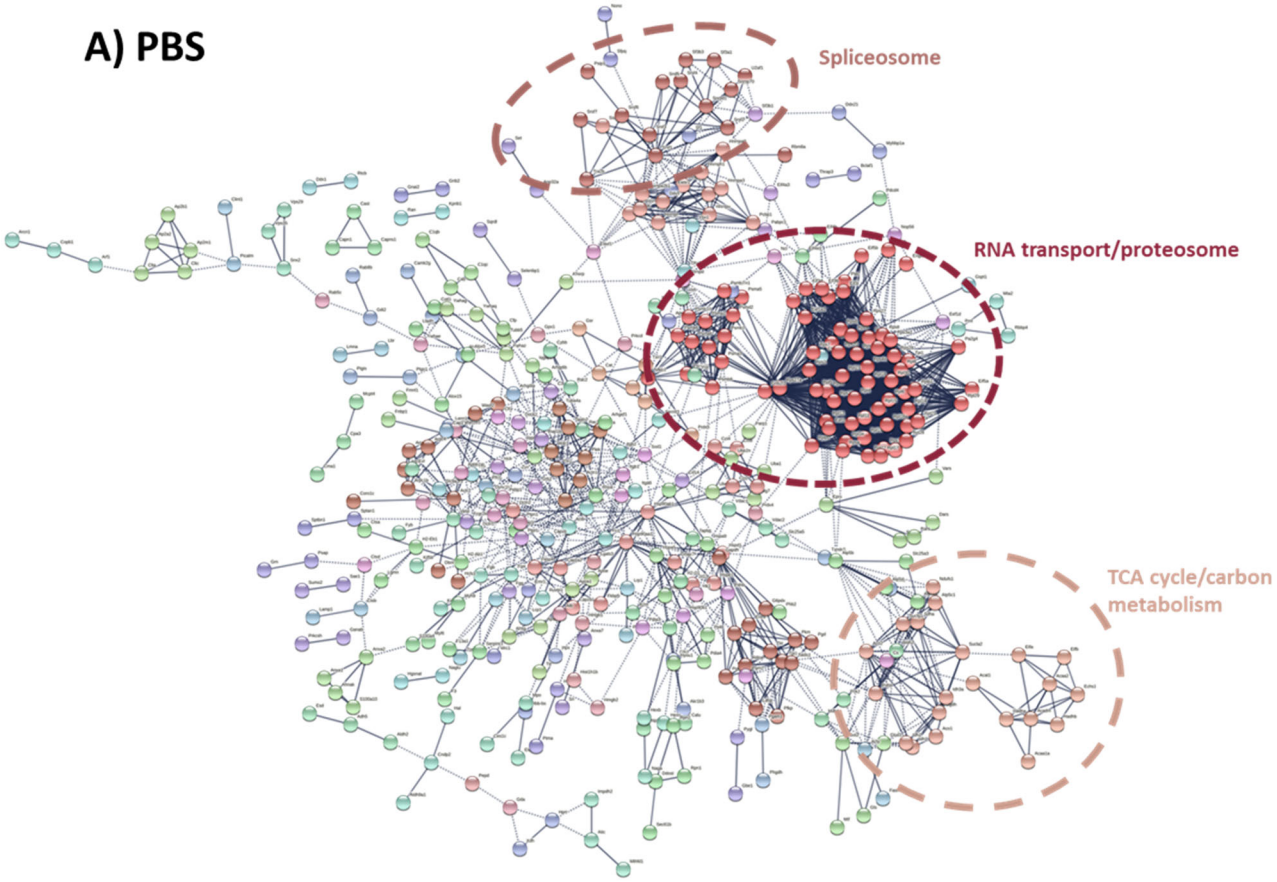
A) PBS
Spliceosome
RNA transport/proteosome
TCA cycle/carbon metabolism

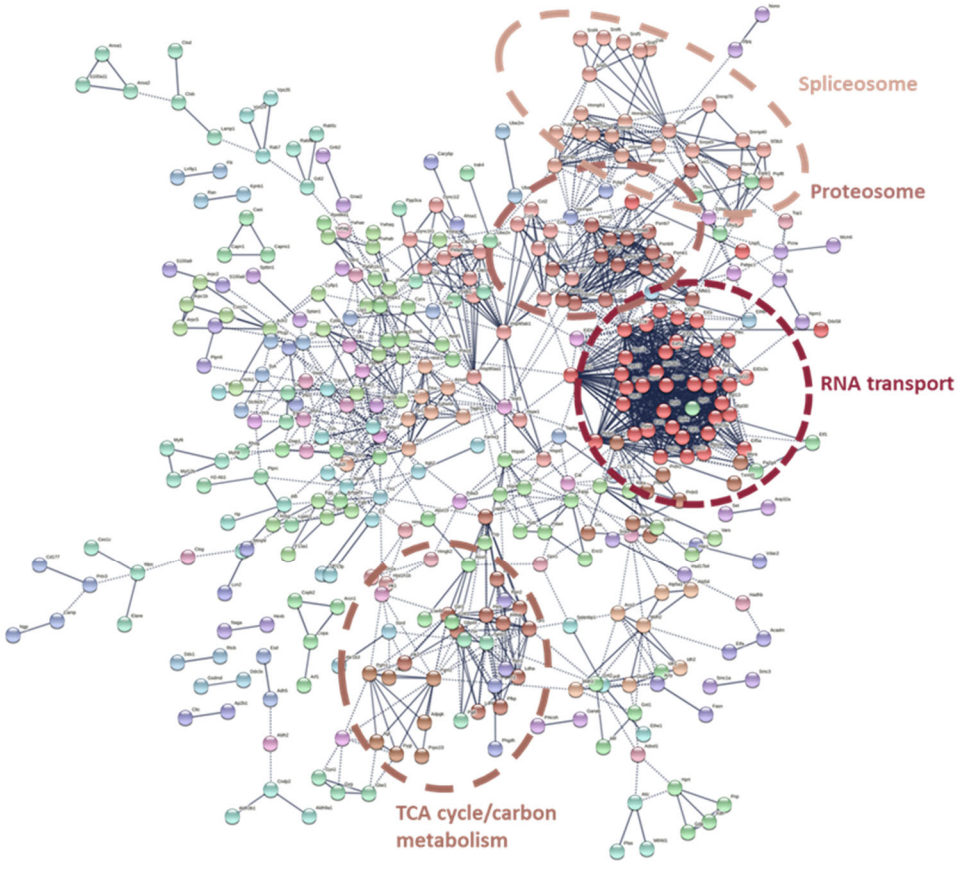
B) L. major (LSH)
Spliceosome
Proteosome
RNA transport
TCA cycle/carbon metabolism

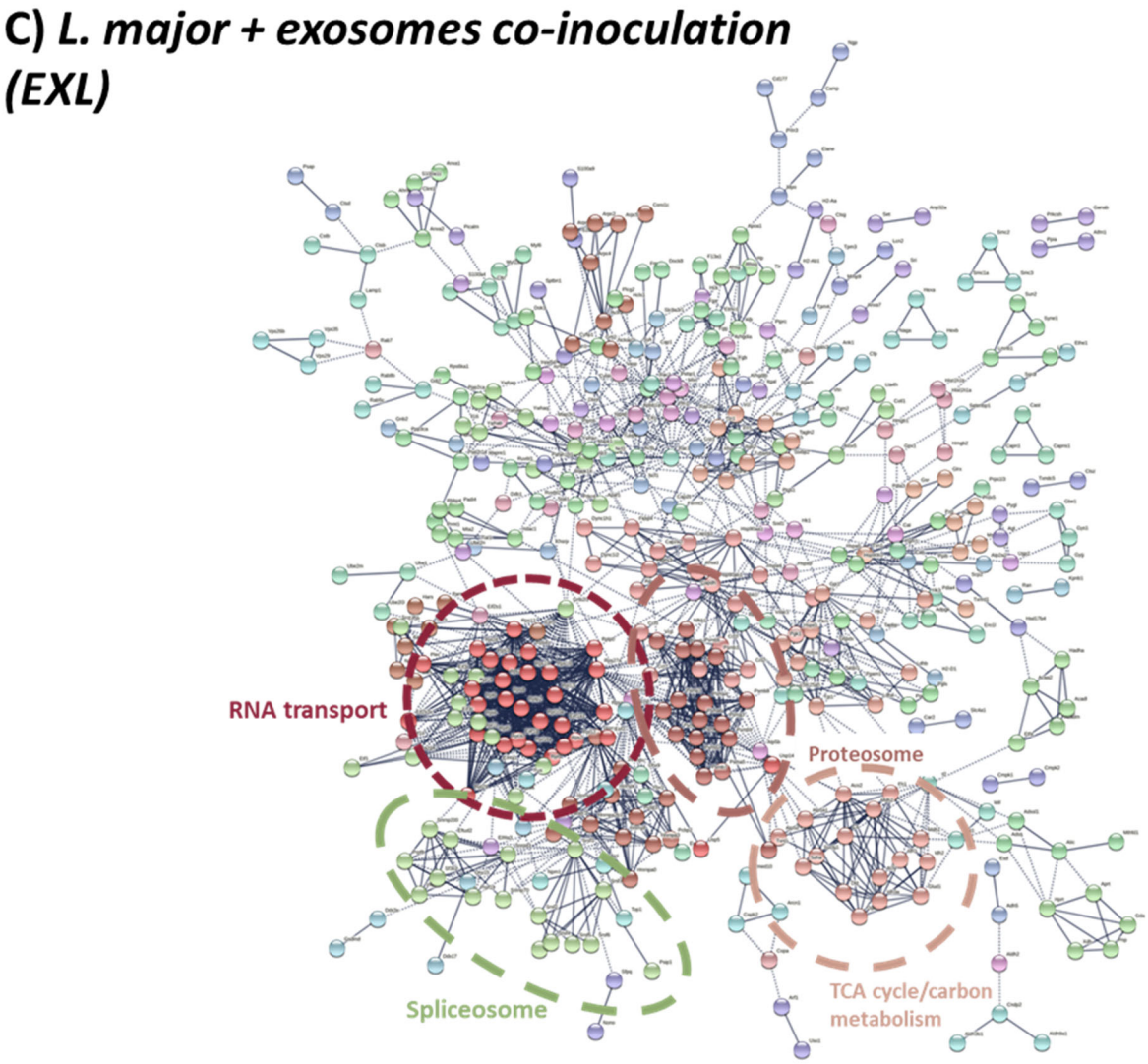

Figure 14: STRING protein network analysis of total proteins in each experimental condition. Analysis was performed using STRING v11.5. Circles represent groups of proteins in the same cluster and their shared functions. Clustering was done using MCL Level 3 clustering.

Further, we dissected unique proteins in these groups. We assumed that unique proteins found in PBS group to be downregulated during *Leishmania* infections. Based on string analysis and gene ontology, most identified proteins are ribosomal proteins involved in mRNA translation and inhibition of ubiquitin activity (Figure 15). A list of unique PBS protein is shown in Table 1.

LSH group had only 15 unique proteins, most involved in positive regulation of the DNA metabolic process, demethylation of DNA, and Leukotriene B metabolic process (Figure 16).

Interestingly, the 76 unique proteins in EXL group had clusters of proteins involved in mRNA splicing, regulation of actin cytoskeleton and protein binding, and vesicle trafficking (Figure 17). The top three enriched GO biological process terms in unique EXL proteins were "neutrophil degranulation," "neutrophil activation involved in immune response," and "neutrophil-mediated immunity."

Analysis of PBS unique proteins

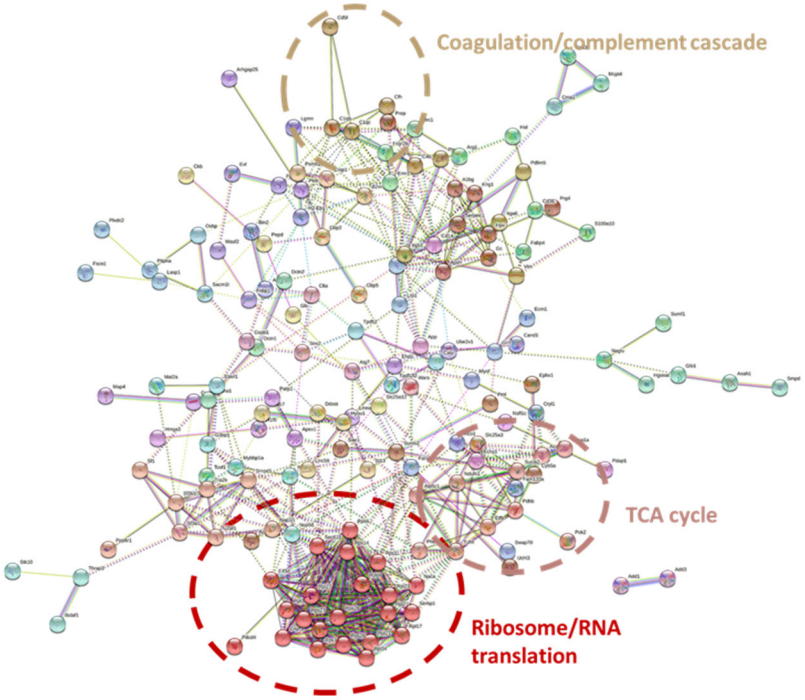

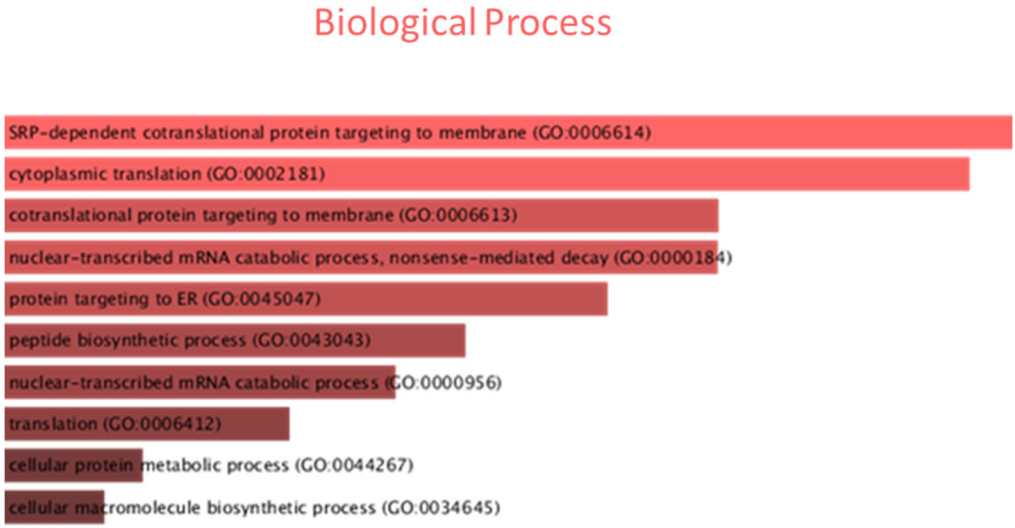

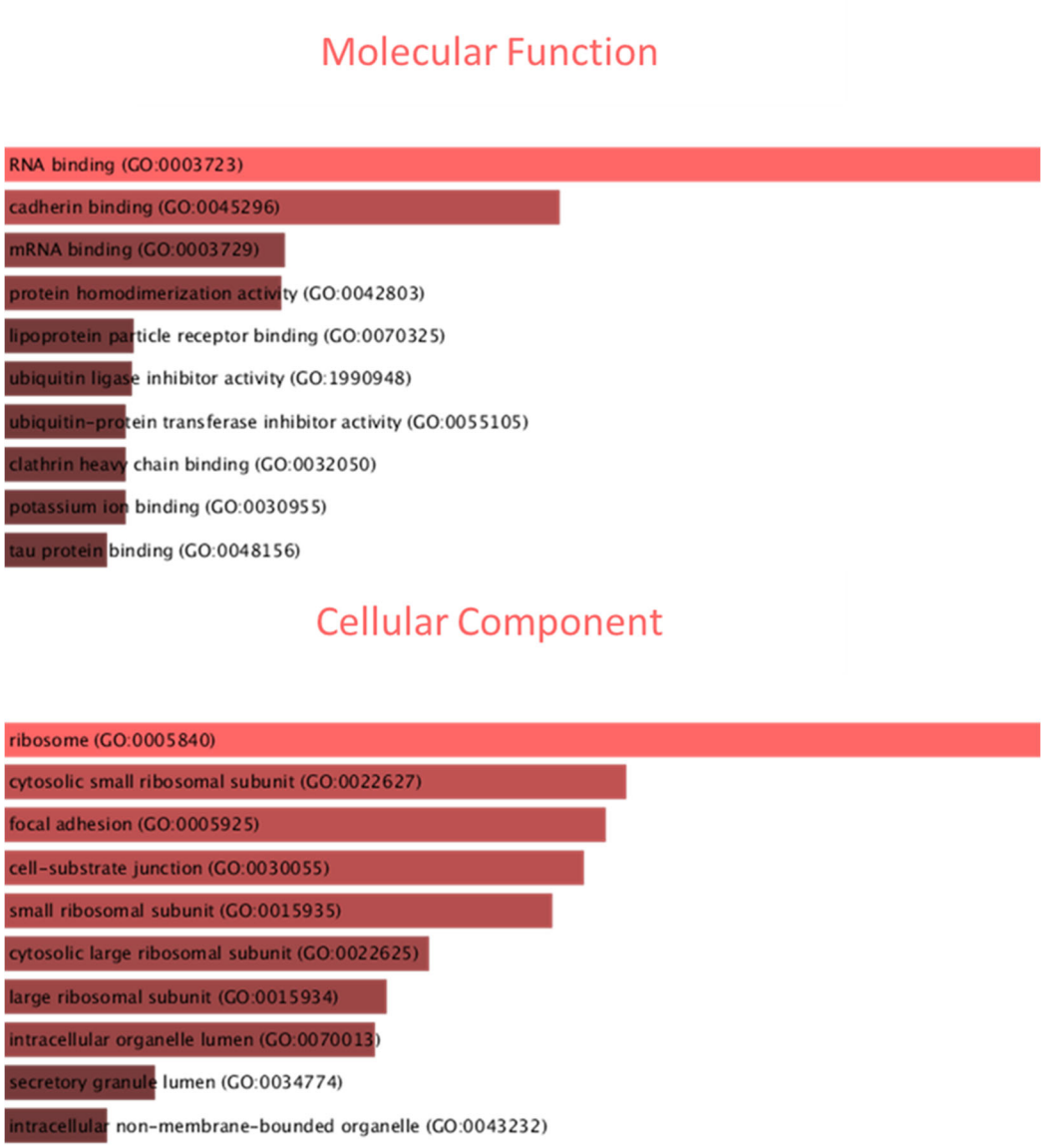

Figure 15: String and Gene ontology analysis of unique proteins obtained from PBS samples. Top: protein network analysis unique PBS proteins (186). Analysis was performed using STRING v11.5. Circles represent proteins in the same cluster and their shared functions. Clustering was done using MCL Level 3 clustering. Bottom: Gene Ontology analysis of PBS unique proteins shows three figures of the top 10 functions for Biological Process, Molecular Function, and Cellular Component.

Table 1: List of unique PBS proteins

	Protein Name	Accession Number
1	Dolichyl-diphosphooligosaccharide--protein glycosyltransferase 48 kDa subunit	OST48_MOUSE (+2)
2	Hypoxia upregulated protein 1	HYOU1_MOUSE
3	40S ribosomal protein S9	RS9_MOUSE
4	Cullin-associated NEDD8-dissociated protein 1	CAND1_MOUSE
5	Arginase-1	ARGI1_MOUSE
6	Monocyte differentiation antigen CD14	Q3U6A3_MOUSE [7]
7	Ubiquitin-conjugating enzyme E2 variant 1	B7ZBY7_MOUSE (+2)
8	Plasminogen activator inhibitor 1 RNA-binding protein	A0A0N4SV32_MOUSE [5]
9	Nucleosome assembly protein 1-like 1	NP1L1_MOUSE (+2)
10	Ras GTPase-activating-like protein IQGAP2	IQGA2_MOUSE
11	SH3 domain-binding glutamic acid-rich-like protein 3	SH3L3_MOUSE
12	Hsc70-interacting protein	F10A1_MOUSE (+2)
13	Fabp4 protein	Q542H7_MOUSE
14	40S ribosomal protein S7	RS7_MOUSE
15	Hemopexin	HEMO_MOUSE
16	Nascent polypeptide-associated complex subunit alpha, muscle-specific form	NACAM_MOUSE
17	40S ribosomal protein S6	RS6_MOUSE
18	Complement C4-B	CO4B_MOUSE
19	MCG10343, isoform CRA_b	G5E902_MOUSE (+2)
20	Xaa-Pro dipeptidase	PEPD_MOUSE
21	Apolipoprotein E	APOE_MOUSE (+2)
22	Pleckstrin	PLEK_MOUSE (+1)
23	AP-2 complex subunit mu	AP2M1_MOUSE (+1)
24	60S ribosomal protein L27a	RL27A_MOUSE
25	Phosphatidylinositol transfer protein alpha isoform	PIPNA_MOUSE (+2)
26	MCG116671	A0A1Y7VKY1_MOUSE [2]
27	Rpl17 protein (Fragment)	Q505B1_MOUSE (+4)
28	Eukaryotic translation initiation factor 3 subunit D	EIF3D_MOUSE
29	Acetyl-CoA acetyltransferase, mitochondrial	THIL_MOUSE
30	IgE L chain kappa	A0A0D5ZY64_MOUSE [7]
31	Ribosomal protein S14	O70569_MOUSE (+2)
32	Elongation factor Tu, mitochondrial	EFTU_MOUSE
33	60S ribosomal protein L34	RL34_MOUSE
34	Bridging integrator 2	BIN2_MOUSE [5]
35	Small ubiquitin-related modifier 2	D3Z794_MOUSE [3]
36	Alpha-adducin	ADDA_MOUSE (+1)

37	Electron transferring flavoprotein, beta polypeptide-like	A0A0N4SVE0_MOUSE
38	Clathrin light chain	B1AWD8_MOUSE (+5)
39	Beta-galactosidase	BGAL_MOUSE
40	Snx2 protein	Q91VZ1_MOUSE
41	Ubiquitin-like modifier-activating enzyme ATG7	A0A0A0MQN4_MOUSE
42	B5 domain-containing protein (Fragment)	Q3TG12_MOUSE (+1)
43	Proteoglycan 4	E0CZ58_MOUSE (+1)
44	Small nuclear ribonucleoprotein Sm D1	SMD1_MOUSE
45	Myb-binding protein 1A	MBB1A_MOUSE
46	Acid sphingomyelinase-like phosphodiesterase 3a	ASM3A_MOUSE
47	Splicing factor 3B subunit 1	G5E866_MOUSE (+1)
48	Low density lipoprotein receptor-related protein 1	A0A0R4J0I9_MOUSE (+1)
49	Glycerol-3-phosphate dehydrogenase 1-like protein	GPD1L_MOUSE
50	Ribosomal_S17_N domain-containing protein	Q9DB79_MOUSE (+1)
51	Cytochrome b5	CYB5_MOUSE (+1)
52	Lactoylglutathione lyase	LGUL_MOUSE
53	Phosphodiesterase	F7D3W5_MOUSE
54	Integrin beta-1	ITB1_MOUSE
55	LIM and SH3 domain protein 1	LASP1_MOUSE
56	Prolyl endopeptidase	PPCE_MOUSE
57	Dynactin subunit 2	DCTN2_MOUSE
58	3-ketoacyl-CoA thiolase A, peroxisomal	THIKA_MOUSE
59	S-adenosylmethionine synthase	A0A0U1RNK6_MOUSE [5]
60	ELAV-like protein	Q8BM84_MOUSE
61	Transformer-2 protein homolog beta	TRA2B_MOUSE
62	Leucine-rich repeat-containing protein 59	LRC59_MOUSE
63	60S ribosomal protein L21	Q9CQM8_MOUSE
64	IF rod domain-containing protein	Q3TFD9_MOUSE [3]
65	Antithrombin-III	ANT3_MOUSE
66	Protein transport protein Sec61 subunit beta	SC61B_MOUSE
67	Transcription elongation factor A protein 1	E9PYD5_MOUSE (+1)
68	Kininogen-1	A0A0R4J038_MOUSE [3]
69	Myoferlin	A0A286YDF5_MOUSE (+3)
70	Lambda-crystallin homolog	CRYL1_MOUSE
71	60S ribosomal protein L27	RL27_MOUSE
72	Predicted gene 7324	A0A2I3BRL8_MOUSE [2]
73	Aldolase_II domain-containing protein	Q8BJH2_MOUSE
74	Acid ceramidase	ASAH1_MOUSE (+1)

75	Creatine kinase B-type	KCRB_MOUSE
76	SUMO-activating enzyme subunit 1	SAE1_MOUSE
77	Coatomer subunit beta	COPB_MOUSE
78	Beta-2-glycoprotein 1	APOH_MOUSE (+1)
79	EH-domain containing 1	Q80ZZ0_MOUSE [2]
80	Methylthioribose-1-phosphate isomerase	MTNA_MOUSE
81	Endoplasmic reticulum aminopeptidase 1	ERAP1_MOUSE
82	Cytosolic endo-beta-N-acetylglucosaminidase	ENASE_MOUSE
83	High mobility group protein HMG-I/HMG-Y	A0A338P6F6_MOUSE (+2)
84	Adiponectin a	A0A3B0ITG8_MOUSE (+3)
85	DNA-(apurinic or apyrimidinic site) lyase	APEX1_MOUSE
86	Extracellular matrix protein 1	F8WI14_MOUSE (+1)
87	Prostacyclin synthase	PTGIS_MOUSE (+1)
88	Mast cell carboxypeptidase A	CBPA3_MOUSE
89	Ribosomal protein L7A	Q5EBG5_MOUSE (+3)
90	Oxysterol-binding protein 1	OSBP1_MOUSE
91	Protein PML	PML_MOUSE
92	Nuclear mitotic apparatus protein 1	NUMA1_MOUSE
93	Fc receptor, IgG, low affinity IIb	A0A0B4J1E6_MOUSE (+3)
94	Electron transfer flavoprotein subunit beta (Fragment)	A0A0U1RQB4_MOUSE
95	Apoptotic chromatin condensation inducer in the nucleus	ACINU_MOUSE [2]
96	Enoyl-CoA hydratase, mitochondrial	ECHM_MOUSE
97	Thyroid hormone receptor-associated protein 3	TR150_MOUSE
98	Chymase	A4QPC5_MOUSE (+1)
99	Inosine-5'-monophosphate dehydrogenase 2	IMDH2_MOUSE [3]
100	Succinate-CoA ligase subunit beta (Fragment)	Q3U6C7_MOUSE (+2)
101	40S ribosomal protein S28 (Fragment)	G3UYV7_MOUSE (+1)
102	Formin-binding protein 1	A2AQ41_MOUSE (+5)
103	Serine/threonine kinase 10	A1A553_MOUSE (+2)
104	Pyruvate dehydrogenase E1 component subunit beta, mitochondrial	ODPB_MOUSE
105	Prohibitin-2	PHB2_MOUSE
106	40S ribosomal protein S27 (Fragment)	A0A0G2JDW7_MOUSE (+1)
107	MKIAA4115 protein (Fragment)	Q571F9_MOUSE
108	Calcium-binding mitochondrial carrier protein Aralar1	CMC1_MOUSE
109	Guanylate-binding protein 4	GBP4_MOUSE [2]
110	Eukaryotic peptide chain release factor GTP-binding subunit ERF3A	ERF3A_MOUSE
111	SAPS domain family, member 1	B2RUA5_MOUSE (+1)

112	ATP synthase subunit gamma	A2AKU9_MOUSE (+3)
113	Rho GTPase-activating protein 25	RHG25_MOUSE
114	Tyrosine-protein phosphatase non-receptor type 1	PTN1_MOUSE (+1)
115	Pyridoxal kinase	PDXK_MOUSE
116	Vitamin D-binding protein	VTDB_MOUSE
117	Slk protein	A2RRK3_MOUSE
118	Ena/VASP-like protein	E9PVP4_MOUSE (+1)
119	FYN binding protein	B2RUR0_MOUSE
120	Splicing factor U2AF 35 kDa subunit	U2AF1_MOUSE
121	Phosphatidylinositide phosphatase SAC1	SAC1_MOUSE
122	NSFL1 cofactor p47	NSF1C_MOUSE (+2)
123	Adhesion G protein-coupled receptor E1	AGRE1_MOUSE (+1)
124	Integrin_alpha2 domain-containing protein	Q8CC06_MOUSE
125	Mast cell protease 4	Q3UN88_MOUSE
126	Septin 9	A2A6U3_MOUSE (+1)
127	40S ribosomal protein S26	RS26_MOUSE
128	Splicing factor 3A subunit 1	SF3A1_MOUSE
129	Fascin	FSCN1_MOUSE
130	Calcium/calmodulin-dependent protein kinase type II subunit gamma	KCC2G_MOUSE [5]
131	Progranulin	GRN_MOUSE (+12)
132	Rpl37a protein	Q5M9N6_MOUSE (+2)
133	Nucleolar protein 56	NOP56_MOUSE [2]
134	EF-hand domain-containing protein	Q3UF30_MOUSE (+1)
135	Cytoplasmic aconitate hydratase	ACOC_MOUSE (+1)
136	Splicing factor 1	D3YZC9_MOUSE (+5)
137	Treacle protein	H3BL37_MOUSE (+2)
138	Brain acid soluble protein 1	BASP1_MOUSE
139	Guanylate binding protein 1	A4UUI2_MOUSE
140	Epoxide hydrolase	E9PWK1_MOUSE (+1)
141	Tumor protein D52 (Fragment)	D3Z125_MOUSE (+4)
142	Cellular nucleic acid-binding protein	A0A0N4SVS6_MOUSE (+2)
143	Adiponectin b	A0A3B0INZ4_MOUSE (+1)
144	Plexin domain-containing protein 2	PXDC2_MOUSE
145	PDZ and LIM domain protein 5	PDLI5_MOUSE
146	WHEP-TRS domain-containing protein	Q3U6U7_MOUSE (+1)
147	CD5 antigen-like	CD5L_MOUSE
148	Ubiquitin carboxyl-terminal hydrolase isozyme L3	UCHL3_MOUSE
149	Microtubule-associated protein 4	MAP4_MOUSE
150	Calumenin	CALU_MOUSE
151	Carbonyl reductase [NADPH] 2	CBR2_MOUSE

152	Glutaminase kidney isoform, mitochondrial	GLSK_MOUSE
153	Steryl-sulfatase	STS_MOUSE
154	Amyloid-beta A4 protein	A0A2I3BPT1_MOUSE (+7)
155	Heparan-alpha-glucosaminide N-acetyltransferase	HGNAT_MOUSE
156	Proteasome subunit beta type-10	PSB10_MOUSE (+2)
157	Platelet glycoprotein 4	CD36_MOUSE (+4)
158	Poly [ADP-ribose] polymerase	Q3TF18_MOUSE (+5)
159	NADH-ubiquinone oxidoreductase 75 kDa subunit, mitochondrial	NDUS1_MOUSE (+2)
160	Histidine ammonia-lyase	HUTH_MOUSE (+1)
161	Dynactin subunit 1	D3YX34_MOUSE (+6)
162	WH2 domain-containing protein	Q3T9Z7_MOUSE
163	Macrophage mannose receptor 1	MRC1_MOUSE
164	Guanylate-binding protein 2	GBP2_MOUSE
165	Prelamin-A/C	LMNA_MOUSE
166	60S ribosomal protein L23	RL23_MOUSE
167	H-2 class II histocompatibility antigen, I-A beta chain (Fragment)	A0A498U6I0_MOUSE (+3)
168	Constitutive coactivator of PPAR-gamma-like protein 1	F120A_MOUSE
169	Switch-associated protein 70	SWP70_MOUSE
170	Complement factor H (Fragment)	A0A0A6YWP4_MOUSE (+3)
171	Histone H1.0	H10_MOUSE (+2)
172	Bcl-2-associated transcription factor 1	A0A087WQA0_MOUSE (+4)
173	28 kDa heat- and acid-stable phosphoprotein	HAP28_MOUSE (+1)
174	MCG113838	A0A2I3BPG9_MOUSE (+1)
175	Beta-2-microglobulin	B2MG_MOUSE (+1)
176	Alpha-1B-glycoprotein	A1BG_MOUSE
177	Legumain	LGMN_MOUSE (+1)
178	ATP-binding cassette sub-family A member 9	ABCA9_MOUSE
179	Tubulin polymerization-promoting protein family member 3	TPPP3_MOUSE
180	Naglu	O54752_MOUSE (+1)
181	DnaJ homolog subfamily C member 7	DNJC7_MOUSE (+1)
182	Coiled-coil domain-containing protein 50	CCD50_MOUSE [2]
183	Tumor protein D54	A2AUD5_MOUSE (+6)
184	Phosphoenolpyruvate carboxykinase [GTP], mitochondrial	A0A0R4J0G0_MOUSE (+7)
185	Programmed cell death protein 4	PDCD4_MOUSE
186	Shootin-1	SHOT1_MOUSE

Analysis of LSH unique proteins

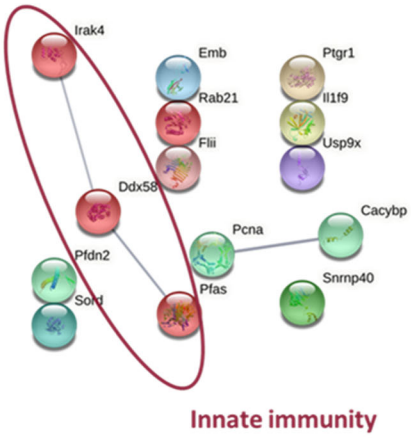

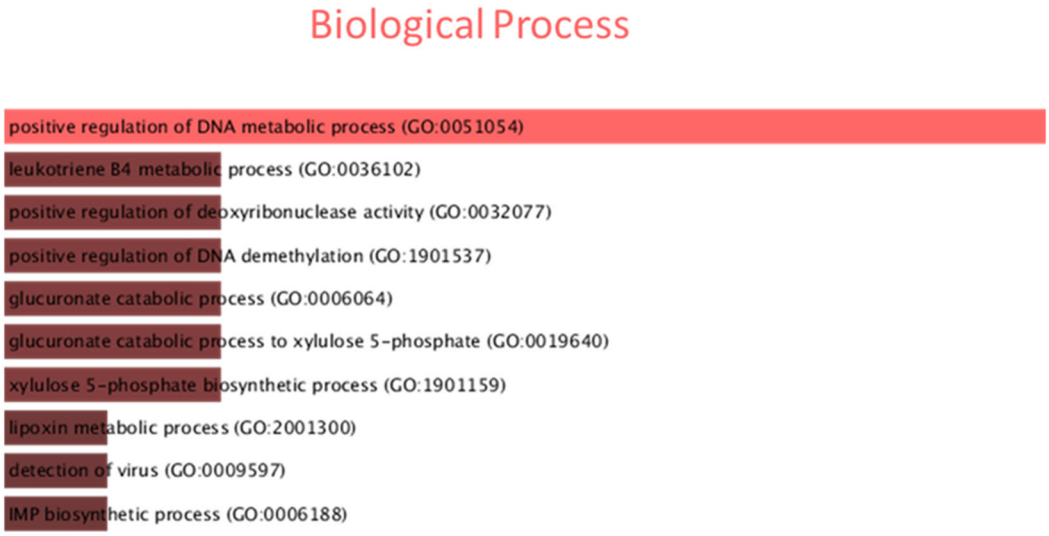

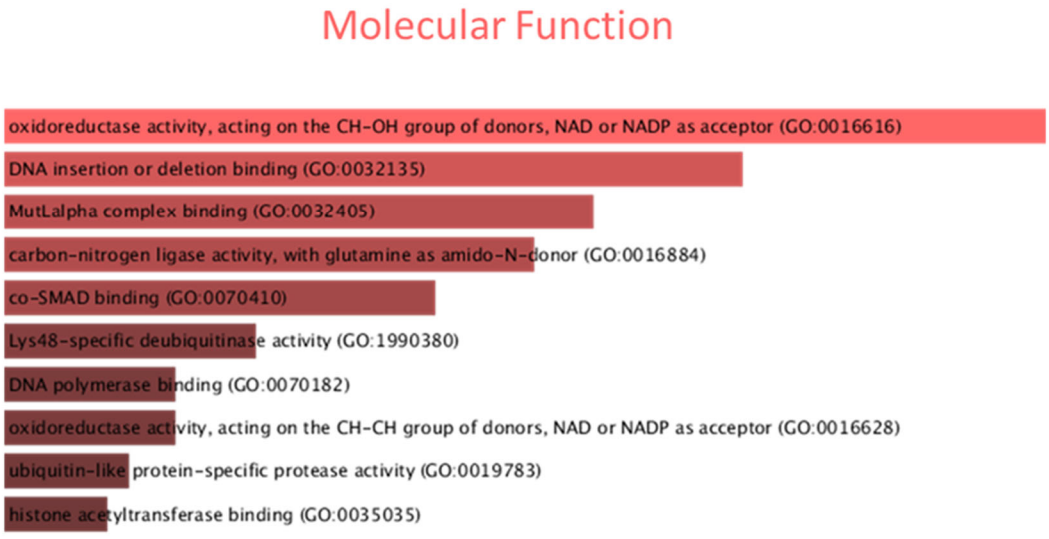

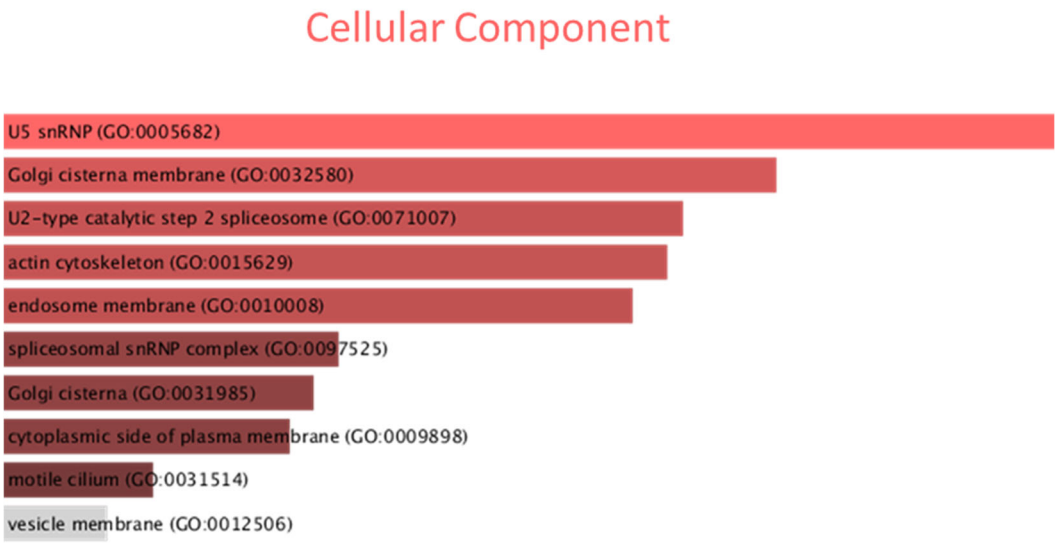

Figure 16: String and gene ontology analysis of unique proteins obtained from L. major (LSH) infected mice. Top: Protein network analysis of unique LSH proteins (15). Analysis was performed using STRING v11.5. Circles represent groups of proteins in the same cluster and their shared functions. Clustering was done using MCL Level 3 clustering. Bottom: gene ontology analysis of LSH unique proteins shows three figures of top 10 functions for Biological Process, Molecular Function, and Cellular Component.

Analysis of EXL unique proteins

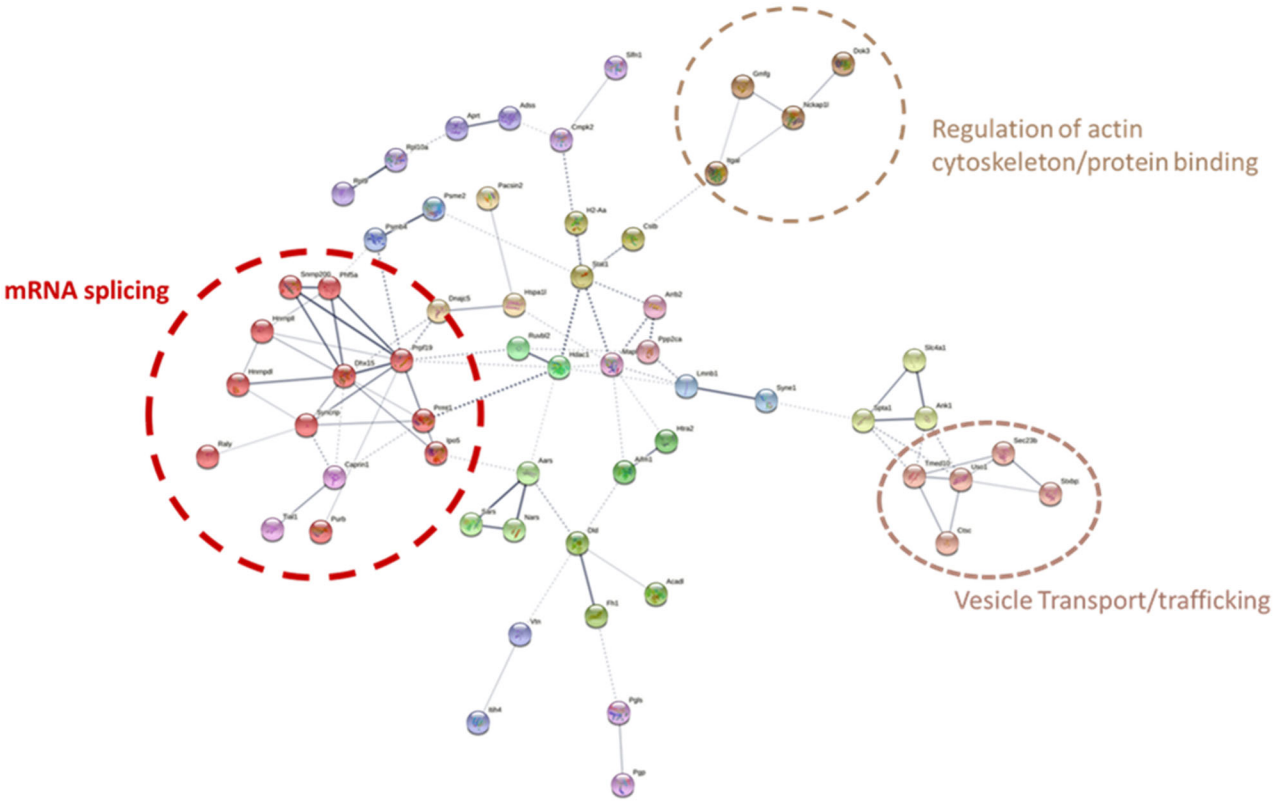

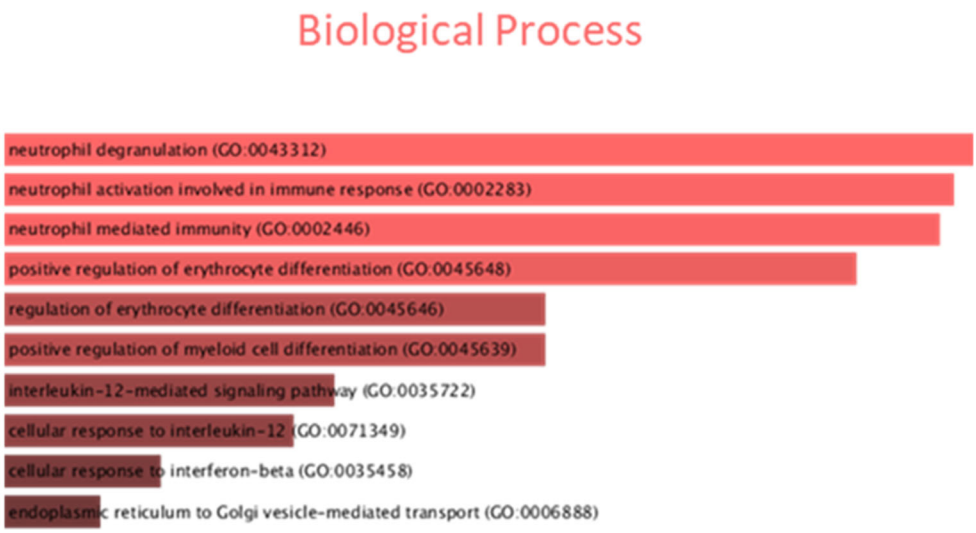

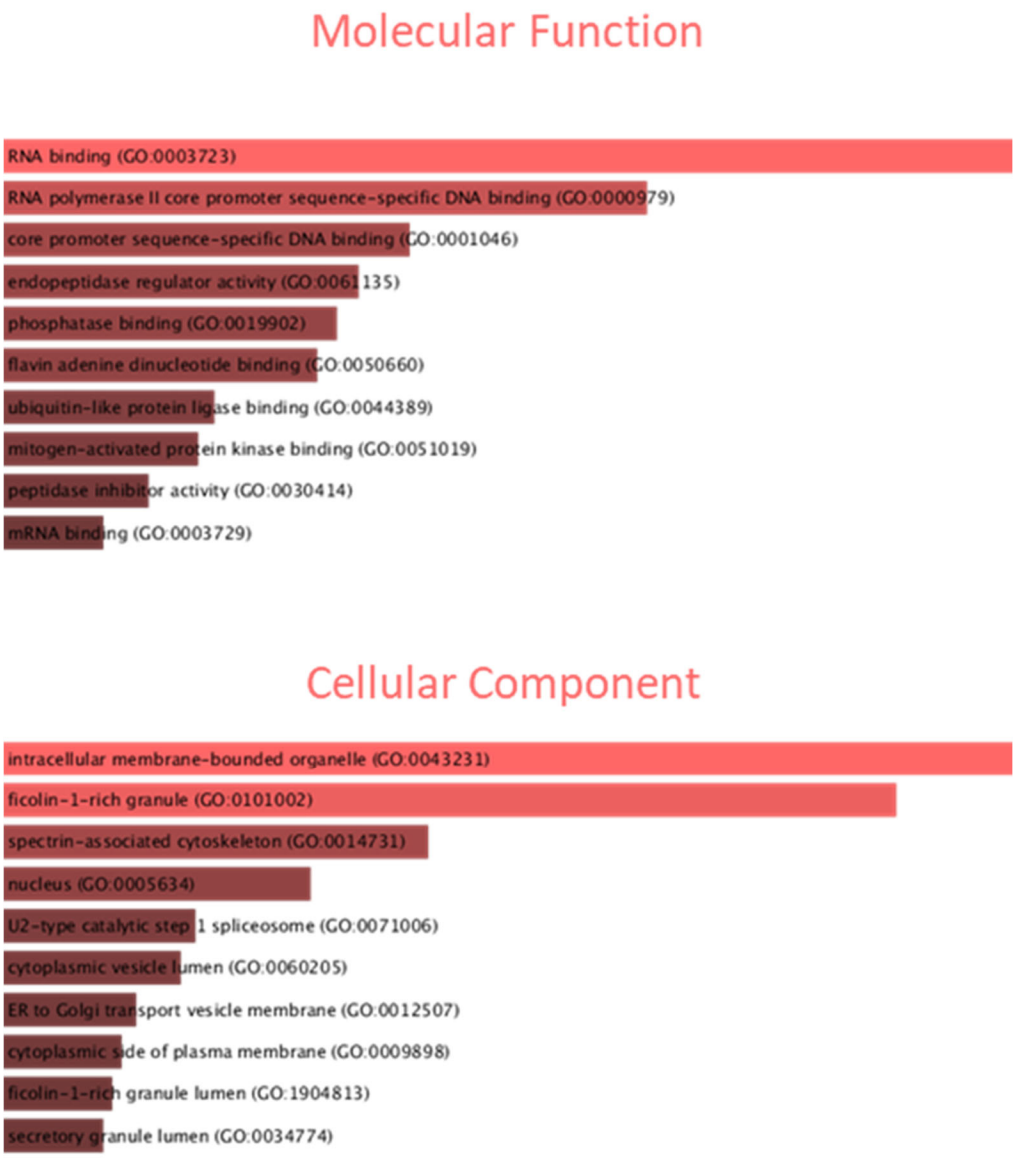

Figure 17: String and gene ontology analysis of unique proteins obtained from L. major + exosome co-inoculation (EXL) mice.
Top: Protein network analysis of unique proteins (76) obtained from *L. major* + exosomes co-inoculation. Analysis was performed using STRING v11.5. Circles represent groups of proteins in the same cluster and their shared functions. Clustering was done using MCL Level 3 clustering. Bottom: Gene Ontology analysis of EXL unique proteins shows three figures of top 10 functions for Biological Process, Molecular Function, and Cellular Component.

To identify differential protein expression due to signaling events initiated by exosomes interacting with FPR2, we compared the proteomic profile of AGO group to LSH and EXL. Most proteins were shared between the three groups (455 proteins), yet AGO and EXL had 72 and 54 unique proteins, respectively, compared to LSH, which had only 18 unique proteins (Figure 18). Like our previous observation, global characterization of GO functions based on biological process and molecular function does not show differentially regulated GO functions. To add, clustering of proteins in the protein interaction network differs in AGO from the other two groups in the size of the largest clusters and identities of smaller clusters (Figure 19).

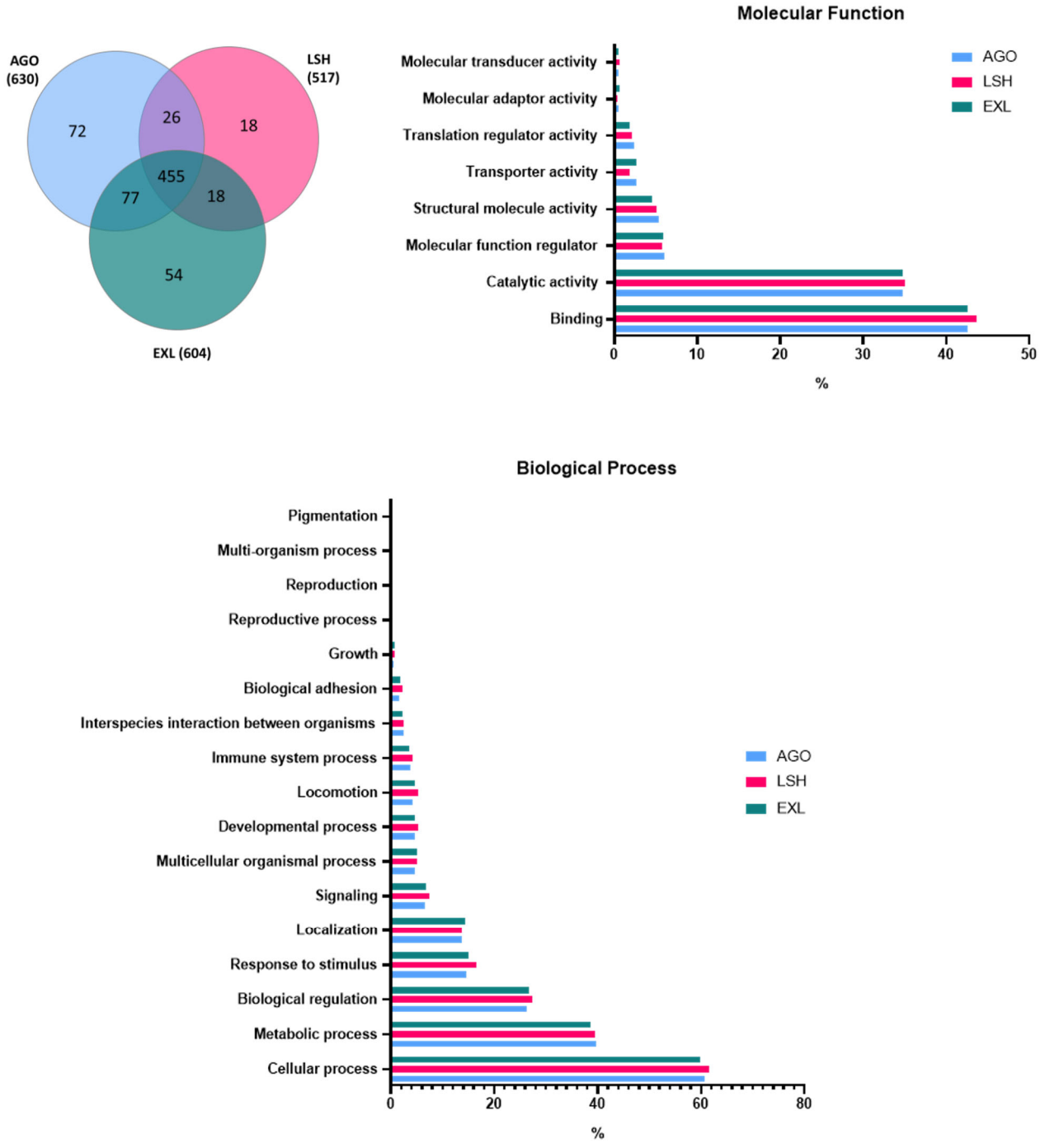

Figure 18: Proteomics analysis of proteins obtained from L. major (LSH), L. major + agonist (AGO), and L. major + exosome (EXL) peritoneal co-inoculation in mice. A) Venn diagram of total proteins identified in LSH, EXL, and AGO, B) Top GO Molecular Function terms, and C) Top GO Biological process terms for proteins identified in the three groups.

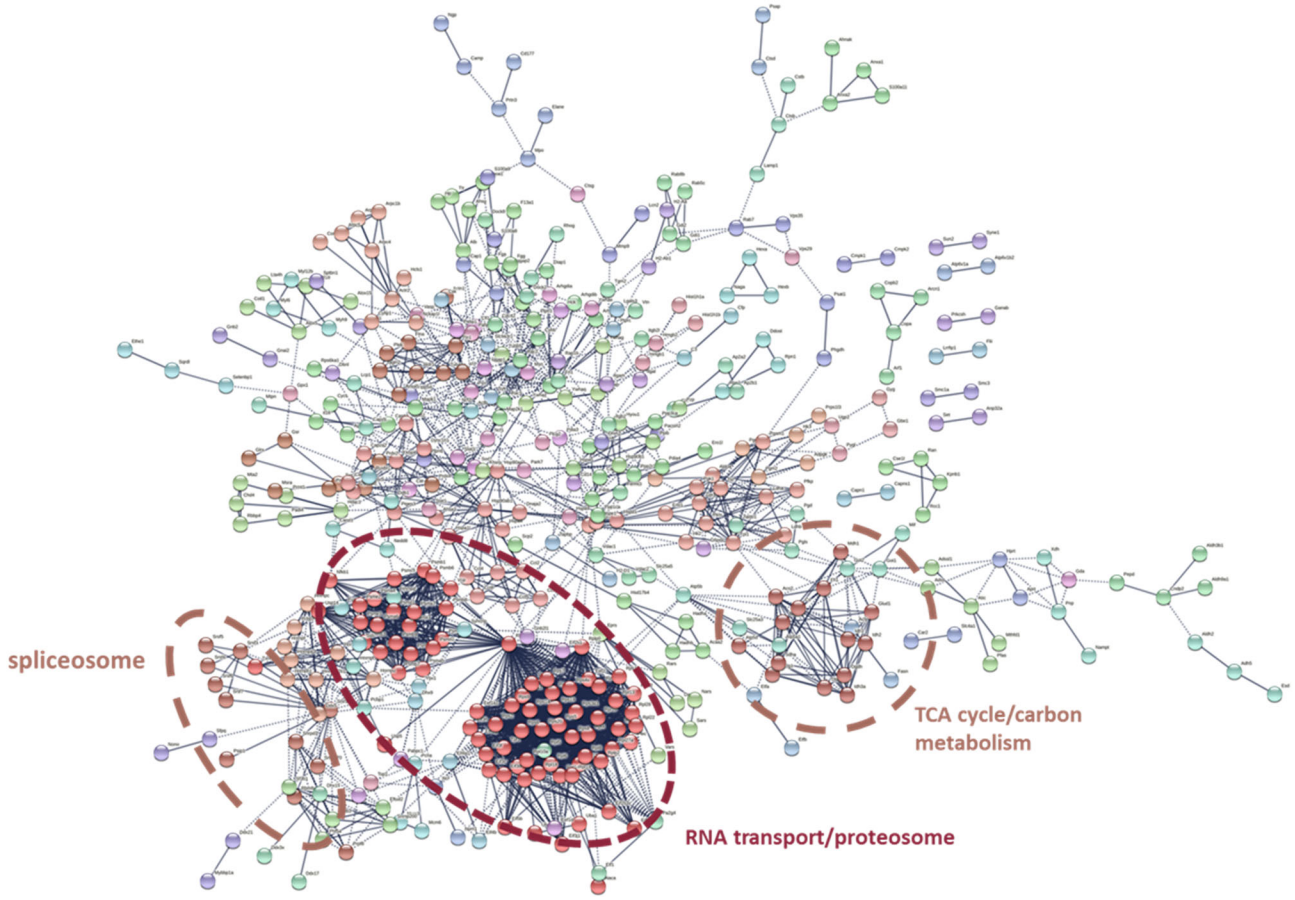

Figure 19: String protein network analysis of total proteins obtained from L. major + agonist (AGO) co-inoculation in mice Analysis was performed using STRING v11.5. Circles represent proteins in the same cluster and their shared functions. Clustering was done using MCL Level 3 clustering.

Unique proteins in AGO formed clusters for transcription and translation, proteosome, membrane vesicle trafficking, and immune cell signaling. GO analysis of unique AGO proteins showed enrichment for neutrophil function, degranulation, and activation in the biological processes. The molecular function of these proteins was mainly in binding protein kinases and RNA (Figure 20). These findings indicate AGO uniquely regulates innate immune function by upregulating proteins differently from LSH and EXL, which could be explained by the potency of FPR2 agonist in activating the receptor compared to exosomes.

Analysis of AGO unique proteins

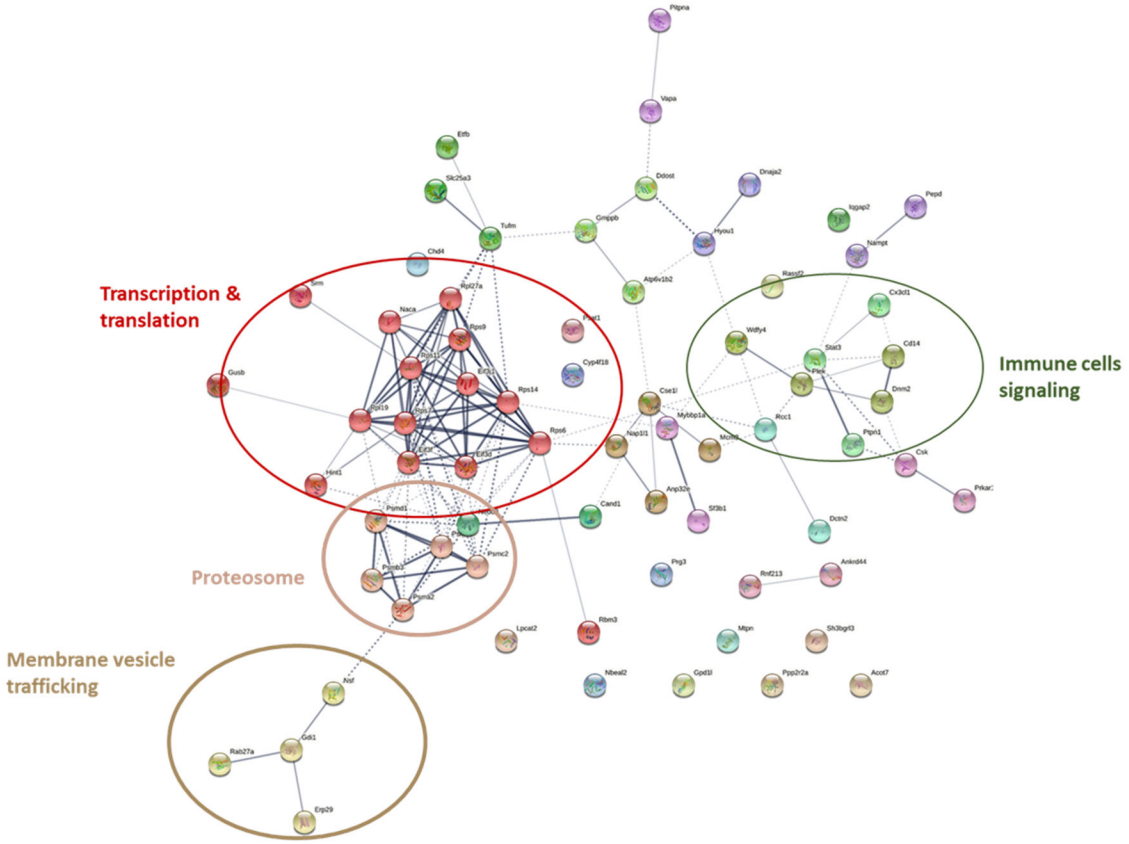

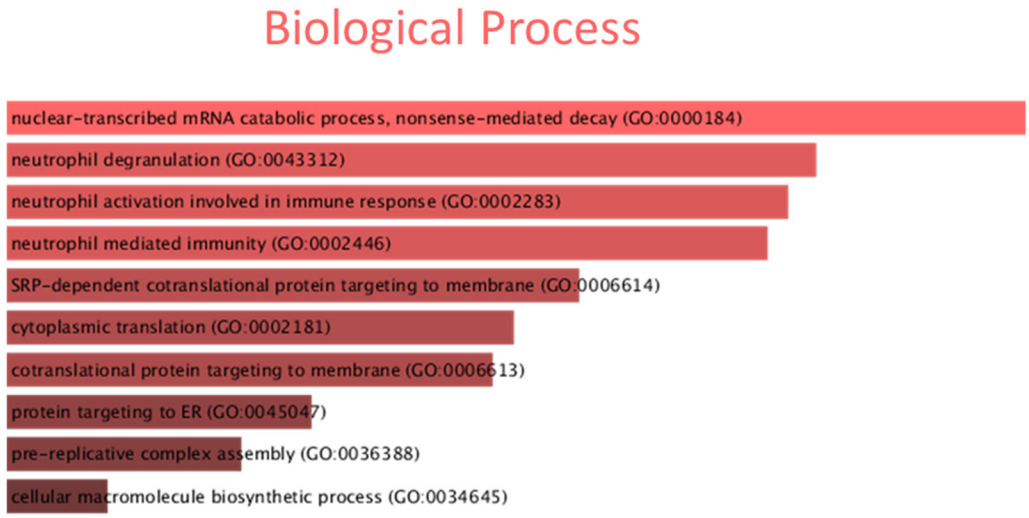

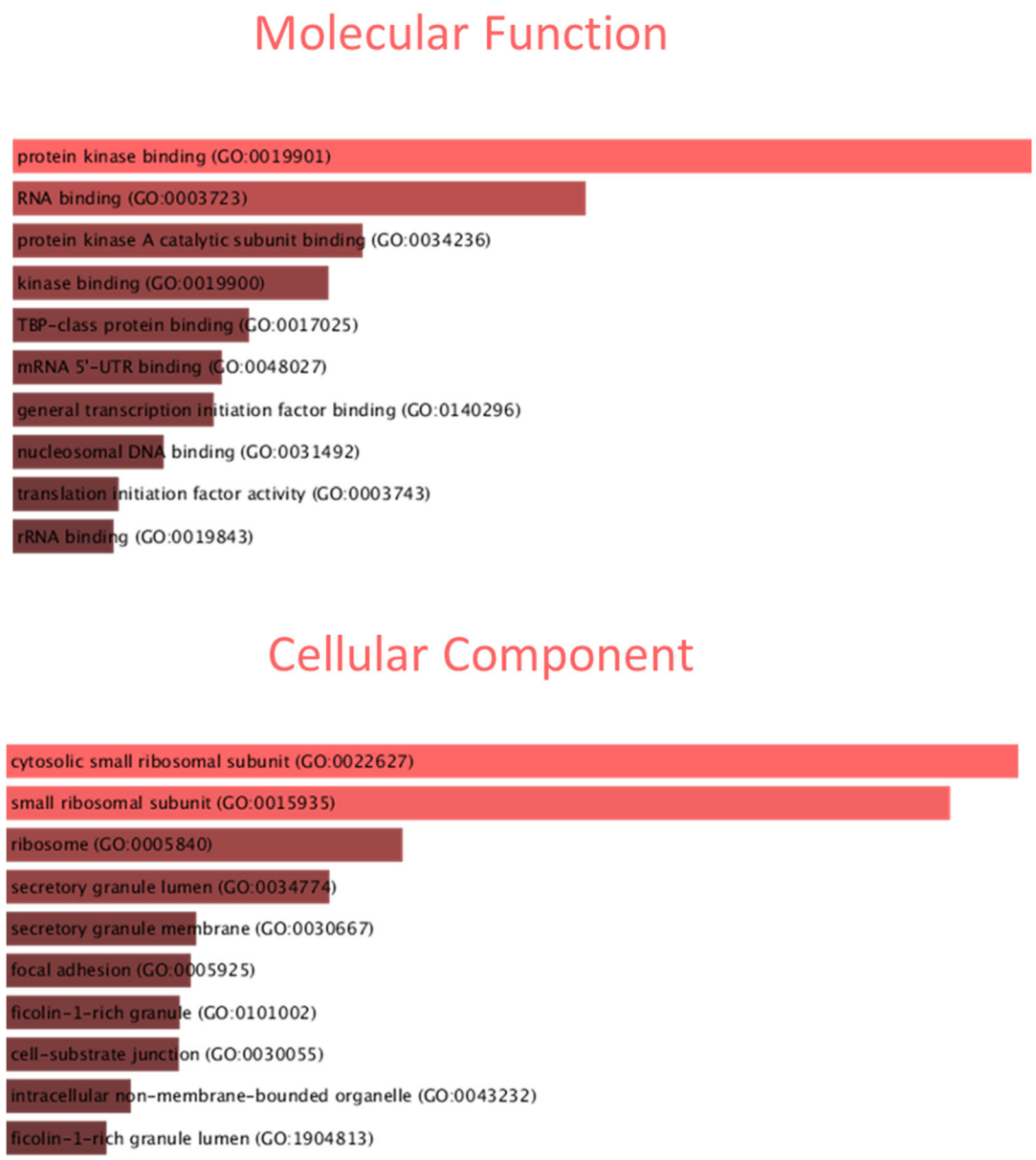

Figure 20: String and gene ontology analysis of unique proteins obtained from L. major + agonist (AGO) co-inoculation Top*:* Protein network analysis of unique AGO proteins (72). Analysis was performed using STRING v11.5. Circles represent groups of proteins in the same cluster and their shared functions. Clustering was done using MCL Level 3 clustering. Bottom: Gene Ontology analysis of AGO unique proteins shows three figures with top 10 functions for Biological Process, Molecular Function, and Cellular Component

Due to the small number of unique proteins in LSH group, protein network analysis did not show any clustering. Yet, top biological process GO terms associated with the 18 unique proteins in LSH group were "stress fiber assembly" and "contractile actin filament bundle assembly" (Figure 21). Table 2 lists unique LSH proteins and their functions obtained from Uniprot.

Analysis of LSH unique proteins

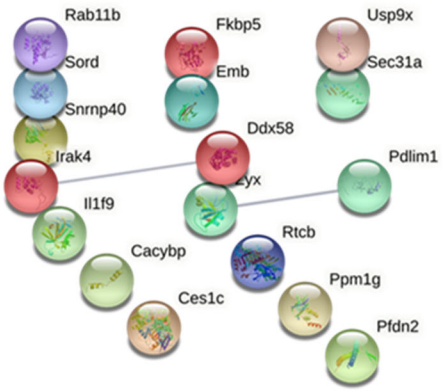

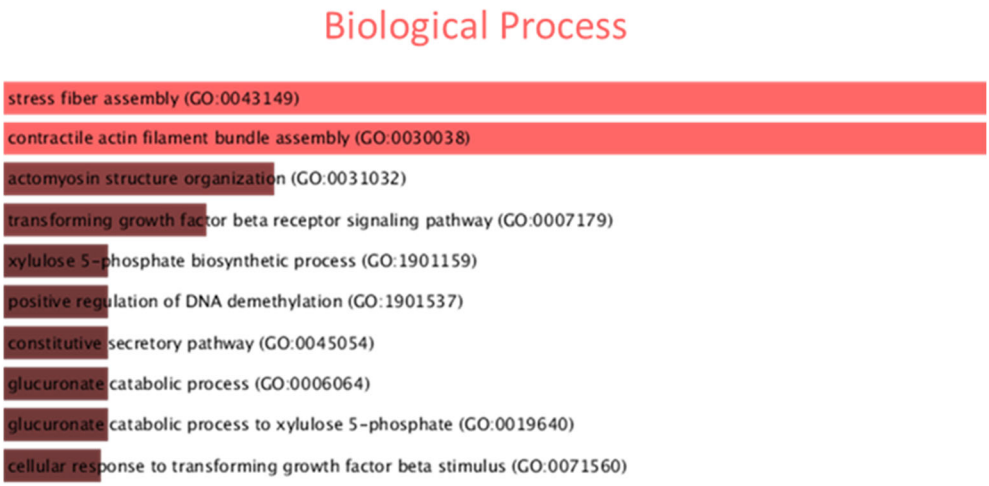

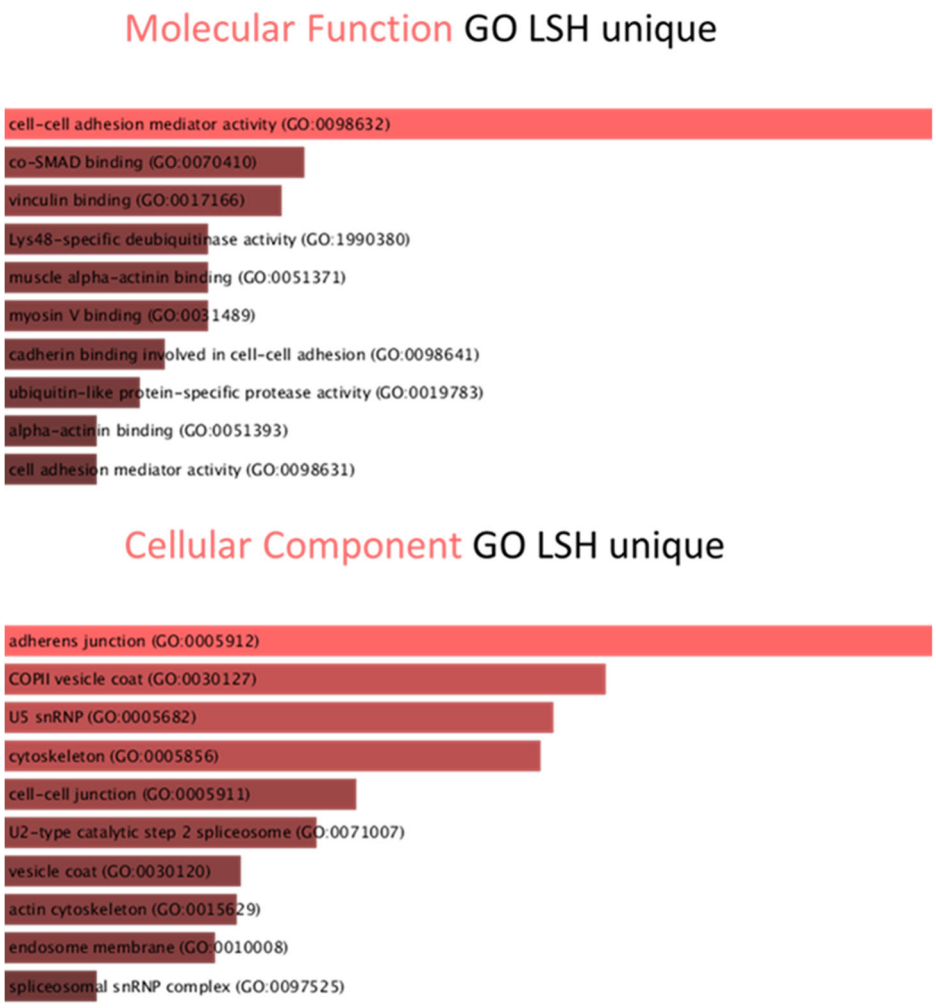

Figure 21: String and Gene Ontology analysis of unique proteins obtained from L. major (LSH) infection in mice. Top left: Protein network analysis of unique LSH proteins (18). Analysis was performed using STRING v11.5. Circles represent proteins in the same cluster and their shared functions. Clustering was done using MCL Level 3 clustering. Bottom and top right: Gene Ontology analysis of LSH unique proteins shows three figures with top 10 functions for Biological Process, Molecular Function, and Cellular Component.

Table 2: List of unique proteins obtained from L. major (LSH) infected mice.

#	ID	Protein names	Function
1	O70591	Prefoldin subunit 2	Binds specifically to cytosolic chaperonin (c-CPN) and transfers target proteins to it
2	Q3TJ01	RNA-splicing ligase RtcB homolog	Catalytic subunit of the tRNA-splicing ligase complex that acts by directly joining spliced tRNA halves to mature-sized tRNAs by incorporating the precursor-derived splice junction phosphate into the mature tRNA as a canonical 3',5'-phosphodiester
3	Q3UPL0	Protein transport protein Sec31A	Component of the coat protein complex II (COPII) which promotes the formation of transport vesicles from the endoplasmic reticulum (ER) (By similarity)
4	O70400	PDZ and LIM domain protein 1	Cytoskeletal protein that may act as an adapter that brings other proteins (like kinases) to the cytoskeleton (By similarity)
5	Q8R460	Interleukin-36 gamma	Functions as an agonist of NF-kappa B activation through the orphan IL-1-receptor-related protein 2/IL1RL2
6	P23953	Carboxylesterase 1C	Involved in the detoxification of xenobiotics and in the activation of ester and amide prodrugs
7	Q9CXW3	Calcyclin-binding protein	May be involved in calcium-dependent ubiquitination and subsequent proteasomal degradation of target proteins
8	P21995	Embigin	Plays a role in targeting the monocarboxylate transporters SLC16A1 and SLC16A7 to the cell membrane (By similarity)
9	Q64442	Sorbitol dehydrogenase	Polyol dehydrogenase that catalyzes the reversible NAD(+)-dependent oxidation of various sugar alcohols (By similarity)
10	Q6PE01	U5 small nuclear ribonucleoprotein 40 kDa protein	Required for pre-mRNA splicing as component of the activated spliceosome
11	Q3USX5	Interleukin-1 receptor-associated kinase 4	Serine/threonine-protein kinase that plays a critical role in initiating innate immune response against foreign pathogens
12	A0A068BFR3	RAS oncogene family protein	Regulation of endocytic recycling
13	Q7TQE2	Zyx protein	Could modulate cytoskeletal reorganization
14	Q4FE56	Ubiquitinyl hydrolase 1	Thiol-dependent hydrolysis of ester, thioester, amide, peptide and isopeptide bonds formed by the C-terminal Gly of ubiquitin

15	A1L0V6	RNA helicase (fragment)	Rearrange RNA secondary structure
16	A0A0J9YVG0	Protein phosphatase 1G	Negative regulator of cell stress response pathway
17	Q8R3H6	Ighg protein	N/A
18	Q3TX72	Peptidylprolyl isomerase	N/A

On the other hand, proteins found in EXL only are assumed to be expressed uniquely due to the presence of exosomes, however, not through FPR2 activation. These proteins formed multiple unique clusters in the protein network analysis (Figure 22). Clusters included vesicle transport and cell cytoskeleton, microtubule-associated proteins, signal transduction, post-transcriptional regulation in immune cells. Top GO terms associated with these proteins indicated their role in vesicle-mediated transport from the endoplasmic reticulum to Golgi apparatus, intracellular protein transport, RNA binding, and mRNA binding. A list of unique EXL proteins and their functions is shown in Table 3.

Analysis of EXL unique proteins

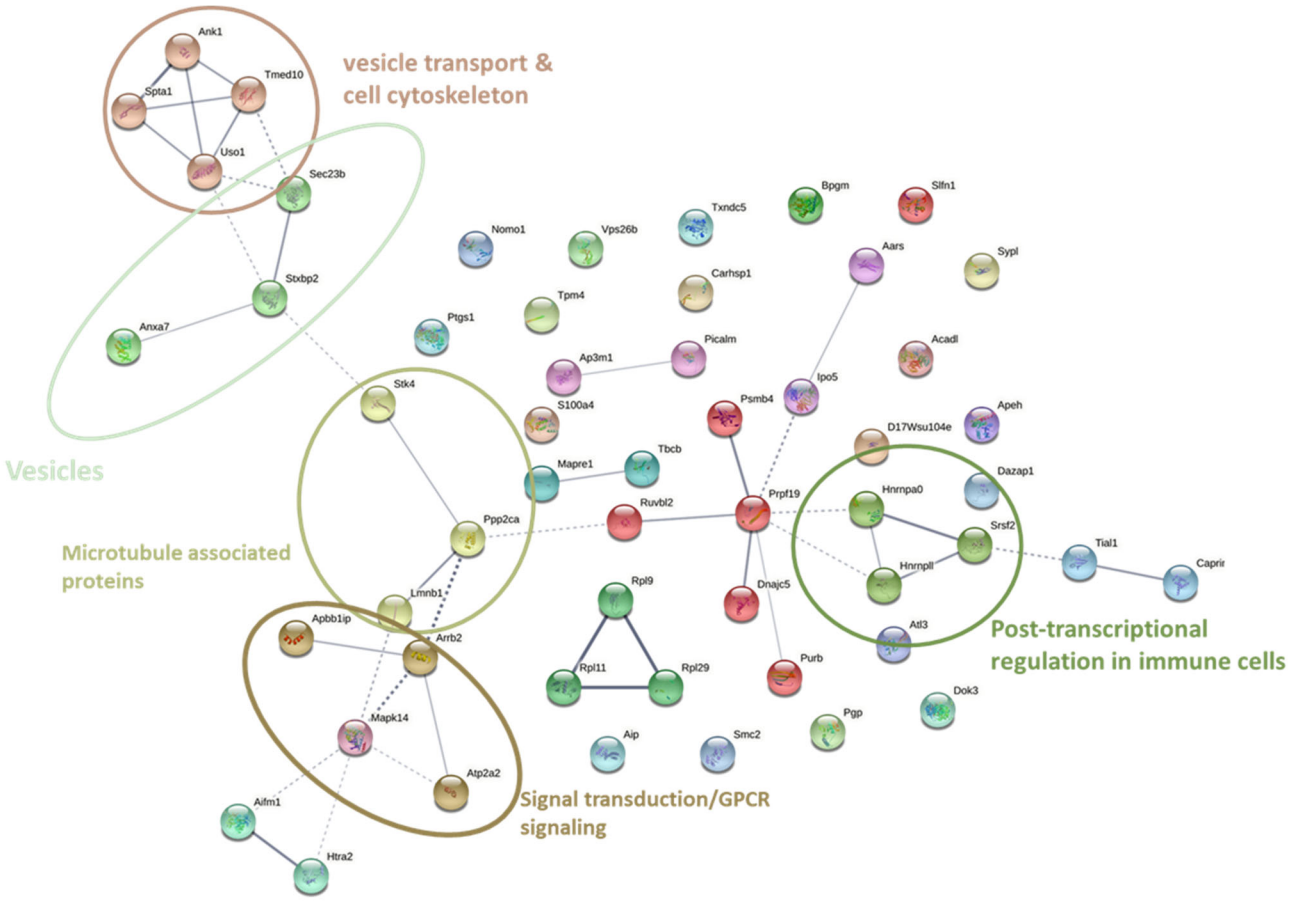

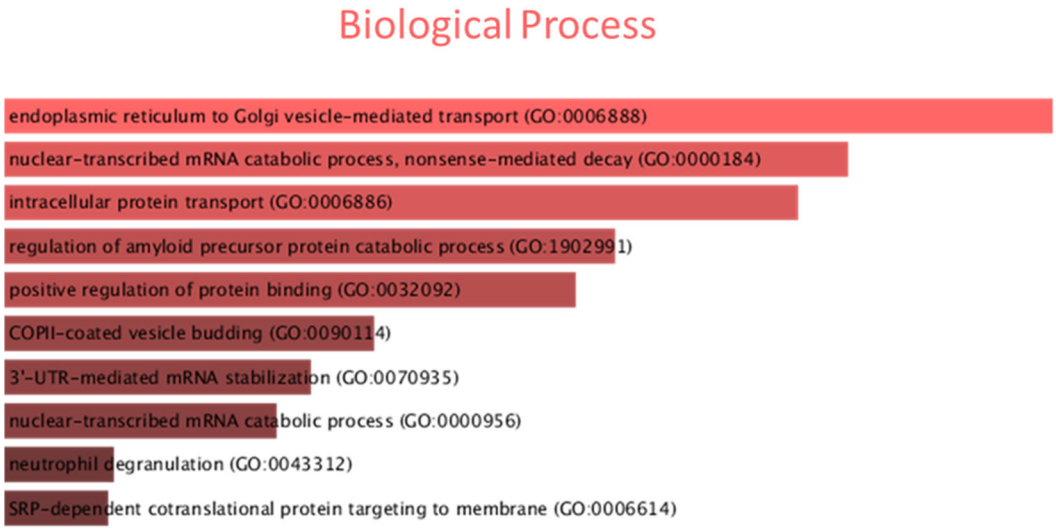

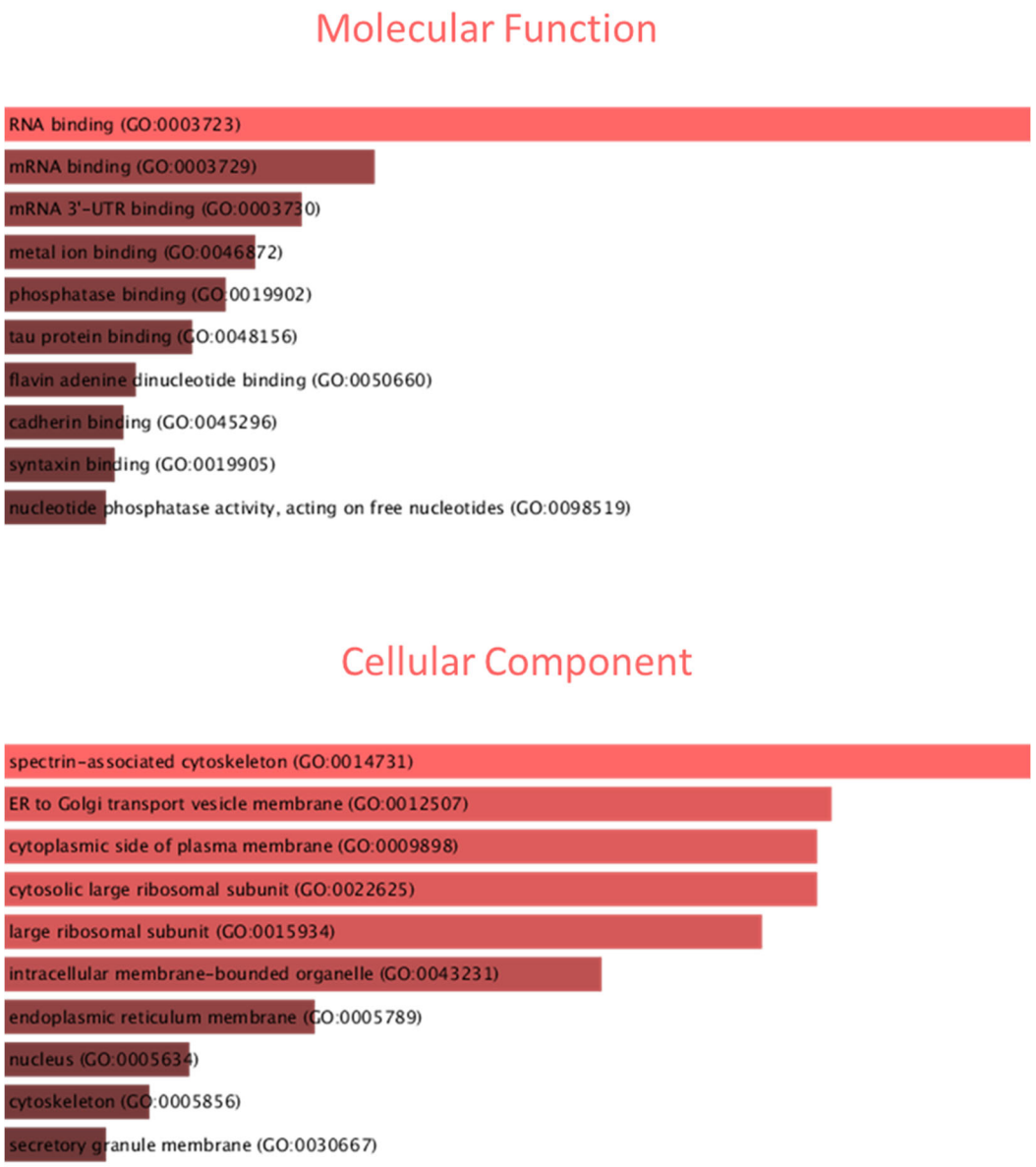

Figure 22: String and Gene Ontology analysis of unique proteins obtained from L. major + exosome co-inoculation (EXL) mice. Top: Protein network analysis of unique EXL proteins (54). Analysis was performed using STRING v11.5. Circles represent groups of proteins in the same cluster and their shared functions. Clustering was done using MCL Level 3 clustering. Bottom: Gene Ontology analysis of EXL unique proteins shows three figures with top 10 functions for Biological Process, Molecular Function, and Cellular Component.

Table 3: A list of unique proteins obtained from L. major + exosome co-inoculation in mice and their functions

#	ID	Protein names	Function
1	Q99KP6	Pre-mRNA-processing factor 19	[Isoform 1]: Ubiquitin-protein ligase which is a core component of several complexes mainly involved in pre-mRNA splicing and DNA repair
2	Q8C0E2	Vacuolar protein sorting-associated protein 26B	Acts as component of the retromer cargo-selective complex (CSC) (PubMed:21040701, PubMed:21920005)
3	Q8R5A3	Amyloid beta A4 precursor protein-binding family B member 1-interacting protein	Appears to function in the signal transduction from Ras activation to actin cytoskeletal remodeling
4	Q9CR86	Calcium-regulated heat stable protein 1	Binds mRNA and regulates the stability of target mRNA
5	Q6IRU2	Tropomyosin alpha-4 chain	Binds to actin filaments in muscle and non-muscle cells
6	Q9D1E6	Tubulin-folding cofactor B	Binds to alpha-tubulin folding intermediates after their interaction with cytosolic chaperonin in the pathway leading from newly synthesized tubulin to properly folded heterodimer (By similarity)
7	Q9CPT4	Myeloid-derived growth factor	Bone marrow-derived monocyte and paracrine-acting protein that promotes cardiac myocyte survival and adaptive angiogenesis for cardiac protection and/or repair after myocardial infarction (MI)
8	Q9D1D4	Transmembrane emp24 domain-containing protein 10	Cargo receptor involved in protein vesicular trafficking and quality control in the endoplasmic reticulum (ER) and Golgi

9	Q3TZ32	Alanine--tRNA ligase	Catalyzes the attachment of alanine to tRNA(Ala) in a two-step reaction: alanine is first activated by ATP to form Ala-AMP and then transferred to the acceptor end of tRNA(Ala)
10	Q6GQT9	Nodal modulator 1	Component of a ribosome-associated endoplasmic reticulum (ER) translocon complex involved in multi-pass membrane protein transport into the ER membrane and biogenesis (By similarity)
11	Q3TIS3	Protein transport protein SEC23	Component of the coat protein complex II (COPII) which promotes the formation of transport vesicles from the endoplasmic reticulum (ER)
12	P47915	60S ribosomal protein L29	Component of the large ribosomal subunit
13	Q7M6Y3	Phosphatidylinositol-binding clathrin assembly protein	Cytoplasmic adapter protein that plays a critical role in clathrin-mediated endocytosis which is important in processes such as internalization of cell receptors, synaptic transmission or removal of apoptotic cells
14	Q9QZK7	Docking protein 3	DOK proteins are enzymatically inert adaptor or scaffolding proteins
15	P22437	Prostaglandin G/H synthase 1	Dual cyclooxygenase and peroxidase in the biosynthesis pathway of prostanoids, a class of C20 oxylipins mainly derived from arachidonate, with a particular role in the inflammatory response
16	Q9Z0X1	Apoptosis-inducing factor 1, mitochondrial	Functions both as NADH oxidoreductase and as regulator of apoptosis (By similarity)
17	Q8BKC5	Importin-5	Functions in nuclear protein import as nuclear transport receptor
18	Q91YI4	Beta-arrestin-2	Functions in regulating agonist-mediated G-protein coupled receptor (GPCR) signaling by mediating both receptor

			desensitization and resensitization processes
19	Q9Z1Z0	General vesicular transport factor p115	General vesicular transport factor required for intercisternal transport in the Golgi stack; it is required for transcytotic fusion and/or subsequent binding of the vesicles to the target membrane
20	Q8CHP8	Glycerol-3-phosphate phosphatase	Glycerol-3-phosphate phosphatase hydrolyzing glycerol-3-phosphate into glycerol
21	Q91YH5	Atlastin-3	GTPase tethering membranes through formation of trans-homooligomers and mediating homotypic fusion of endoplasmic reticulum membranes
22	O35295	Transcriptional activator protein Pur-beta	Has capacity to bind repeated elements in single-stranded DNA such as the purine-rich single strand of the PUR element located upstream of the MYC gene
23	P14733	Lamin-B1	Lamins are components of the nuclear lamina, a fibrous layer on the nucleoplasmic side of the inner nuclear membrane, which is thought to provide a framework for the nuclear envelope and may also interact with chromatin
24	O08915	AH receptor-interacting protein	May play a positive role in AHR-mediated (aromatic hydrocarbon receptor) signaling, possibly by influencing its receptivity for ligand and/or its nuclear targeting
25	Q60865	Caprin-1	May regulate the transport and translation of mRNAs of proteins involved in synaptic plasticity in neurons and cell proliferation and migration in multiple cell types (PubMed:20516077)
26	Q9CX86	Heterogeneous nuclear ribonucleoprotein A0	mRNA-binding component of ribonucleosomes
27	P99026	Proteasome subunit beta type-4	Non-catalytic component of the 20S core proteasome complex involved in the proteolytic

			degradation of most intracellular proteins
28	Q9JKC8	AP-3 complex subunit mu-1	Part of the AP-3 complex, an adaptor-related complex which is not clathrin-associated
29	P15327	Bisphosphoglycerate mutase	Plays a major role in regulating hemoglobin oxygen affinity by controlling the levels of its allosteric effector 2,3-bisphosphoglycerate (2,3-BPG)
30	Q61166	Microtubule-associated protein RP/EB family member 1	Plus-end tracking protein (+TIP) that binds to the plus-end of microtubules and regulates the dynamics of the microtubule cytoskeleton
31	P63330	Serine/threonine-protein phosphatase 2A catalytic subunit alpha isoform	PP2A is the major phosphatase for microtubule-associated proteins (MAPs)
32	Q3UXP2	RuvB-like helicase	Proposed core component of the chromatin remodeling Ino80 complex which exhibits DNA- and nucleosome-activated ATPase activity and catalyzes ATP-dependent nucleosome sliding
33	Q921F4	Heterogeneous nuclear ribonucleoprotein L-like	RNA-binding protein that functions as regulator of alternative splicing for multiple target mRNAs, including PTPRC/CD45 and STAT5A
34	Q9JII5	DAZ-associated protein 1	RNA-binding protein, which may be required during spermatogenesis
35	P47811	Mitogen-activated protein kinase 14	Serine/threonine kinase which acts as an essential component of the MAP kinase signal transduction pathway
36	P08032	Spectrin alpha chain, erythrocytic 1	Spectrin is the major constituent of the cytoskeletal network underlying the erythrocyte plasma membrane
37	Q9JI11	Serine/threonine-protein kinase 4	Stress-activated, pro-apoptotic kinase which, following caspase-cleavage, enters the nucleus and induces chromatin condensation

			followed by internucleosomal DNA fragmentation
38	Q8VC94	60S ribosomal protein L11	Component of the ribosome
39	Q5DTI2	P-type Ca(2+) transporter	A p-type ATPase functions to transport calcium from the cytoplasm to the sarcoplasmic reticulum
40	A0A0R4J083	Long-chain specific acyl-CoA dehydrogenase, mitochondrial	catalyzes the first step of mitochondrial fatty acid beta-oxidation. A process that breaks down lipids to acetyle-coA
41	Q8C671	Serine/arginine-rich splicing factor 2	N/A
42	A0A0R4J1N7	Ankyrin-1	Found in Red blood cells, brain cells, and muscles. Plays a role in maintaining cellular stability and movement
43	P51410	60S ribosomal protein L9	A component of the ribosomes, resposnbile for protein synthesis.
44	A0A0R4J107	Acyl-peptide hydrolase	May play a role in destroying oxidatively damaged proteins in cells
45	A0A0G2JGD2	Protein S100-A4 (Fragment)	Involved in various cellular processes including motility, angiogenesis, cell differentiation, apoptosis, and autophagy
46	A0A0R4J1Y7	Thioredoxin domain-containing protein 5	Possesses thioredoxin activity. Has been shown to reduce insulin disulfide bonds
47	Q9Z0I7	Schlafen 1	Induces growth arrest in some cells types.
48	Q3ULS2	Structural maintenance of chromosomes protein	Involved in cell cycle regulation
49	A0A2C9F2D2	Annexin 7	A member of the annexin family which can function as scaffolding proteins to anchor other proteins to the cell membrane
50	A2AUE1	DnaJ homolog subfamily C member 5 (Fragment)	N/A
51	Q3TVX7	MARVEL domain-containing protein	Microtubule-associated protein that exhibits cell cycle-dependent localization and can inhibit cell proliferation and migration

52	F8WGM5	Syntaxin-binding protein 2 (Fragment)	Involved in intracellular vesicle trafficking and vesicle fusion with membranes
53	D3YX27	Serine protease HTRA2, mitochondrial	Promotes cell death
54	Q921W2	Nucleolysin TIAR	RNA binding protein, may be involved in apoptosis

Furthermore, despite AGO and EXL groups having unique proteins, 77 proteins were exclusively shared between the two groups. We expect uniquely shared proteins in AGO and EXL to provide an insight into potential pathways upregulated when exosomes interact with FPR2. Hence, we identified 77 shared proteins and performed protein network analysis and GO analysis (Figure 23). Protein clusters of interest functioned in actin cytoskeleton regulation, immune system regulation, protein synthesis, methylation and histone deacetylation, and protein synthesis. To add, neutrophil-related terms ranked in top 10 enriched terms in GO biological processes.

Analysis of shared EXL-AGO proteins

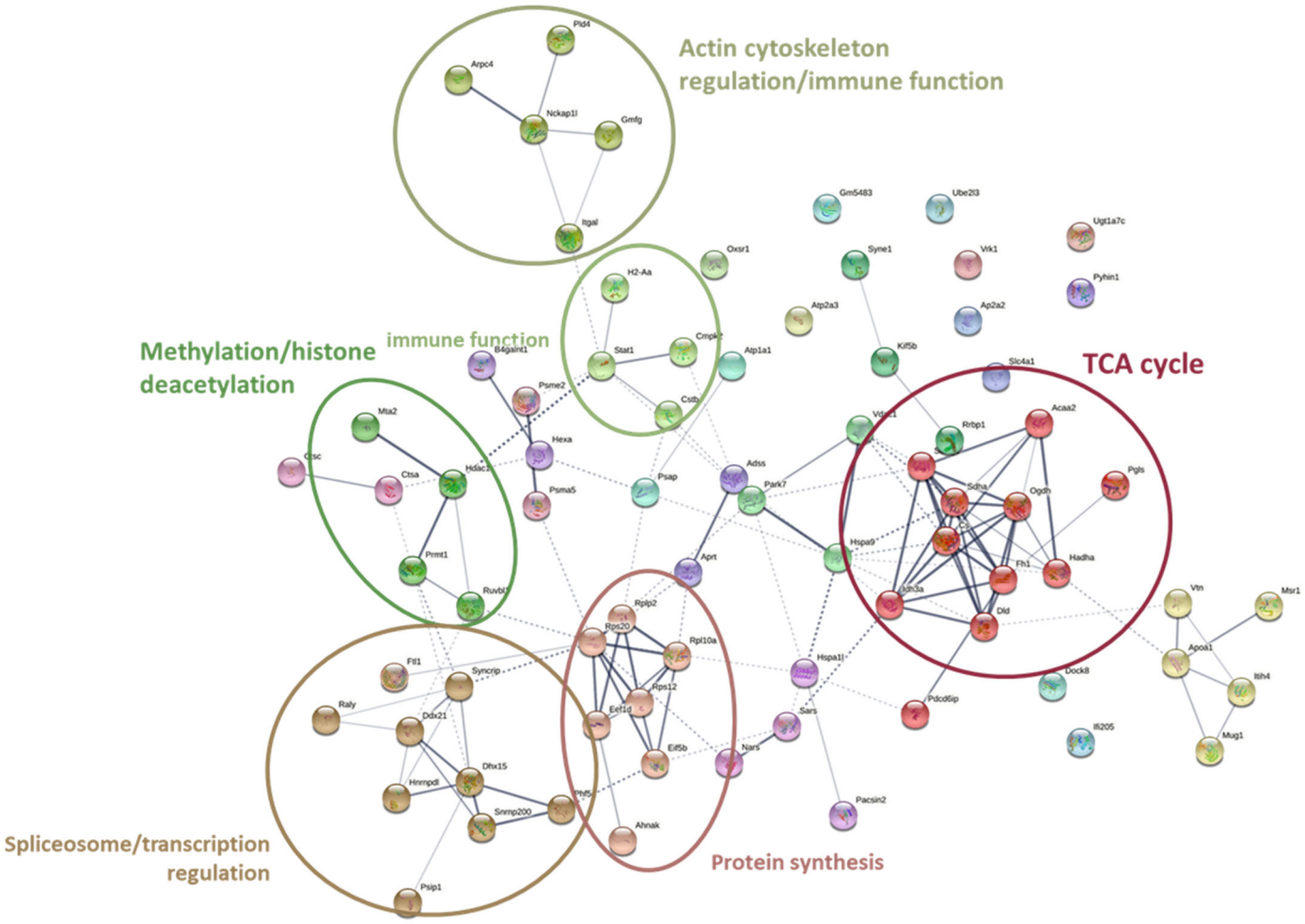

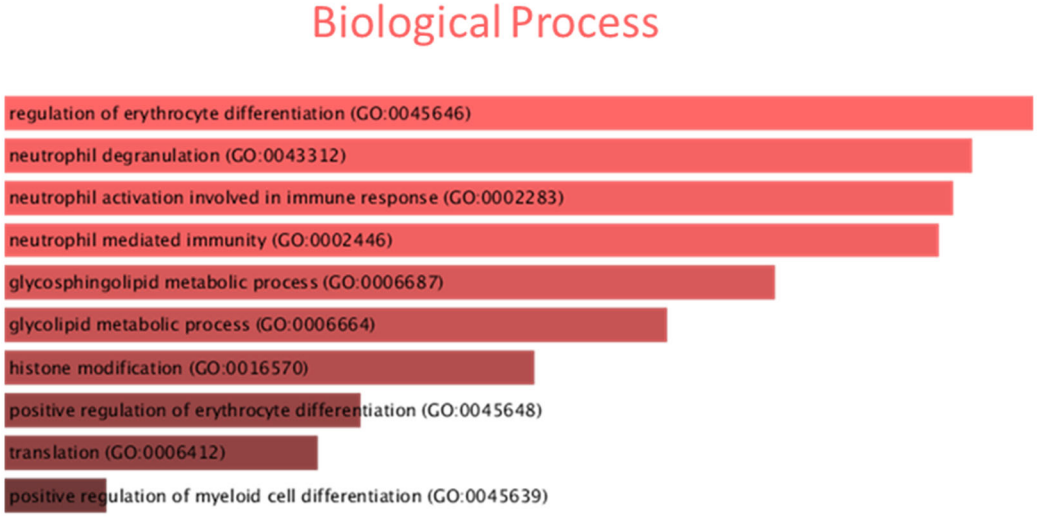

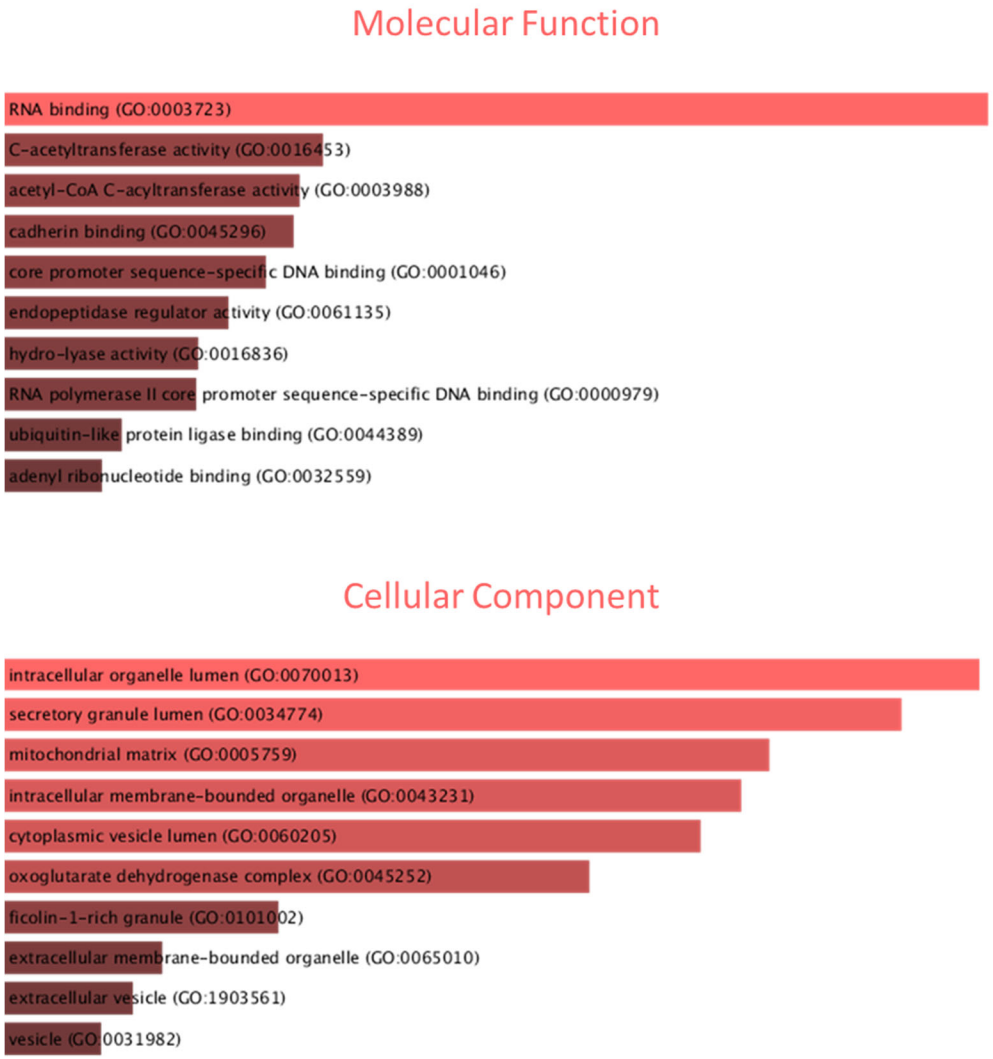

Figure 23: String and Gene Ontology analysis of AGO-EXL shared proteins. Top: Protein network analysis of shared proteins between AGO-EXL (77). Analysis was performed using STRING v11.5.Circles represent groups of proteins in the same cluster and their shared functions. Clustering was done using MCL Level 3 clustering. Bottom: Gene Ontology analysis of AGO-EXL shared proteins shows three figures with the top 10 functions for Biological Process, Molecular Function, and Cellular Component.

We were also interested in identifying differentially regulated common proteins. A cut-off of 1.5-fold change between EXL or AGO and LSH groups was set for a protein to be considered upregulated. Overall, AGO had 97 upregulated proteins against LSH, while EXL had 41 upregulated proteins against LSH, 28 were upregulated in both (Figure 24-Table 4). The top three GO biological process terms for the 28 proteins were related to neutrophil recruitment and activation. GO molecular functions of these proteins were mainly enzymatic activity such as arylesterase and oxidoreductase activity; however, the GO term "cytoskeleton-nuclear membrane anchor activity" was in top 10 terms for this group.

Analysis of upregulated proteins in EXL and AGO

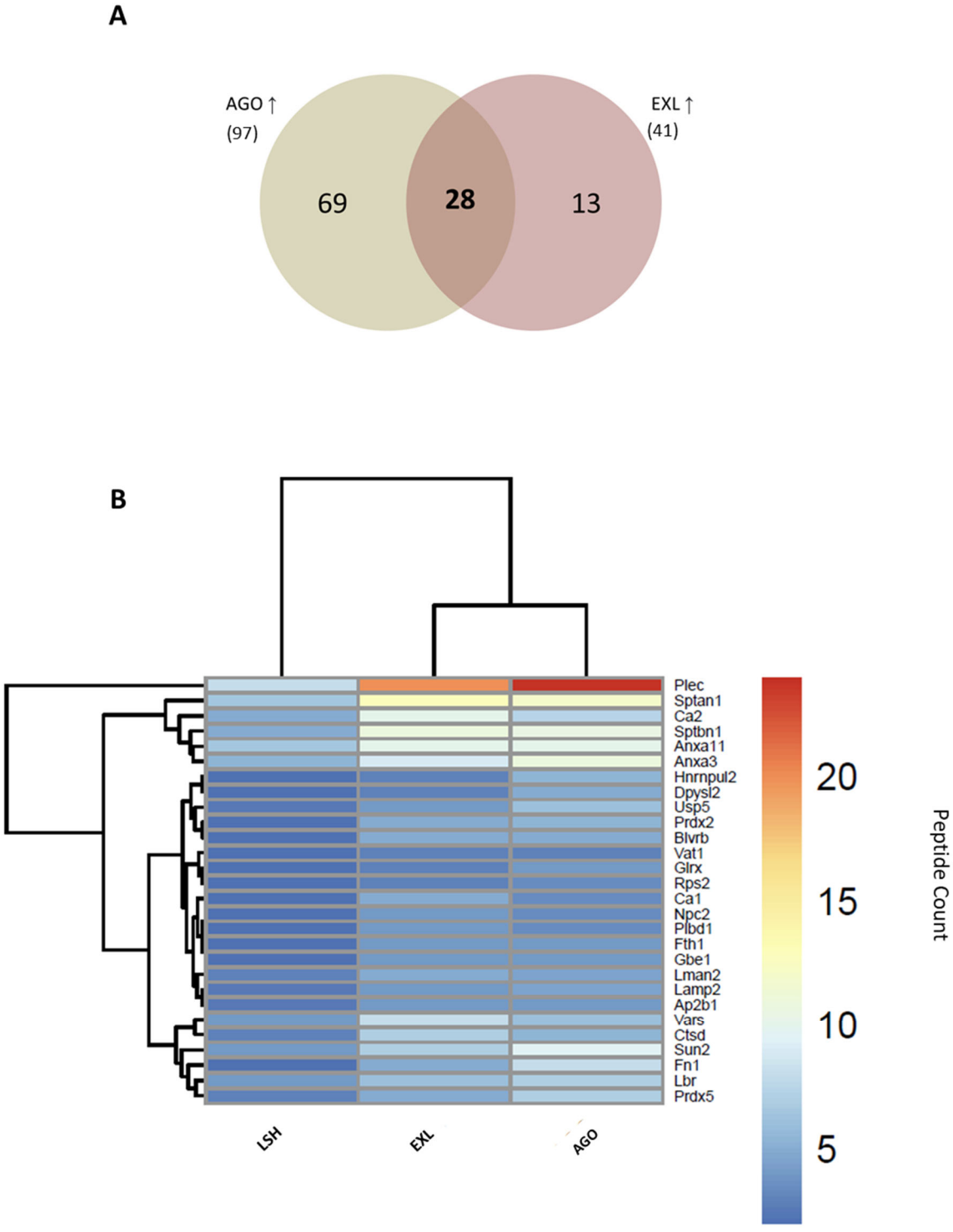

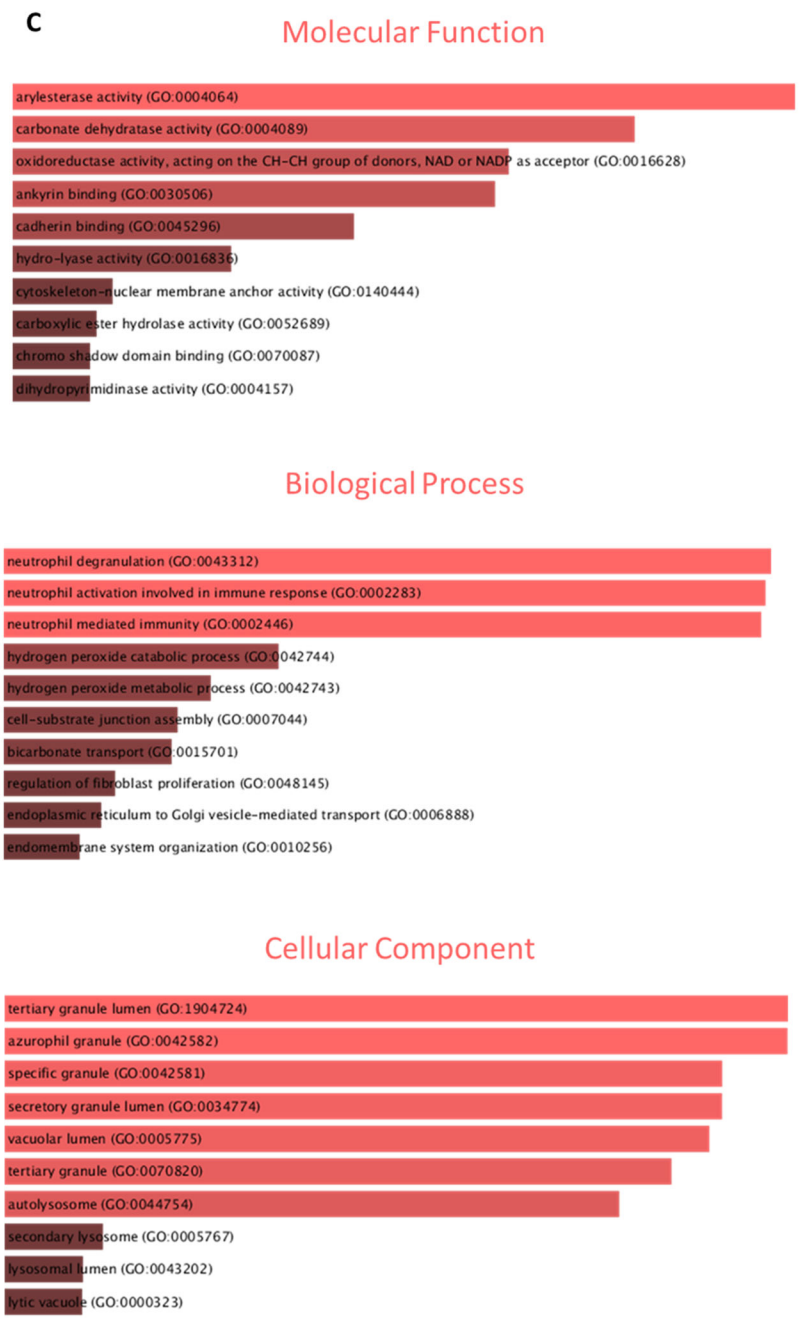

Figure 24: Analysis of upregulated proteins in L. major co-infected with exosomes (EXL) and agonist (AGO). Results are obtained from EXL and AGO experimental groups in mice peritoneal infections. A) Venn diagram of upregulated > 1.5-fold change proteins in AGO and EXL compared to LSH. B) A heat map of the 28 shared upregulated proteins in AGO and EXL compared to LSH. C) Gene Ontology *a*nalysis of proteins upregulated in both AGO-EXL *(28)* represented in three figures showing results of Biological Process, Molecular Function, and Cellular component analysis and the top 10 terms in each section.

Table 4: List of upregulated proteins in EXL and AGO.

#	**Protein Name**	**Gene**	**Accession Number**	**LSH**	**EXL**	**AGO**
1	Plectin	Plec	PLEC_MOUSE [6]	8	20	24
2	Fibronectin	Fn1	A0A087WR50_MOUSE (+2)	2	5	8
3	Peroxiredoxin-2	Prdx2	PRDX2_MOUSE	2	5	5.5
4	Flavin reductase (NADPH)	Blvrb	BLVRB_MOUSE	2	5	5
5	Carbonic anhydrase 1	Ca1	CAH1_MOUSE	2	5	3.5
6	Peptidase A1 domain-containing protein	Ctsd	Q3U651_MOUSE (+1)	3	7	5.5
7	Spectrin beta chain, non-erythrocytic 1	Sptbn1	SPTB2_MOUSE [4]	5	11	10.5
8	Spectrin alpha chain, non-erythrocytic 1	Sptan1	SPTN1_MOUSE	6.5	13	12
9	Carbonic anhydrase 2	Ca2	CAH2_MOUSE	5	10	7.5
10	Valyl-tRNA synthetase	Vars	Q7TPT7_MOUSE [2]	4	8	6
11	NPC intracellular cholesterol transporter 2	Npc2	NPC2_MOUSE (+2)	2	4	3.5
12	Ferritin heavy chain	Fth1	FRIH_MOUSE	2	4	4
13	Phospholipase B-like	Plbd1	A0A0R4J0B2_MOUSE (+1)	2	4	3.5
14	1,4-alpha-glucan-branching enzyme	Gbe1	F6ZHD8_MOUSE	2	4	4
15	SUN domain-containing protein 2	Sun2	SUN2_MOUSE	4	7	9.5
16	Peroxiredoxin-5, mitochondrial	Prdx5	PRDX5_MOUSE [3]	3	5	7
17	Vesicular integral-membrane protein VIP36	Lman2	LMAN2_MOUSE	3	5	4.5
18	Annexin A3	Anxa3	ANXA3_MOUSE (+2)	5.5	9	11
19	Ubiquitin carboxyl-terminal hydrolase	Usp5	Q3U4W8_MOUSE (+1)	2.5	4	6

20	Lysosome-associated membrane glycoprotein 2	Lamp2	LAMP2_MOUSE (+2)	2.5	4	4.5
21	AP-2 complex subunit beta	Ap2b1	AP2B1_MOUSE [7]	2.5	4	4
22	Annexin A11	Anxa11	ANX11_MOUSE	6.5	10	10
23	Delta(14)-sterol reductase LBR	Lbr	LBR_MOUSE	4	6	7
24	Heterogeneous nuclear ribonucleoprotein U-like protein 2	Hnrnpul2	HNRL2_MOUSE	2	3	5.5
25	Glutaredoxin-1	Glrx	GLRX1_MOUSE	2	3	4
26	Dihydropyrimidinase-related protein 2	Dpysl2	DPYL2_MOUSE [2]	2	3	5
27	PKS_ER domain-containing protein	Vat1	Q3TXD3_MOUSE (+3)	2	3	3
28	S5 DRBM domain-containing protein	Rps2	Q3TXS9_MOUSE	2	3	3.5

Table 5: List of upregulated proteins in EXL only.

#	**Protein Name**	**Accession Number**	**LSH**	**EXL**	**AGO**
1	S-formylglutathione hydrolase	H3BKH6_MOUSE	2.5	5	2.5
2	Apoptotic protease-activating factor 1	APAF_MOUSE	2.5	5	2
3	Fibrinogen alpha chain	FIBA_MOUSE	3	5	2.5
4	Fatty acid binding protein 5, epidermal	Q497I3_MOUSE	2.5	4	3
5	60 kDa heat shock protein, mitochondrial	CH60_MOUSE	2.5	4	3.5
6	Coatomer subunit delta	COPD_MOUSE	2.5	4	3.5
7	Nardilysin, N-arginine dibasic convertase, NRD convertase 1	A2A9Q2_MOUSE [4]	2.5	4	2.5
8	Tropomyosin alpha-3 chain	D3Z6I8_MOUSE [5]	7	11	7.5
9	Tyrosine-protein kinase	F6UND7_MOUSE [7]	4.5	7	6
10	Coatomer subunit beta'	COPB2_MOUSE	4	6	3.5
11	Dehydrogenase/reductase SDR family member 7 (Fragment)	A0A1Y7VN19_MOUSE (+1)	2	3	2
12	Vacuolar protein sorting-associated protein 29	D3Z645_MOUSE (+1)	2	3	2

13	Dehydrogenase/reductase SDR family member 1	DHRS1_MOUSE	2	3	2.5

Table 6: List of upregulated proteins in AGO only.

#	Protein Name	Accession Number	LSH	EXL	AGO
1	Vacuolar protein sorting-associated protein 35	VPS35_MOUSE	2	2	7.5
2	T-complex protein 1 subunit delta	Q3TII0_MOUSE (+1)	2	2	5
3	Beta-hexosaminidase subunit beta	HEXB_MOUSE	2.5	3	6
4	Importin subunit beta-1	IMB1_MOUSE (+1)	3	2	7
5	Ras-related protein Rab-7a	RAB7A_MOUSE	2.5	2	5.5
6	Splicing factor 3B subunit 3	SF3B3_MOUSE	3.5	5	7.5
7	Guanine nucleotide-binding protein G(I)/G(S)/G(T) subunit beta-2	E9QKR0_MOUSE [4]	4	5	8
8	Histone-binding protein RBBP4	RBBP4_MOUSE [2]	3.5	3	7
9	Electron transfer flavoprotein subunit alpha, mitochondrial	ETFA_MOUSE	2.5	2	5
10	Protein kinase C delta type	KPCD_MOUSE [3]	4	3	8
11	Staphylococcal nuclease domain-containing protein	Q3TW51_MOUSE [3]	5	6	9.5
12	ATP synthase subunit alpha, mitochondrial	ATPA_MOUSE	3	4	5.5
13	Malate dehydrogenase, cytoplasmic	MDHC_MOUSE	3	4	5.5
14	Heterogeneous nuclear ribonucleoprotein F	HNRPF_MOUSE	3	3	5.5
15	Rps16 protein	Q5CZY9_MOUSE (+2)	3	2	5.5
16	Eukaryotic initiation factor 4A-I	IF4A1_MOUSE [6]	5.5	6	10
17	T-complex protein 1 subunit gamma	TCPG_MOUSE	5	7	9
18	Phosphoglycerate mutase 1	PGAM1_MOUSE	5	6	9
19	Annexin A5	ANXA5_MOUSE	4.5	4	8
20	Protein-arginine deiminase type-4	PADI4_MOUSE	6.5	9	11.5
21	Pyr_redox_2 domain-containing protein	Q3UDS4_MOUSE (+1)	2	2	3.5
22	Eukaryotic translation initiation factor 3 subunit C	EIF3C_MOUSE	2	2	3.5
23	DEAD (Asp-Glu-Ala-Asp) box polypeptide 5	A1L333_MOUSE (+4)	10	9	17.5
24	Rab GDP dissociation inhibitor (Fragment)	Q3UC72_MOUSE (+1)	7.5	6	13
25	Annexin A2	ANXA2_MOUSE [2]	7	10	12
26	Interferon-activable protein 204	IFI4_MOUSE [2]	6.5	9	11
27	Ddx3x protein	B7ZWF1_MOUSE [3]	6.5	6	11

28	Lysosomal alpha-mannosidase	MA2B1_MOUSE (+1)	3	3	5
29	Lymphocyte-specific protein 1	LSP1_MOUSE [2]	4.5	3	7.5
30	Eukaryotic peptide chain release factor subunit 1	ERF1_MOUSE (+3)	3	2	5
31	Serine/threonine-protein phosphatase PP1-alpha catalytic subunit	PP1A_MOUSE [4]	7	7	11.5
32	Heterogeneous nuclear ribonucleoprotein L (Fragment)	G5E924_MOUSE (+1)	5.5	6	9
33	Clathrin heavy chain 1	CLH1_MOUSE [2]	24	24	39
34	40S ribosomal protein S8	RS8_MOUSE	4	4	6.5
35	F-actin-capping protein subunit alpha	Q3UBZ3_MOUSE	4	4	6.5
36	von Willebrand factor A domain-containing protein 5A	VMA5A_MOUSE	4	4	6.5
37	ATP-dependent RNA helicase A	A0A087WPL5_MOUSE [2]	6.5	9	10.5
38	Coronin-7	CORO7_MOUSE	5	7	8
39	Heterogeneous nuclear ribonucleoprotein D0	HNRPD_MOUSE [3]	5	6	8
40	MCG1051009	A0A0R4J0I1_MOUSE [2]	2.5	3	4
41	Phosphatidylethanolamine-binding protein 1	PEBP1_MOUSE (+1)	2.5	3	4
42	Platelet-activating factor acetylhydrolase IB subunit alpha	LIS1_MOUSE (+1)	2.5	3	4
43	Aspartyl aminopeptidase	DNPEP_MOUSE (+2)	2.5	3	4
44	60S ribosomal protein L12	RL12_MOUSE	2.5	2	4
45	Mitotic checkpoint protein BUB3	A0A140LHA2_MOUSE (+1)	2.5	2	4
46	ATP synthase subunit beta, mitochondrial	ATPB_MOUSE	7.5	4	12
47	Cytoplasmic dynein 1 heavy chain 1	DYHC1_MOUSE	12	11	19
48	Fibrinogen gamma chain	FIBG_MOUSE (+1)	3.5	4	5.5
49	Immunoglobulin heavy constant mu (Fragment)	A0A075B5P6_MOUSE (+2)	3.5	4	5.5
50	Transitional endoplasmic reticulum ATPase	TERA_MOUSE	12.5	11	19.5
51	Copine-1	CPNE1_MOUSE	4.5	5	7
52	Transgelin-2	TAGL2_MOUSE	4.5	4	7
53	Hexokinase-2	HXK2_MOUSE	5.5	5	8.5
54	Arachidonate 15-lipoxygenase	LOX15_MOUSE	12	7	18.5
55	Aminopeptidase B	AMPB_MOUSE	6.5	8	10
56	Arachidonate 5-lipoxygenase	LOX5_MOUSE	6.5	6	10
57	Proteasome subunit beta type-1	PSB1_MOUSE	3	4	4.5

58	Thioredoxin-like protein 1	A0A498WGD8_MOUSE (+3)	3	4	4.5
59	Methanethiol oxidase	SBP1_MOUSE	3	4	4.5
60	Protein DEK	DEK_MOUSE	4	5	6
61	Leucine-rich repeat flightless-interacting protein 1	LRRF1_MOUSE	6	7	9
62	Acidic leucine-rich nuclear phosphoprotein 32 family member A	AN32A_MOUSE	6	6	9
63	Proteasome subunit alpha type-6	PSA6_MOUSE	5	5	7.5
64	Heterogeneous nuclear ribonucleoprotein A/B	Q20BD0_MOUSE (+4)	4	4	6
65	UDP-glucose:glycoprotein glucosyltransferase 1	UGGG1_MOUSE	4	4	6
66	Eukaryotic translation initiation factor 3 subunit B	EIF3B_MOUSE (+1)	3	3	4.5
67	Nap1l4 protein	B7ZNL2_MOUSE (+2)	2	2	3
68	Eukaryotic translation initiation factor 2 subunit 1	IF2A_MOUSE	2	2	3
69	Serine/threonine-protein phosphatase 2B catalytic subunit alpha isoform	PP2BA_MOUSE	3	2	4.5

Proteomics data show a differential expression of proteins due to co-inoculation of exosomes during *L. major* infection. At the same time, unique proteins appear in GO terms involved in innate immune signaling. We observed a similarity in protein profiles of peritoneal cells obtained from mice infected with *Leishmania* and exosomes or agonist. These two groups shared 77 unique proteins not found in *Leishmania* only treated groups and were involved in innate immunity and modifying cellular metabolism. Similarly, of the 455 shared proteins between all three groups, 28 were upregulated in both AGO and EXL groups. Interestingly, these proteins appeared in GO terms related to immune regulation and cytoskeleton rearrangement.

8.5.5 ***Leishmania*** **exosomes alter phosphorylation levels of proteins**

We sought phosphoproteomic analysis for our data to have a snapshot of signaling pathways activated when cells are stimulated with these conditions. For phosphoproteomic analysis, we analyzed data from three groups only, *L. major* only (LSH), *L. major* and agonist (AGO), and *L. major* with exosomes (EXL), to identify potential differences in signaling pathways activated in AGO and EXL groups compared to LSH.

A Venn diagram of phosphopeptides identified in each group shows a total of 819 phosphorylated peptides in AGO, 987 in LSH, and 903 in EXL (Figure 25A). Although AGO had 73 unique phosphopeptides and LSH had 42, the EXL group did not have any unique phosphopeptides. EXL did not have phosphopeptides shared exclusively with AGO either. However, it had 197 phosphopeptides shared with LSH. The majority of phosphopeptides (691) in all groups were shared.

Seeing that all phosphopeptides in EXL group were shared with LSH, we were interested in learning whether EXL led to phosphorylation of these peptides in unique sites. All phosphorylation sites on the shared proteins between of EXL and LSH were identical (Figure 25B).

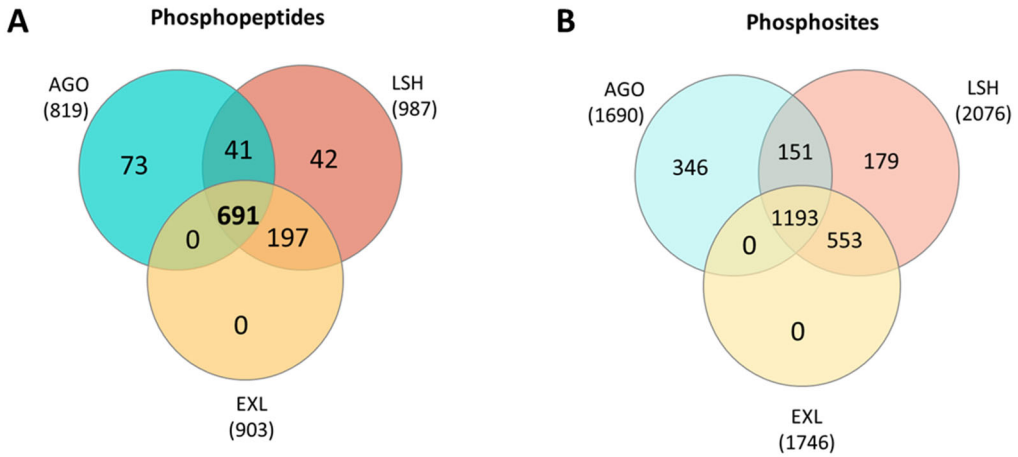

Figure 25: Venn diagrams of phosphoproteomic data Venn Diagrams of total phosphoproteins obtained from mice intraperitoneal infections show three experimental conditions *L. major* infection (LSH), *L. major* + exosome co-inoculation (EXL), *L. major* + FPR2 agonist (AGO). A) A Venn diagram of the total phosphopeptides identified in AGO, LSH, and EXL. B) A Venn diagram of the total phosphosites identified in AGO, LSH, and EXL accounting for unique phosphorylation sites on each identified phosphopeptide.

Furthermore, we were interested in identifying phosphopeptides unique to LSH, as these peptides do not appear in EXL group (Figure 26). In total, 42 phosphopeptides were unique to LSH. STRING analysis shows protein clusters involved in immune regulation and protein trafficking. GO terms in biological processes were linked to metabolism and immune system activation. Table 7 shows a list of unique LSH phosphoproteins and their functions as obtained from the Uniprot database.

Analysis of unique LSH phosphopeptides

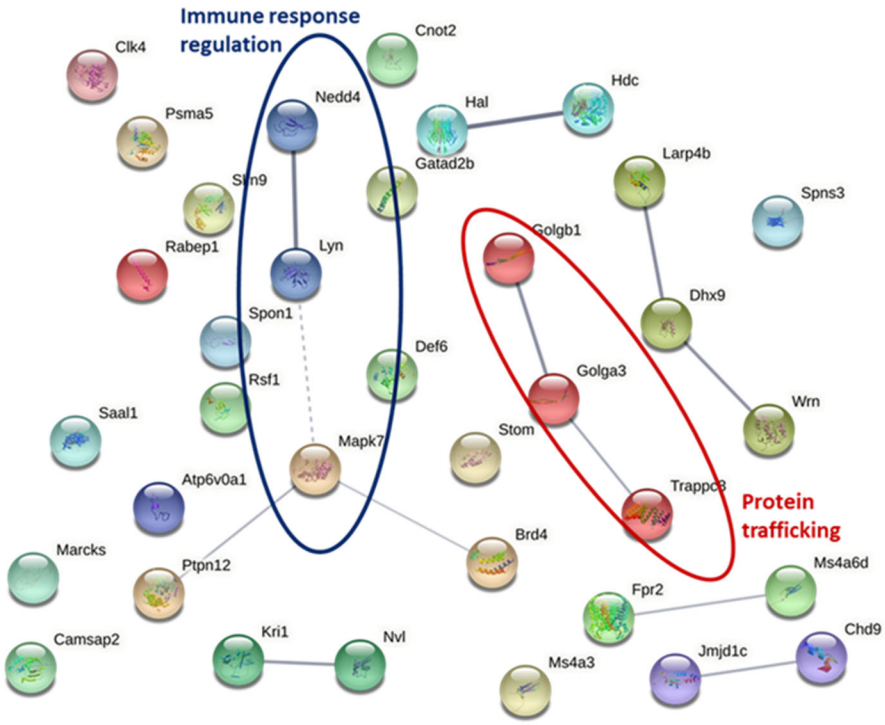

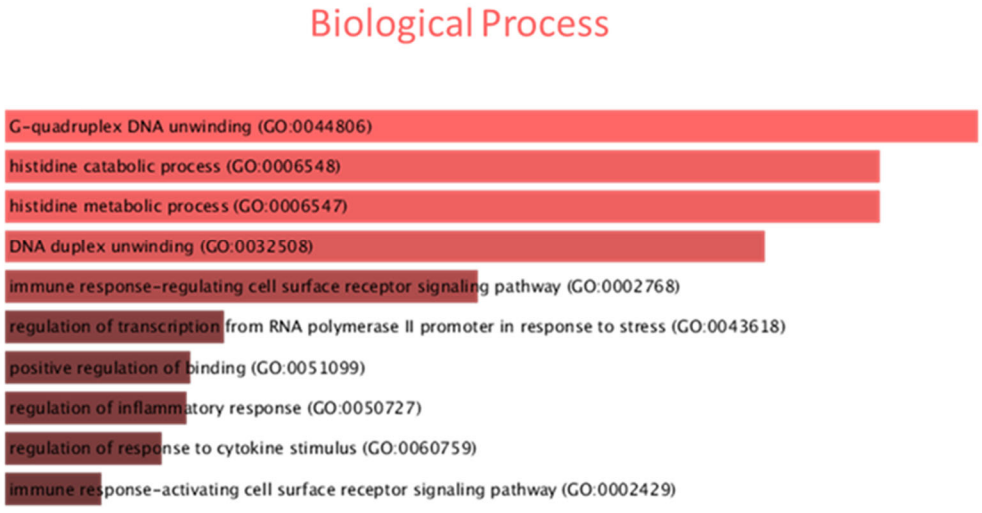

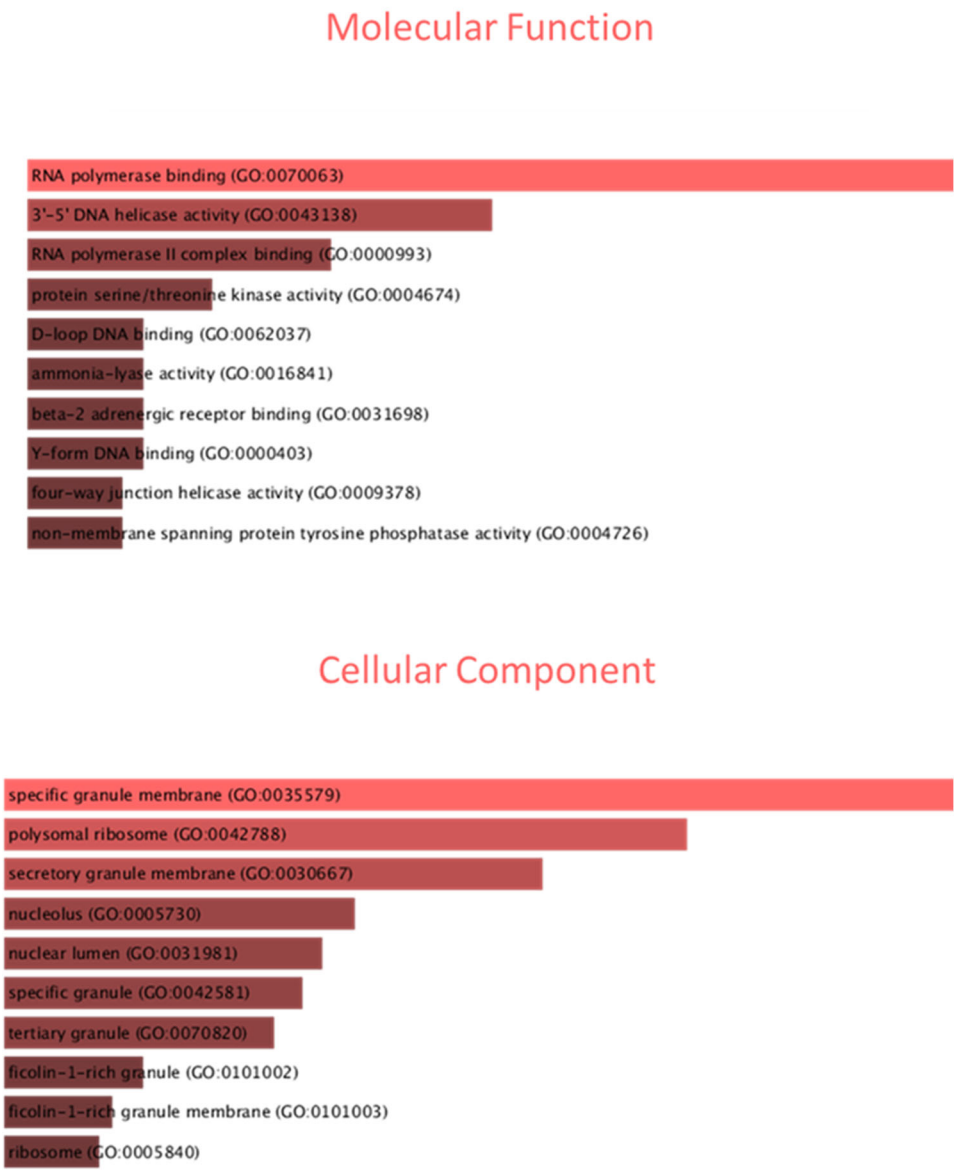

*Figure 26: String and Gene Ontology analysis of unique phosphopeptides obtained from L. major (LSH) intraperitoneal infections.*Top: protein network analysis was performed using STRING v11.5. Circles represent groups of proteins in the same cluster and their shared functions. Clustering was done using MCL Level 3 clustering. Bottom: GO analysis of the unique LSH proteins shows three figures with top 10 functions for Biological Process, Molecular Function, and Cellular Component.

Table 7: Unique LSH phosphopeptides and their functions

#	ID	Protein names	Function
1	P0CG50	Polyubiquitin-C	[Ubiquitin]: Exists either covalently attached to another protein, or free (unanchored).
2	Q8VCC9	Spondin-1	Cell adhesion protein that promotes the attachment of spinal cord and sensory neuron cells and the outgrowth of neurites in vitro.
3	P35831	Tyrosine-protein phosphatase non-receptor type 12	Dephosphorylates a range of proteins, and thereby regulates cellular signaling cascades.
4	Q3TY98	V-type proton ATPase subunit a	Essential component of the vacuolar proton pump (V-ATPase), a multimeric enzyme that catalyzes the translocation of protons across the membranes.
5	O88536	Formyl peptide receptor 2	High affinity receptor for N-formyl-methionyl peptides (FMLP), which are powerful neutrophil chemotactic factors. Stimulates chemotaxis in immune cells to site of infection or tissue damage upon recognition of several ligands, such as FMLP, or ligand involved in cell damage, disease or inflammation.
6	F6V7U2	Membrane-spanning 4-domains subfamily A member 6D	May be involved in signal transduction as a component of a multimeric receptor complex.
7	Q6A0A2	La-related protein 4B	Stimulates mRNA translation.
8	Q05BL6	Marcks protein (Fragment)	MARCKS is the most prominent cellular substrate for protein kinase C. This protein binds calmodulin, actin, and synapsin. MARCKS is a filamentous (F) actin cross-linking protein.
9	G3UYW3	Probable JmjC domain-containing histone demethylation protein 2C (Fragment)	Propable histone demythelase
10	B2RRE3	Camsap1l1 protein	Could be involved in microtuble binding

11	A0A0R4IZX1	Differentially-expressed in FDCP 6	In humans, plays a role in the activation of Rho GTPases RAC1, RhoA and CDC42.
12	D3Z0Q8	Golgin subfamily A member 3 (Fragment)	Possibly involved in maintaining golgi structure
13	A0A1B0GR76	DNA helicase	An enzyme that unwinds DNA
14	A0A1G5SK24	Schlafen family member 9 isoform 2	N/A
15	E9Q8D5	CCR4-NOT transcription complex subunit 2	Component of the CCR4-NOT complex which is one of the major cellular mRNA deadenylases and is linked to various cellular processes including bulk mRNA degradation
16	Q8BJI6	Uncharacterized protein	N/A
17	A1L3S7	Gatad2b protein	Transcriptional repressor
18	A2A4P4	Predicted gene, 27029	N/A
19	A4FUQ2	Vomeronasal type-1 receptor	Putative pheromone receptor
20	B0QZP9	Dual-specificity protein kinase CLK4 (Fragment)	may be a constituent of a network of regulatory mechanisms that enable SR proteins to control RNA splicing
21	B2RSE4	Bromodomain containing 4	Chromatin reader protein that recognizes and binds acetylated histones and plays a key role in transmission of epigenetic memory across cell divisions and transcription regulation
22	Q571K1	MKIAA4151 protein (Fragment)	N/A
23	Q9D3I5	Uncharacterized protein	N/A
24	Q3V3T8	PHD-type domain-containing protein (Fragment)	Could be involved in chromatin mediated gene regulation
25	Q3UKQ7	IRF tryptophan pentad repeat domain-containing protein	Involved in DNA binding and transcription regulation
26	E9Q7S1	Zinc finger protein 106	RNA binding protein. Essential for maintenance of peripheral motor neuron and skeletal muscle function
27	E9QNN1	DEAH box protein 9	DNA/RNA helicase activity
28	V9GXJ9	Protein KRI1 homolog	RNA binding protein
29	G1UCX4	Synoviocyte proliferation-associated in collagen-induced arthritis 1	Plays a role in promoting the proliferation of synovial fibroblasts

			in response to proinflammatory stimuli
30	J3QJV7	Rab GTPase-binding effector protein 1	Involved in endocytic membrane fusion and membrane trafficking of recycling endosomes
31	Q7TMW5	Histidine decarboxylase	Catalyzes the biosynthesis of histamine from histidine
32	Q8BPA1	PHB domain-containing protein	An integral component of the plasma membrane
33	Q3TN98	Uncharacterized protein (Fragment)	N/A
34	Q3UPK6	Proteasome subunit alpha type	A subunit of the proteosome that plays a role in the regulation of proteins that control cell-cycle progression and apoptosis
35	Q53ZU3	Membrane-spanning 4-domains subfamily A member 3	Hematopoietic modulator for the G1-S cell cycle transition. Modulates the level of phosphorylation of cyclin-dependent kinase 2 (CDK2) through its direct binding to cyclin-dependent kinase inhibitor 3 (CDKN3/KAP)
36	Q5NCN8	Mitogen-activated protein kinase 7	Plays a role in various cellular processes such as proliferation, differentiation and cell survival
37	Q9CRW9	Nucleolin_bd domain-containing protein (Fragment)	An ATP binding protein
38	Q3TMV6	DNA helicase	Functions in unwinding the DNA
39	A2AD84	Serine/threonine-protein kinase 26	Meidator of growth and modulates apoptosis
40	Q3TUU1	Uncharacterized protein	N/A
41	A0A0R4J1V6	Homeodomain-interacting protein kinase 1	Involved in transcription regulation and TNF-mediated cellular apoptosis.
42	Q8CEI0	Tyrosine-protein kinase	Plays an important role in the signal transduction process

LSH and EXL groups shared 197 phosphopeptides. Protein interaction network identified clusters involved in translation regulation, apoptosis, endocytic vesicles, and innate immunity (Figure 27). Of the 197 shared proteins between LSH and EXL, 31 were upregulated with a 1.5-fold increase in EXL (Figure 28-Table 8). Interestingly, three of the top 10 GO biological process

terms for these phosphoproteins are related to regulation of protein localization to the plasma membrane or periphery. The GO terms negative regulation of autophagy, regulation of calcineurin-NFAT signaling cascade, calcium ion transmembrane import into the cytosol, and regulation of proteasomal catabolic process also appeared in the top 10 for GO biological process. Top enriched GO molecular function terms for these phosphopeptides are protein phosphatase 2B binding, nitric-oxide synthase binding, methylated histone binding, protein phosphatase binding, histone demethylase activity, and cytoskeleton-nuclear membrane anchor activity. These findings indicate upregulation of protein binding activity and demethylation in EXL compared to LSH.

Analysis of shared phosphopeptides between LSH and EXL

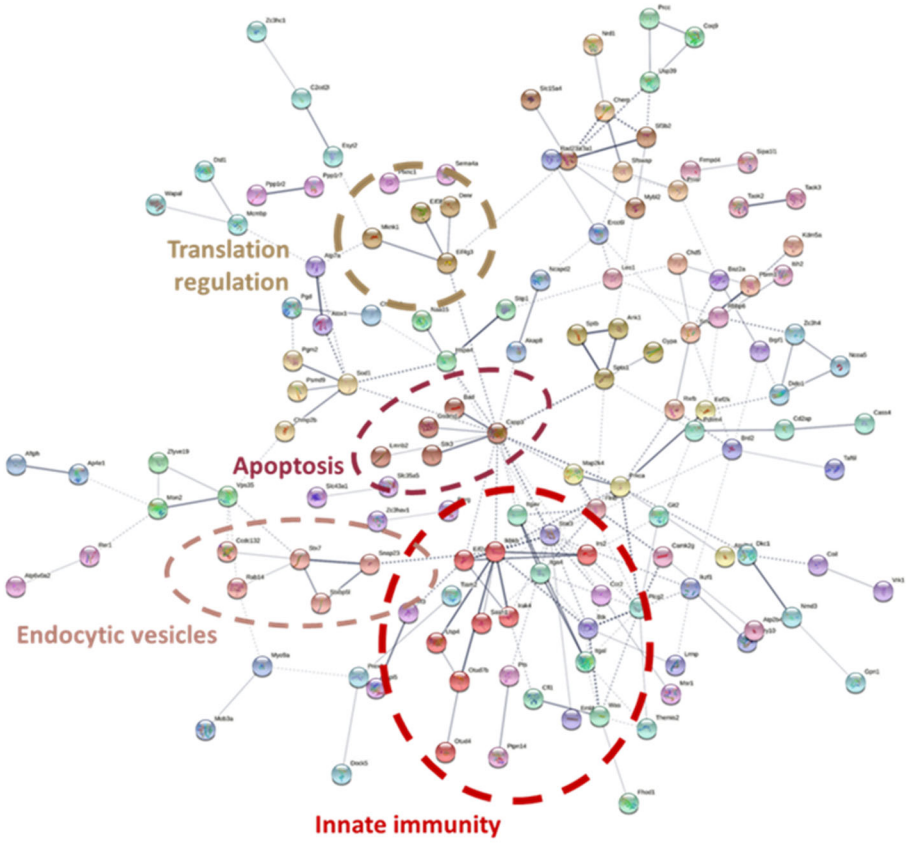

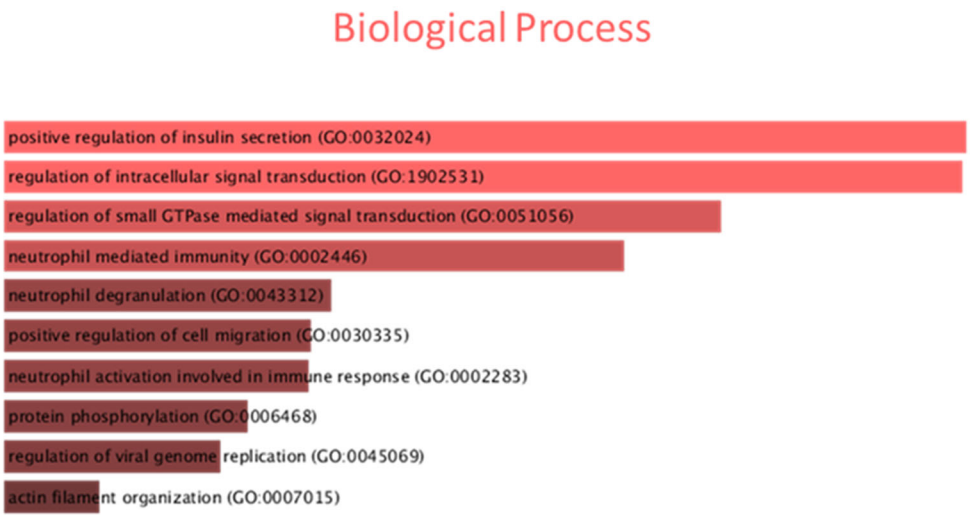

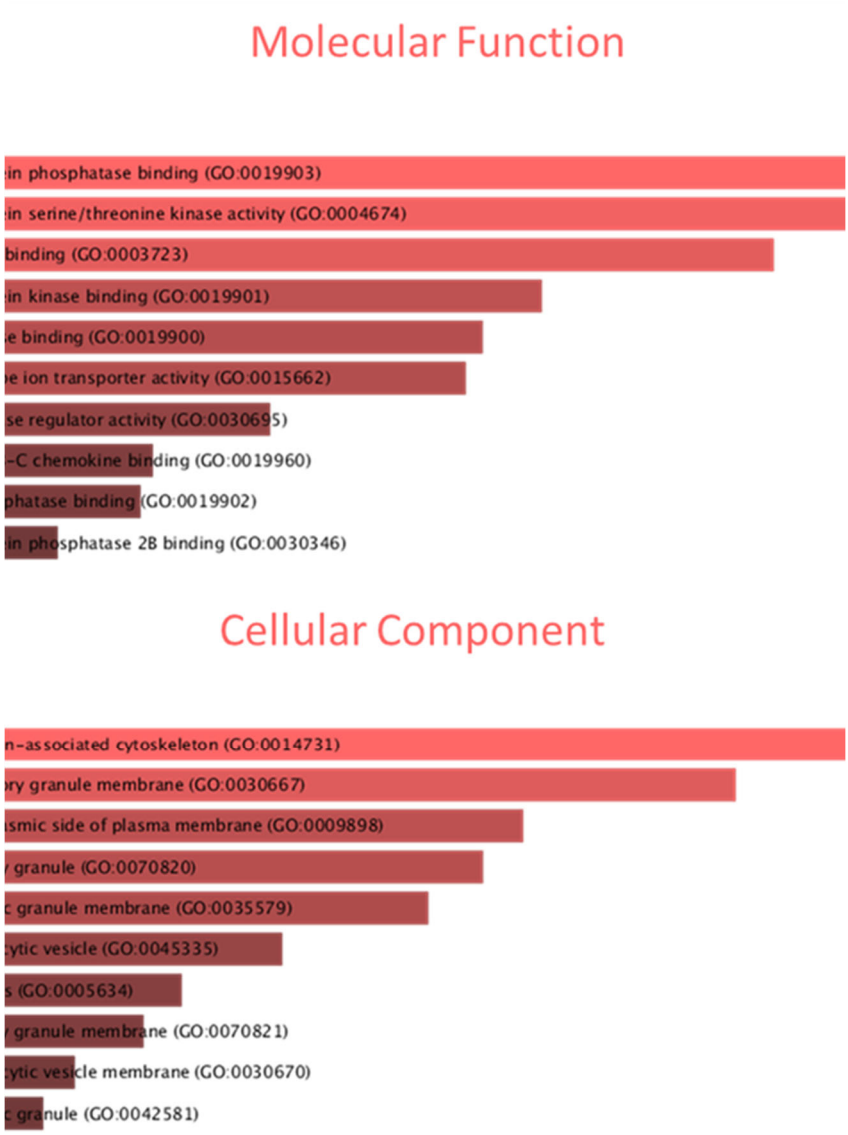

Figure 27: String and Gene Ontology analysis of shared phosphopeptides (197) between LSH and EXL. Top: Protein network analysis was performed using STRING v11.5. Circles represent groups of proteins in the same cluster and their shared functions. Clustering was done using MCL Level 3 clustering. Bottom: GO analysis of shared proteins shows three figures with top 10 functions for Biological Process, Molecular Function, and Cellular Component.

Gene Ontology analysis of upregulated phosphopeptides in EXL shared between LSH and EXL

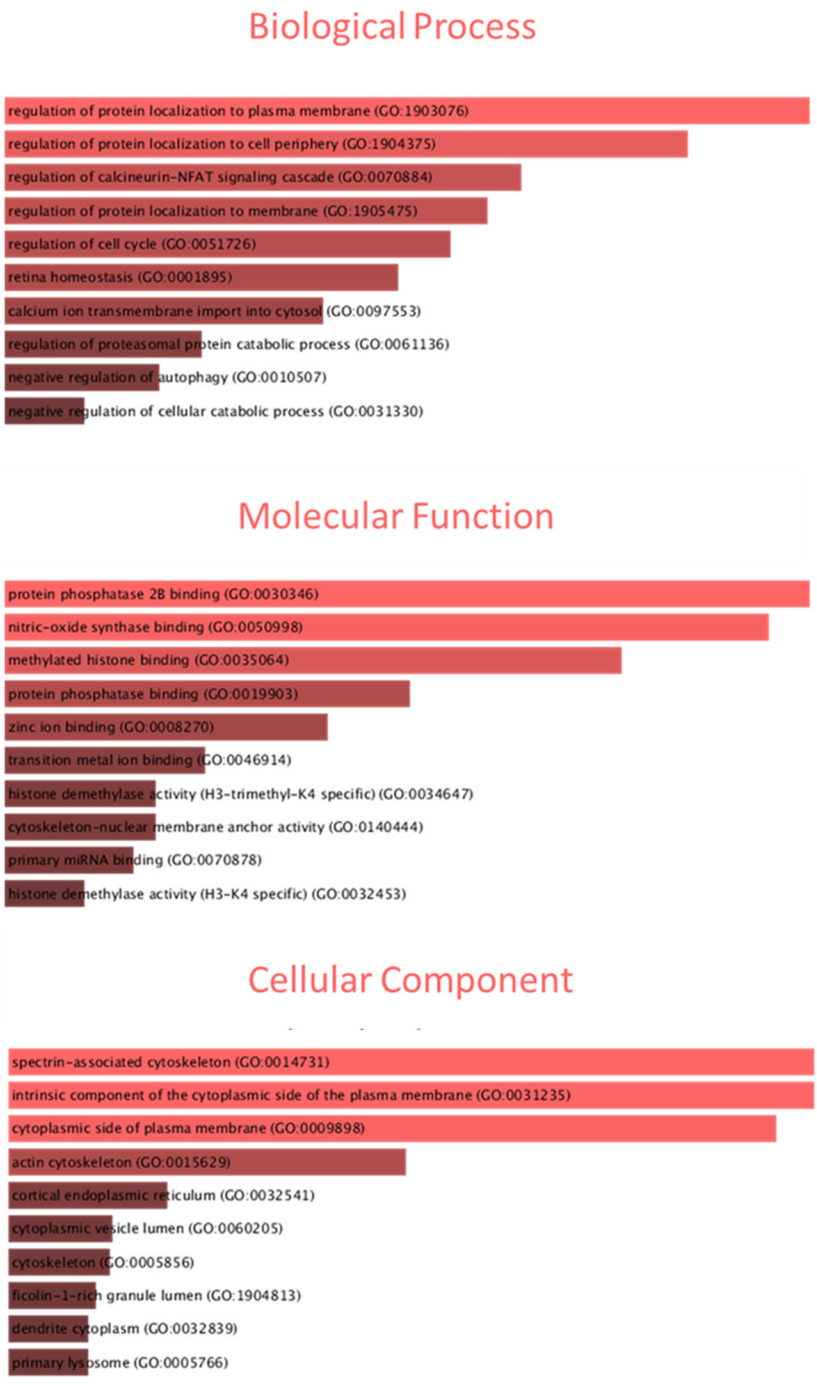

Figure 28: Gene Ontology analysis of upregulated phosphopeptides (31) shared between EXL and LSH. Three figures are shown for Biological Process, Molecular Function, and Cellular Component analysis with the top 10 enriched functions for each term.

Table 8: Upregulated phosphopeptides in EXL shared with LSH.

#	ID	Name	function
1	P60710	Actin, cytoplasmic 1	Actin is a highly conserved protein that polymerizes to produce filaments that form cross-linked networks in the cytoplasm of cells
2	P08228	Superoxide dismutase	Destroys radicals which are normally produced within the cells and which are toxic to biological systems.
3	Q3UDW8	Heparan-alpha-glucosaminide N-acetyltransferase (EC 2.3.1.78) (Transmembrane protein 76)	Lysosomal acetyltransferase that acetylates the non-reducing terminal alpha-glucosamine residue of intralysosomal heparin or heparan sulfate, converting it into a substrate for luminal alpha-N-acetyl glucosaminidase.
4	Q8CAP3	UV excision repair protein RAD23	Multiubiquitin chain receptor involved in modulation of proteasomal degradation. Involved in nucleotide excision repair.
5	P08032	Spectrin alpha chain, erythrocytic 1 (Erythroid alpha-spectrin)	Spectrin is the major constituent of the cytoskeletal network underlying the erythrocyte plasma membrane. It associates with band 4.1 and actin to form the cytoskeletal superstructure of the erythrocyte plasma membrane.
6	F7AAP4	Calcium-transporting ATPase	This magnesium-dependent enzyme catalyzes the hydrolysis of ATP coupled with the transport of calcium.
7	P48972	Myb-related protein B (B-Myb) (Myb-like protein 2)	Transcription factor involved in the regulation of cell survival, proliferation, and differentiation. Transactivates the expression of the CLU gene.
8	A0A338P6P6	Arf-GAP with coiled-coil, ANK repeat and PH domain-containing protein 2	GTPase activating protein
9	A0A0G2JF47	Phosphoglucomutase-2 (Fragment)	Catalyzes the conversion of the nucleoside breakdown products ribose-1-phosphate and deoxyribose-1-phosphate to the corresponding 5-phosphopentoses.
10	A0A1L1STZ1	Cysteine and histidine-rich domain-containing protein 1	Involved in the stress response. Plays a role in ensuring the localization of the tyrosine kinase receptor EGFR to the plasma membrane, and thus ensures the subsequent regulation of EGFR activity and EGF-induced actin cytoskeleton remodeling

11	A0A3B2W812	CD2-associated protein	May act as an adapter protein between membrane proteins and the actin cytoskeleton
12	E0CXY0	Fibronectin type-III domain-containing protein 3A (Fragment)	Involved in RNA binding
13	E9PYU4	DNA helicase	DNA unwinding
14	E9Q397	Spectrin beta chain	Spectrin is the major constituent of the cytoskeletal network underlying the erythrocyte plasma membrane
15	F2Z423	Tubulin--tyrosine ligase-like protein 12	Negatively regulates post-translational modifications of tubulin
16	G3X8X3	Large neutral amino acids transporter small subunit 3	Sodium-independent, high affinity transport of large neutral amino acids
17	G5E8I8	Calcium homeostasis endoplasmic reticulum protein	Involved in calcium homeostasis, growth and proliferation
18	Q3TRN7	Uncharacterized protein (Fragment)	N/A
19	Q3TU08	Uncharacterized protein (Fragment)	N/A
20	Q3URL4	Uncharacterized protein	N/A
21	Q3UZ11	PHD-type domain-containing protein (Fragment)	N/A
22	Q3V075	Uncharacterized protein (Fragment)	N/A
23	Q3V159	Uncharacterized protein	N/A
24	Q4QQM3	Unc84b protein	An integral component of the nuclear inner membrane
25	Q6GU23	Signal transducer and activator of transcription	Contribute to signal transduction by cytokines, hormones, and growth factors
26	Q6PHC0	C2cd2l protein	Plays a key role in the coordination of Ca^{2+} and phosphoinositide signaling
27	Q8BXH8	Integrator complex subunit 10	In humans, Component of the Integrator (INT) complex, a complex involved in the small nuclear RNAs (snRNA) U1 and U2 transcription and in their 3'-box-dependent processing
28	Q9DA64	CMT1A duplicated region transcript 4 protein homolog	N/A

29	Q9DD05	Delta-aminolevulinic acid dehydratase	Catalyzes an early step in the biosynthesis of tetrapyrroles
30	Q9JMJ6	Syntaxin 7	Involved in protein tranfficking from the plasma membrane to the early endosome
31	U3KLT0	Deleted.	N/A

Then, we investigated the largest phosphoprotein cluster in our data, the 691 shared phosphoproteins between all groups. To identify upregulated phosphoproteins in this group, we compared EXL and AGO to LSH. If the log intensity value in EXL or AGO was greater than 1.5-fold change or more than LSH, the phosphopeptide is considered upregulated. Figure 29 shows a Venn diagram of upregulated proteins in EXL and LSH. Forty-two were upregulated in AGO, 26 in EXL, and 43 upregulated in both groups. Because our main goal is to identify signaling pathways activated by exosomes when interacting with FPR2, we focused our analysis on the 43 shared upregulated phosphopeptides Table 9.

The top GO biological process term for this group was regulation of cytoskeleton organization, followed by the term positive regulation of Notch signaling pathway. In top 10 GO biological process terms, a total of three terms were related to upregulation of Notch signaling pathway, two terms related to positive regulation of transforming growth factor-beta, and two terms in negative regulation of insulin signaling. On the other hand, molecular function top GO term was histone deacetylase binding. Other terms of interest appearing in top 10 enriched GO terms in molecular function were Notch binding, protein kinase regulator activity, and cytoskeleton-nuclear membrane anchor activity. As for cellular component GO terms, four out of top 10 enriched terms were cytoskeleton and microtubule-related terms. We also created a heatmap of the 43 upregulated proteins showing their log2 intensities compared to LSH (Figure 30)

Figure 29: String and Gene Ontology analysis of upregulated phosphopeptides in AGO and EXL. Top: A Venn diagram of the upregulated > 1.5-fold change phosphopeptides in AGO and EXL. Bottom: GO analysis of shared upregulated phosphopeptides (43) AGO-EXL represented in three figures showing Biological Process, Molecular Function, and Cellular component analysis and top 10 terms in each section.

Table 9: Upregulated shared AGO-EXL phosphoproteins and their functions.

#	Gene	ID	Protein names	Function
1	Srrt	Q99MR6	Serrate RNA effector molecule homolog	Acts as a mediator between the cap-binding complex (CBC) and the primary microRNAs (miRNAs) processing machinery during cell proliferation.
2	Terf2ip	Q8BPK1	Telomeric repeat-binding factor 2-interacting protein 1	Acts both as a regulator of telomere function and as a transcription regulator.
3	Akna	Q80VW7	Microtubule organization protein AKNA	Centrosomal protein that plays a key role in cell delamination by regulating microtubule organization.
4	Atg4b	A0A0R4J065	Cysteine protease	Cysteine protease required for the cytoplasm to vacuole transport (Cvt) and autophagy.
5	Vasp	P70460	Vasodilator-stimulated phosphoprotein	Ena/VASP proteins are actin-associated proteins involved in a range of processes dependent on cytoskeleton remodeling and cell polarity such as axon guidance, lamellipodial and filopodial dynamics, platelet activation and cell migration.
6	Fcho2	Q3UQN2	F-BAR domain only protein 2	Functions in an early step of clathrin-mediated endocytosis.
7	Psd4	Q8BLR5	PH and SEC7 domain-containing protein 4	Guanine nucleotide exchange factor for ARF6 and ARL14/ARF7.

8	Purb	O35295	Transcriptional activator protein Pur-beta	Has capacity to bind repeated elements in single-stranded DNA such as the purine-rich single strand of the PUR element located upstream of the MYC gene.
9	Snw1	Q3TM37	SNW domain-containing protein 1 (Fragment)	Involved in pre-mRNA splicing.
10	Dcaf6	Q9DC22	DDB1- and CUL4-associated factor 6	Ligand-dependent coactivator of nuclear receptors. Enhance transcriptional activity of the nuclear receptors NR3C1 and AR.
11	Bmp2k	Q91Z96	BMP-2-inducible protein kinase	May be involved in osteoblast differentiation.
12	Ccny	Q8BGU5	Cyclin-Y	Positive regulatory subunit of the cyclin-dependent kinase CDK14/PFTK1.
13	Cir1	Q9DA19	Corepressor interacting with RBPJ 1	Regulates transcription and acts as corepressor for RBPJ.
14	Evi2b	Q8VD58	Protein EVI2B	Required for granulocyte differentiation and functionality of hematopoietic progenitor cells through the control of cell cycle progression and survival of hematopoietic progenitor cells.

15	Cast	Q921U7	Calpain inhibitor	Specific inhibition of calpain (calcium-dependent cysteine protease). Plays a key role in postmortem tenderization of meat and have been proposed to be involved in muscle protein degradation in living tissue.
16	Rbm17	Q8JZX4	Splicing factor 45	Splice factor that binds to the single-stranded 3'AG at the exon/intron border and promotes its utilization in the second catalytic step.
17	Faf1;FAF1	P54731	FAS-associated factor 1	Ubiquitin-binding protein.
18	Nck1	A0A087WQD1	Cytoplasmic protein NCK1 (Fragment)	Plays a role in the DNA damage response
19	Suds3	A0A0R4J243	Sin3 histone deacetylase corepressor complex component SDS3	Regulatory protein which represses transcription and augments histone deacetylase activity of HDAC1
20	Xpo4	A0A0R4J254	Exportin-4	It mediates nuclear export of eIF-5A
21	Crebbp	A0A0U1RPL2	Histone acetyltransferase (Fragment)	An epigenetic enzyme that acetylates cellular proteins
22	Uhrf1bp1l	A0A1W2P7J6	UHRF1-binding protein 1-like (Fragment)	Involved in protein homodimerization
23	Elmsan1	Q8BUZ9	Uncharacterized protein (Fragment)	N/A
24	Cog3	A0A2I3BQD7	Deleted.	N/A

25	Sh3bp1	A2A5V3	SH3 domain-binding protein 1	Through its GAP activity toward RAC1 and/or CDC42 plays a specific role in phagocytosis of large particles. Specifically recruited by a PI3 kinase/PI3K-dependent mechanism to sites of large particles engagement, inactivates RAC1 and/or CDC42 allowing the reorganization of the underlying actin cytoskeleton required for engulfment
26	Ermap	A2A7P7	Erythroid membrane-associated protein	Possible role as a cell-adhesion or receptor molecule of erythroid cells
27	Rere	A2A7T3	Arginine-glutamic acid dipeptide repeats protein	Plays a role as a transcriptional repressor during development. May play a role in the control of cell survival
28	Dync1i2	A2BFF8	Cytoplasmic dynein 1 intermediate chain 2	Acts as a motor for the intracellular retrograde motility of vesicles and organelles along microtubules
29	Supt3	Q8BWQ2	Uncharacterized protein	N/A
30	Cad	Q80VF8	CAD protein (Fragment)	This protein is a 'fusion' protein encoding four enzymatic activities of the pyrimidine pathway (GATase, CPSase, ATCase and DHOase)
31	Rbm39	B7ZD61	RNA-binding protein 39 (Fragment)	Acts as a pre-mRNA splicing factor

32	Ccdc6	D3YZP9	Coiled-coil domain-containing protein 6	Involved in SH3 domain binding
33	Gsk3a	D3Z7E5	[Tau protein] kinase	N/A
34	Syne2	F7BX34	Nesprin-2 (Fragment)	Multi-isomeric modular protein which forms a linking network between organelles and the actin cytoskeleton to maintain the subcellular spatial organization
35	Ncor2	E9PY55	Nuclear receptor corepressor 2	Transcriptional corepressor
36	Phf6	E9QAG2	PHD finger protein 6	Transcriptional regulator that associates with ribosomal RNA promoters and suppresses ribosomal RNA (rRNA) transcription
37	S100a8	Q53X15	Protein S100	Weakly binds calcium but binds zinc very tightly-distinct binding sites with different affinities exist for both ions on each monomer
38	G3bp1	Q3UR88	NTF2 domain-containing protein	Transport of moelcules into the nucleus
39	Rictor	Q8CB99	RICTOR_N domain-containing protein	Plays a role in TOR signaling
40	Nsfl1c	Q3KQQ1	NSFL1 cofactor p47 (Fragment)	educes the ATPase activity of VCP
41	Tomm70a	Q80TT4	MKIAA0719 protein (Fragment)	N/A
42	Adrbk1	Q3U5J8	PH domain-containing protein (Fragment)	Protein phosphatase involved in regulation of Akt and PKC signaling
43	Tppp	Q3URG1	Uncharacterized protein	N/A

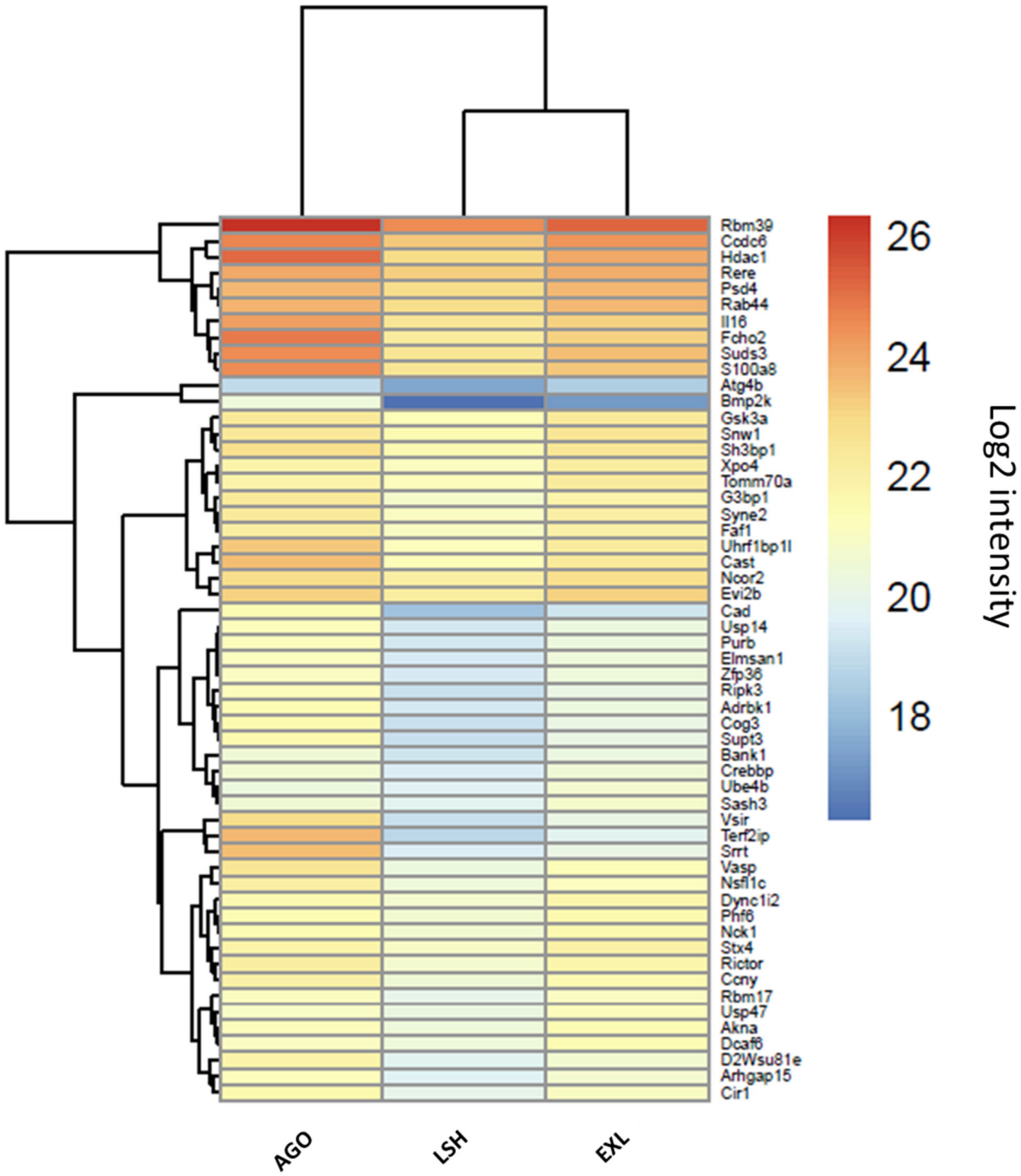

Figure 30: A heatmap of the shared upregulated phosphopeptides (43) in AGO and EXL. Proteins correspond to the list in Table 9.

Using X2K platform, we obtained a list of predicted transcription factors, and kinases the 43 upregulated phosphopeptides interact with. This platform is useful to predict upstream kinases that might have subtle changes in their phosphorylation levels due to the nature of signal transduction. The platform requires a gene list for its analysis, so we provided corresponding gene IDs of the phosphopeptides. Putative enriched transcription factors are obtained, followed by a protein-protein interactions subnetwork that connects the enriched transcription factors with known protein-protein interactions. Then, a list of ranked enriched kinases is created using the overlap of proteins in the subnetwork created and known kinase-substrate phosphorylation interactions (Figure 31)

Major transcription factors identified were RUNX1, UBTF, and FOXA2. Furthermore, based on KEA scores, the top 20 kinases in the list involved MAPKs, ERK1/2, CDKs, and CKs. Top hits were for CK2ALPHA, CSNK2A1, and MAPK1.

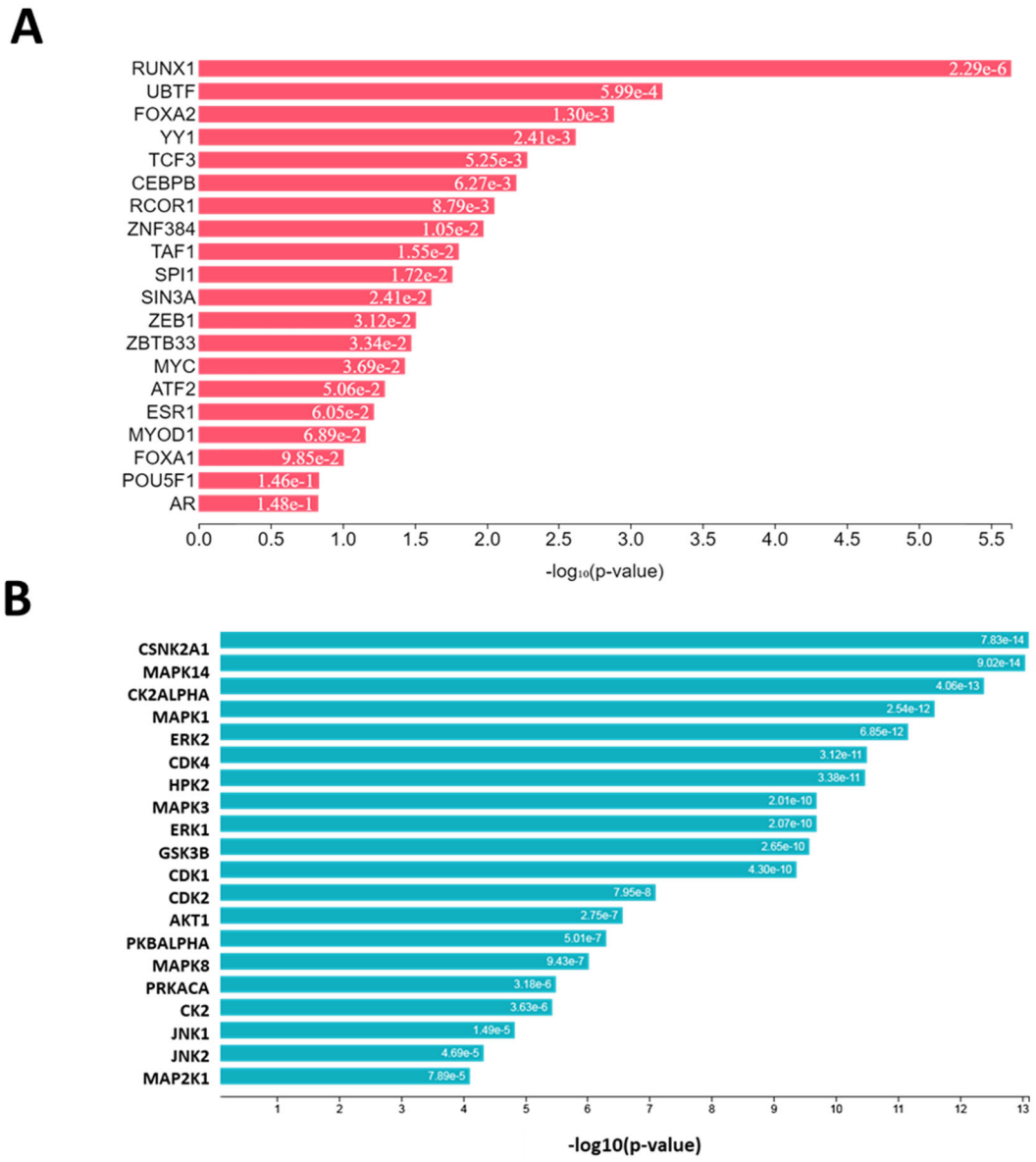

Figure 31: Analysis of shared upregulated phosphopeptides in EXL and AGO using X2K platform. A) Transcription Factor Enrichment Analysis (TFEA) of predicted transcription factors regulating input phosphoproteins. B) Kinase enrichment analysis (KEA) shows the top 20 ranked kinases predicted to regulate the 43 phosphoproteins upregulated in both AGO and EXL compared to LSH. C) subnetwork of transcription factors, intermediate proteins, and protein kinases indicating most enriched transcription factors and kinases upstream of input gene list. The size of the node indicates connectivity.

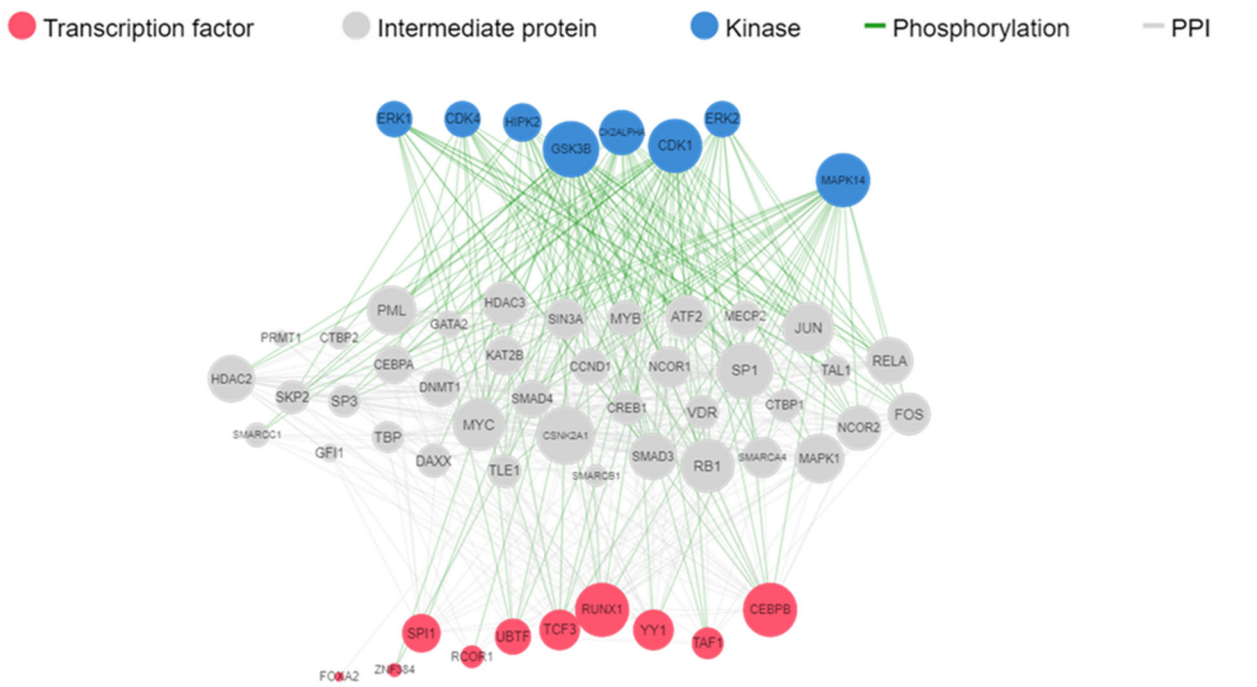

Figure 32: Subnetwork of X2K analysis of shared upregulated phosphoproteins in EXL and AGO.
Subnetwork of transcription factors, intermediate proteins, and protein kinases indicating the most enriched transcription factors and kinases upstream of the input gene list in
Figure *31*. The size of the node indicates connectivity.

8.6 Discussion

Leishmaniasis is a highly prevalent disease, infecting millions of individuals worldwide. However, its pathogenesis's cellular and molecular mechanisms are not fully characterized [160]. Besides, current therapeutic strategies have a risk of toxicity, the possibility of severe side effects, and increasing parasite resistance, necessitating discoveries of new therapies and vaccines. A potential target is *Leishmania* exosomes, extracellular vesicles released by the parasite and classified as virulence factors. Previous work from our lab and others has shown that exosomes released by *Leishmania* parasites exacerbate infection and favors parasite survival within macrophages [72, 99, 100]. Recently, our lab has identified a potential interaction between *L. major* exosomes and FPR2, a receptor present on the surface of many cells, including innate immune cells (Lira Filho and Olivier, unpublished). Studies stemming from my project expands the research on host proteins and signaling pathways modulated by the exosome-FPR2 axis during early infection using molecular and bioinformatic methods.

8.6.1 *Exosomes significantly increase parasite load in macrophages*

Leishmania infections in macrophages are usually quantified by staining infected macrophages and visually quantifying parasites. Instead, in this paper, we used *L. major* tagged with the luciferase enzyme to quantify parasite load, which provides an accurate and reliable representation of *Leishmania* infections [150]. To confirm the reliability of our model, we serially diluted a known concentration of parasites, lysed them, and measured the RLU using a luminometer. Our results showed an almost linear correlation between parasite counts above thousand parasites and measured RLUs, indicating that the system quantifies parasites reliably. These results correspond to a previous publication on the correlation between RLU and parasite count using *L. major*-LUC [150].

Work from our lab has shown that exosomes exacerbate *L. major* infections by increasing lesion size in mice and parasite load [72]. To confirm this finding in our model, we infected LM1 macrophages with different concentrations of exosomes. Per previous findings, *L. major* exosomes increased the parasite load in macrophages significantly in a dose-dependent manner [72].

8.6.2 *L. major* exosomes augmentation of infection via FPR2

Formyl peptide receptors (FPRs) play an important role in signaling in phagocytes by sensing pathogens and eliciting inflammatory responses. Limited studies have been done to

explore the role of FPR2 in *Leishmania* infections. A recent study has shown that *Leishmania infantum* infections activate FPR2 in neutrophils leading to neutrophil extracellular traps (NETs) extrusion and increased expression of citrullinated histone H3, a biomarker of NETs [161]. Wenzel and Van Zandbergen reported that using ANXA1, a known FPR2 ligand, increases *L. major* infection rates in neutrophils and their survival. Blocking FPR2 with the antagonist bNLP inhibited the increase in infection rate by ANXA1 [162].

Interestingly, *L. major* alone appears to suppress ANXA1 production in early infection while benefitting from FPR2 activation in later stages [162, 163]. Data from our lab showed that in BMDMs obtained from ANXA (-/-) mice do not exhibit increase in infection observed with exosomes in WT mice (Lira Filho and Olivier, unpublished). These findings suggest that exosomes could utilize the ANXA1/FPR2 axis in promoting *L. major* entry and survival in macrophages and neutrophils. Furthermore, in *L. braziliensis* infected mice, the levels of ANXA1 were increased in lesions, and ANXA1 levels were also increased in infected BMDMs [164]. Similarly, lesions obtained from patients' sera with the mucosal form of the disease showed increased ANXA1 levels [164]. In the absence of ANXA1 using knockout mice, the inflammatory profile and lesion size were altered [164].

In addition, evidence from our laboratory showed that blocking FPR2 in macrophages using WRW4 resulted in attenuation of the augmentation of infection seen with exosomes. These results indicate that exosomes' effect on infection could be FPR2 dependent (Lira Filho and Olivier, unpublished). This study used WRW4 in *L. major*-LUC infections with exosomes which attenuated the effect of exosomes. When we used FPR2 agonist WKYMVm, we observed a significant increase in *L. major-LUC* activity compared to cells infected with parasites only. Our results suggest and further support that exosomes mediated exacerbation of infection is mediated by FPR2 activation.

8.6.3 **FPR2 does not alter selected cytokine/chemokine release in macrophages during *L. major* infection**

L. major parasites modulate the host immune response to favor their internalization and survival. Cutaneous leishmaniasis, caused by multiple *Leishmania* species, including *L. major,* triggers the production of multiple chemokines that ultimately attract immune cells like macrophages and neutrophils to the site of infection. Biopsies of patients with cutaneous

Leishmaniasis show high levels of MCP-1 and MIP-1α. Similarly, *in vivo* and *in vitro L. major* infections show an increase in the levels of many CC chemokines like MCP-1 and MIP1-α alongside other chemokines [159, 165, 166].

L. major infections alter the levels of inflammatory cytokines release like TNF-α, IL-1β, and IL-6 [159]. In biopsies obtained from *L. major* lesions in infected patients, TNF-α, IL-6, and IFN-γ were detected in 90% of biopsies [167]. Different cell types, including macrophages, produce IL-6. It is found to promote Th2 response in cutaneous Leishmaniasis [168]. TNF-α, a cytokine mainly produced by macrophages also plays an important role in parasite clearance during *Leishmania* infections by increasing the activity of macrophages and NO production [169]. Another cytokine with a role in Leishmaniasis progression is IL-1β, which is produced following NLRP3 inflammasome activation. IL-1β promotes inflammatory responses leading to increased IL-17 levels [170, 171]. Due to the role played by these chemokines and cytokines in *Leishmania* infections, we analyzed their expression levels in macrophages stimulated with FPR2 agonist and antagonist alone or with co-inoculation with *L. major.* Cells infected with *L. major* showed increased all chemokines/cytokines gene expression consistent with current literature. However, the level of IL-1β expression was unchanged. This finding is supported by the role of GP63 in *L. major* in inhibiting inflammasome activation and release of IL-1β [172].

In the context of *L. major* infection, levels of gene expression of MIP-1α, MIP-1β, MCP-1, IL-1β, and IL-6 were not changed in cells co-induced with *L. major* and FPR2 agonist or antagonist in comparison to cells infected with *L. major* only. However, we observed a trend of lower TNF-α gene expression in co-induction with *L. major* and FPR2 agonist. The role of the agonist WKYMVm in regulating TNF-α production is differential depending on the co-stimulatory condition. In a sepsis model, WKYMVm reduced TNF-α production, while in an ulcerative colitis mouse model, it markedly increased TNF-α levels [173, 174]. Additionally, Kang et al. reported that DCs stimulated with LPS and WKYMVm did not influence TNF-α production [175]. TNF-α promotes NO synthesis, and its inhibition in our model indicates the potential promotion of parasite survival within macrophages by FPR2 agonist. Repeating these experiments with a larger sample number is required to have higher statistical power and confirm this finding.

Similarly, when we measured IL-6, TNF-α, and MCP-1 in cell culture supernatants, we found a lower level of TNF-α in samples treated with agonist and *L. major* compared to cells

infected with *L. major* only. On the other hand, there was a trend of a higher level of IL-6 in the antagonist *L. major* co-inoculation group, which could indicate an interaction between *L. major* and FPR2 to suppress IL-6 production. However, the increase was insignificant, possibly because of the small sample size (n=3). The levels MCP-1 were unchanged in all conditions, indicating that the regulation of MIP-1α, MIP-1β, and MCP-1 does not occur via FPR2 during *L. major* infection. However, FPR2 activation could lead to the suppression of TNF-α production.

Further analysis using a cytokine/chemokine multiplex assay with a broader panel of analytes known to be activated by both FPR2 and *L. major* could provide greater insight on the role of FPR2 during *L.major*-exosome infection. For example, measuring the level of IL-10, a pro-resolution cytokine synthesized in macrophages/monocytes upon FPR2 activation, and is also released during *L. major* infection enhancing parasite survival would be an interesting avenue for research [176, 177]. Overall, our observations suggest that modulation of FPR2 does not significantly modify the capacity of *Leishmania* to induce inflammatory mediators.

8.6.4 FPR2 does not influence NO production in *L. major* infected LM1 macrophages

Nitric oxide (NO) is one of the most critical molecules produced by macrophages to control *Leishmania* infections. Release of IFN-γ and TNF-α during *Leishmania* infection in vivo promotes NO synthesis and release [178]. Although NO's role in parasite killing is well studied, limited data on the role of FPR2 in NO release is available. Recently, Horewicz et al. showed that WKYMVm reduces NO production in A7r5 smooth muscles cells and mice aorta [179]. However, according to our knowledge, the role of FPR2 in promoting NO production in macrophages is not reported in the literature.

We measured NO levels in the supernatants of stimulated LM1 cells after overnight incubation. FPR2 agonist and antagonist did not modulate NO production alone, nor did they modulate NO production during *L. major* infection. Similarly, no change in NO production was observed when LPS, a potent inducer of NO, was used in conjunction with the agonist or antagonist.

8.6.5 *L. major* exosomes alter the proteomic and phosphoproteomic profiles of macrophages

Our laboratory has recently established that co-inoculating *Leishmania* with exosomes exacerbates infection and releases different inflammatory molecules compared to *Leishmania*-

only infection [72]. Considering the ability of FPR2 antagonist to block the action of exosomes and FPR2 agonist mimicking the effect of exosomes during *L. major* infections; we hypothesized that exosomes interact with FPR2 to elicit dynamic changes in cells to enhance infections. Thus, we analyzed the protein content and phosphorylation patterns in inflammatory cells obtained from mice infected with *L. major* with or without exosomes and FPR2 agonist to decipher the differential signaling events occurring via the exosome-FPR2 axis.

We used *L. major* only infected mice (LSH), *L. major* with exosomes (EXL), *L. major* with agonist (AGO), and *L. major* with the antagonist (ANTA-EXL). To confirm patterns observed in *L. major*-LUC experiments and the validity of the mice trial, we measured the percentage of infected neutrophils and macrophages in obtained samples. Similar to our results with *L. major*-LUC, we observed a significant increase in the percentage of infected macrophages with EXL and AGO. At the same time, ANTA-EXL attenuated the effect of exosomes. We observed a similar trend in the percentage of infected neutrophils; however, the results were not significant.

To identify potential mechanisms of FPR2 activation by exosomes that lead to increased phagocytosis and parasite internalization, we analyzed the lysates of inflammatory recruited cells in treated mice using LC MS/MS analysis. Herein, we report for the first time proteomic and phosphoproteomic profiling of peritoneal myeloid cells during *L. major* infection with exosomes and FPR2 agonist. Using the powerful mass spectrometry proteomic/phosphoproteomic analysis, we show that mice infected with *L. major* and exosomes have a differential expression of proteins and phosphoproteins compared to *L. major* only infected mice. We also report shared protein expression patterns and upregulation in phosphorylated proteins between exosomes and agonist co-induced groups.

As expected, co-induction of macrophages in EXL led to a differential protein expression compared to LSH only. Although most proteins were shared between the three groups, 77 proteins were shared between AGO and EXL only. We hypothesize that these shared proteins are the proteins recruited as a result of FPR2 activation by exosomes.

Based on GO analysis and String analysis, the unique AGO-EXL proteins are involved in many immune system processes, mainly related to neutrophil function. These results correlate with the role of neutrophils as key players in *Leishmania* infection development and persistence

[180]. Shared upregulated proteins between AGO-EXL found in the enriched neutrophil activity groups included Hem-1 and ITGAL proteins. Hem-1 protein (alternatively named NCKAP1L) is a protein subunit of the WAVE protein complex in immune cells that is crucial for the activation of ARP2/3, a regulator of actin nucleation. Neutrophils deficient in Hem-1 exhibit defective migration and impaired phagocytosis [181]. Similarly, Hem-1 knockout macrophages have deficient phagocytic abilities and adhesion process [182]. ITGAL is a part of the lymphocyte function-associated antigen-1 (LFA-1) intergin is involved in neutrophil adhesion and migration, and it also enhances phagocytosis of apoptotic neutrophils by macrophages [183, 184].

Likewise, terms associated with glycolipid and glycosphingolipid metabolism were significantly enriched in AGO-EXL shared protein group indicating that FPR2 activation also results in changes in the metabolism of infected cells during *L. major* infections.

Of the 455 shared proteins between the three groups, 28 were upregulated in EXL and AGO (> 1.5-fold change). We considered these proteins to be differentially upregulated in the two groups compared to LSH. Like the shared proteins, the 28 upregulated proteins top enriched GO biological process terms were neutrophil degranulation, neutrophil activation involved in immune response, and neutrophil-mediated immunity. Other terms of interest enriched in this group were hydrogen peroxide catabolic process and hydrogen peroxide metabolic process. Cellular localization of these proteins based on GO cellular function showed high enrichment of terms related to neutrophil granules suggesting higher activation of neutrophils in AGO and EXL than LSH. To this end, proteomics data show upregulation in neutrophil activation proteins and proteins involved in the process of phagocytosis.

To capture signaling events altered due to FPR2 activation during *L. major* infection, we also analyzed the phosphoproteome of the samples. Interestingly, AGO and EXL did not have unique shared proteins, and all shared phosphoproteins were common between the three groups. LSH had 47 unique phosphoproteins that were not found in either AGO or EXL. GO analysis of unique LSH proteins showed enrichment in immune activation of cells, response to cytokine stimulus, and regulation of inflammation. To add, LSH and EXL uniquely shared 201 phosphoproteins of those; 31 were upregulated in EXL. GO analysis of upregulated protein showed enriched GO biological process terms related to the regulation of protein localization within the cell.

We identified 43 upregulated phosphoproteins in both AGO and EXL. Based on GO analysis, the terms cytoskeleton organization, positive regulation of TGF-β signaling, positive regulation of Notch signaling pathway, and the regulation of hemopoiesis were enriched in biological process terms. The process of phagocytosis requires remodeling of actin cytoskeleton to allow uptake of foreign particles [185]. Hence, we correlated the enrichment of proteins involved in cytoskeleton organization to the observed increased uptake of *Leishmania* parasites in myeloid cells. For instance, SH3 Domain-binding Protein 1 (SH3BP1) was differentially upregulated in both AGO and EXL and found in phosphoproteins enriched in cytoskeleton reorganization GO term. SH3BP1 is a GTpase activating protein (GAP) required for the completion of phagocytosis of large particles in a process dependent on PI3K activation, a process requiring actin disassembly [186]. Similarly, SA100A8 is differentially upregulated in AGO and EXL. SA100A8 is a calcium binding protein expressed in neutrophils and monocytes and plays a role in regulating inflammation and immune response. In addition to the vast role played by SA100A8 in immune modulation, it also mediates the rearrangement of the cytoskeleton, a requirement for successful phagocytosis and cell migration [187].

Enrichment in TGF-β positive signaling GO terms correlates with the role of TGF-β activation in enhancing macrophage phagocytic ability [188]. Interestingly, TGF-β also drives IL-17 production, a highly produced cytokine during the exacerbated L. major and exosome mice infections [72, 188]. In addition, multiple Notch signaling pathway terms appeared in the top enriched terms list. Activation of Notch signaling appears to promote increased phagocytosis in macrophages [189]. However, the role of FPR2 in regulating Notch signaling is not well studied. In microglia, specialized macrophages in the nervous system, FPR2 inhibits Notch signaling and promotes M2 polarization [190, 191]. To our knowledge, no studies have investigated the role of FPR2 in regulating Notch signaling in microbial infections. These observations suggest that multiple signaling pathways and protein phosphorylation events are activated during exosome-mediated infection exacerbation by FPR2, activating phagocytic cells and promoting parasite uptake. Further studies on the identified enriched phosphoproteins would provide an insight on mechanisms of increased phagocytosis of *L. major* induced by exosomes via FPR2.

Moreover, we performed kinase enrichment analysis on the 43 upregulated phosphoproteins in AGO and EXL using X2K software to determine upstream kinases [157].

The analysis predicted enrichment of ERK1/2 and other MAPK signaling components, known signaling pathways activated by FPR2 [106]. It also predicted the enrichment of Cyclin-dependent kinases (CDKs) like CDK1, CDK2, and CDK4 that are important for cell cycle and proliferation [192]. Out of the top 10 enriched kinases, five are components of ERK1/2 signaling.

To subvert the host immune system and promote its survival, *Leishmania* alters many signaling pathways, including ERK1/2 [193]. ERK1/2 signaling cascades mainly regulate cellular survival, proliferation, differentiation, apoptosis, and stress response. Signaling events initiated by ERK1/2 substrates are regulated by multiple components, thus resulting in distinct and sometimes opposing effects.

The downstream pathways of ERK1/2 that enhance phagocytosis are not well identified. However, multiple reports have shown that ERK1/2 enhances phagocytosis in macrophages. For instance, ERK1/2 is required for enhanced phagocytosis of THP-1 monocytes through C1q, and fibronectin-dependent enhanced FcγR mediated phagocytosis. Pharmacological inhibition of ERK1/2 results in the inhibition of phagocytosis. In addition, ERK1/2 activation is necessary for Syk phagocytosis of *Francisella tularensis* [194].

Similarly, in *E. coli* infections, hydrogen peroxide release promotes ERK1/2 and increases the uptake of bacteria [195]. ERK1/2 is also enhanced in *L. major* infections. Activation of ERK1/2 promotes parasite survival within neutrophils by delaying spontaneous apoptosis of mature neutrophils [193]. ERK1/2 activation cascade favors parasite survival and increased parasite burden in macrophages infected with *L. major.* Further studies confirming the role of ERK1/2 in exosome-FPR2 enhanced phagocytosis of macrophages are required to verify our findings.

Overall, our proteomic and phosphoproteomic data suggest exosomes activate neutrophils and macrophages to enhance phagocytosis and parasite survival via FPR2 using unique signaling pathways not utilized by *L. major* only. The bioinformatics data presented in this thesis is preliminary, owing to the limited sample size. Experiments must be repeated with a larger sample size to increase confidence and permit statistical analysis. As a future direction, we propose evaluating the association select identified proteins and phosphoproteins using other proteomic and genetic analyses such as western blots and gene expression analysis. We also

propose exploring the role of the exosome-FPR2 axis in activating TGFβ, Notch, and ERK1/2 signaling pathways to promote phagocytosis and survival of macrophages

8.7 Conclusion

This study was conducted to decipher signaling mechanisms of FPR2 and exosome interactions leading to enhanced infection. We used gene expression, biochemical, and proteomic/phosphoproteomic analysis to identify proteins involved in phagocytosis and signaling events regulating parasite internalization via the exosome-FPR2 axis. We conclude that the use of mass spectrometry for proteomics and phosphoproteomic analysis is a powerful method to identify those mechanisms utilized by exosomes to promote *L. major* internalization. We report differential regulation of proteins and phosphorylated proteins in exosomes plus *Leishmania* co-induced macrophages for the first time compared to *L. major* only infected macrophages. We also explore common proteins/phosphoproteins between exosomes and FPR2 agonist co-induced mice to highlight the interaction of exosomes with FPR2. Our results show that the exosome-FPR2 axis upregulates phagocytosis and cytoskeletal organization-related processes in mice peritoneal infections. This study opens a new perspective for the role played by exosomes in *L. major* infections. However, A more detailed exploration of the role of exosomes in activating ERK1/2, TGFβ, and Notch signaling pathways via FPR2 is needed to validate the results shown in this study.

9 References

1. Alvar, J., et al., *Leishmaniasis worldwide and global estimates of its incidence.* PloS one, 2012. **7**(5): p. e35671.
2. Georgiadou, S.P., K.P. Makaritsis, and G.N. Dalekos, *Leishmaniasis revisited: Current aspects on epidemiology, diagnosis and treatment.* Journal of translational internal medicine, 2015. **3**(2): p. 43-50.
3. Hotez, P.J., *The rise of leishmaniasis in the twenty-first century.* Transactions of the Royal Society of Tropical Medicine and Hygiene, 2018. **112**(9): p. 421-422.
4. García Miss, M. and A.d.Y. Mérida, *Cellular response to leishmaniasis.* Rev Biomed, 1995. **6**: p. 92-100.
5. mondiale de la Santé, O. and W.H. Organization, *Global leishmaniasis update, 2006–2015: a turning point in leishmaniasis surveillance–Le point sur la situation mondiale de la leishmaniose, 2006-2015: un tournant dans la surveillance de la maladie.* Weekly Epidemiological Record= Relevé épidémiologique hebdomadaire, 2017. **92**(38): p. 557-565.
6. Roatt, B.M., et al., *Recent advances and new strategies on leishmaniasis treatment.* Applied Microbiology and Biotechnology, 2020. **104**(21): p. 8965-8977.
7. Akhoundi, M., et al., *A Historical Overview of the Classification, Evolution, and Dispersion of Leishmania Parasites and Sandflies.* PLoS neglected tropical diseases, 2016. **10**(3): p. e0004349-e0004349.
8. Akhoundi, M., et al., *A historical overview of the classification, evolution, and dispersion of Leishmania parasites and sandflies.* PLoS neglected tropical diseases, 2016. **10**(3).
9. MAROLI, M., et al., *Phlebotomine sandflies and the spreading of leishmaniases and other diseases of public health concern.* Medical and Veterinary Entomology, 2013. **27**(2): p. 123-147.
10. Harkins, K.M., et al., *Phylogenomic reconstruction supports supercontinent origins for Leishmania.* Infection, Genetics and Evolution, 2016. **38**: p. 101-109.
11. Akhoundi, M., et al., *Leishmania infections: Molecular targets and diagnosis.* Molecular aspects of medicine, 2017. **57**: p. 1-29.
12. David, C.V. and N. Craft, *Cutaneous and mucocutaneous leishmaniasis.* Dermatologic Therapy, 2009. **22**(6): p. 491-502.
13. Silveira, F.T., R. Lainson, and C.E. Corbett, *Clinical and immunopathological spectrum of American cutaneous leishmaniasis with special reference to the disease in Amazonian Brazil: a review.* Memórias do Instituto Oswaldo Cruz, 2004. **99**(3): p. 239-251.
14. Akhoundi, M., et al., *A historical overview of the classification, evolution, and dispersion of Leishmania parasites and sandflies.* PLoS neglected tropical diseases, 2016. **10**(3): p. e0004349.
15. Ready, P., *Epidemiology of visceral leishmaniasis. Clin Epidemiol 6: 147–154*. 2014.
16. Choi, C.M. and E.A. Lerner. *Leishmaniasis as an emerging infection*. in *Journal of Investigative Dermatology Symposium Proceedings*. 2001. Elsevier.
17. WHO, E.C., *Control of the Leishmaniases.* Wld. Hlth. Org. techn. Rep. Ser., 1990. **793**.
18. Lainson, R. and J.J. Shaw, *Evolution, classification and geographical distribution*. 1987: Academic Press.
19. Rogers, M.E., M. Chance, and P. Bates, *The role of promastigote secretory gel in the origin and transmission of the infective stage of Leishmania mexicana by the sandfly Lutzomyia longipalpis.* Parasitology, 2002. **124**(5): p. 495-507.
20. Gossage, S.M., M.E. Rogers, and P.A. Bates, *Two separate growth phases during the development of Leishmania in sand flies: implications for understanding the life cycle.* International journal for parasitology, 2003. **33**(10): p. 1027-1034.

21. Kamhawi, S., *Phlebotomine sand flies and Leishmania parasites: friends or foes?* Trends in parasitology, 2006. **22**(9): p. 439-445.
22. Sacks, D.L. and P.V. Perkins, *Development of infective stage Leishmania promastigotes within phlebotomine sand flies.* The American journal of tropical medicine and hygiene, 1985. **34**(3): p. 456-459.
23. Serafim, T.D., et al., *Sequential blood meals promote Leishmania replication and reverse metacyclogenesis augmenting vector infectivity.* Nature microbiology, 2018. **3**(5): p. 548-555.
24. Giraud, E., et al., *Quantifying Leishmania metacyclic promastigotes from individual sandfly bites reveals the efficiency of vector transmission.* Communications Biology, 2019. **2**(1): p. 1-12.
25. Peters, N.C. and D.L. Sacks, *The impact of vector-mediated neutrophil recruitment on cutaneous leishmaniasis.* Cellular microbiology, 2009. **11**(9): p. 1290-1296.
26. De Almeida, M., et al., *Leishmanial infection: analysis of its first steps. A review.* Memorias do Instituto Oswaldo Cruz, 2003. **98**(7): p. 861-870.
27. Wells, A., A. Nuschke, and C.C. Yates, *Skin tissue repair: matrix microenvironmental influences.* Matrix Biology, 2016. **49**: p. 25-36.
28. Silva-Almeida, M., et al., *Extracellular matrix alterations in experimental Leishmania amazonensis infection in susceptible and resistant mice.* Veterinary research, 2012. **43**(1): p. 10.
29. de Menezes, J.P., E.M. Saraiva, and B. da Rocha-Azevedo, *The site of the bite: Leishmania interaction with macrophages, neutrophils and the extracellular matrix in the dermis.* Parasites & vectors, 2016. **9**(1): p. 264.
30. McGwire, B.S., K.-P. Chang, and D.M. Engman, *Migration through the extracellular matrix by the parasitic protozoan Leishmania is enhanced by surface metalloprotease gp63.* Infection and immunity, 2003. **71**(2): p. 1008-1010.
31. Kulkarni, M.M., et al., *Fibronectin binding and proteolytic degradation by Leishmania and effects on macrophage activation.* Infection and immunity, 2008. **76**(4): p. 1738-1747.
32. Carlsen, E.D., et al., *Leishmania amazonensis amastigotes trigger neutrophil activation but resist neutrophil microbicidal mechanisms.* Infection and immunity, 2013. **81**(11): p. 3966-3974.
33. Guimarães-Costa, A.B., et al., *Leishmania amazonensis promastigotes induce and are killed by neutrophil extracellular traps.* Proceedings of the National Academy of Sciences, 2009. **106**(16): p. 6748-6753.
34. Guimarães-Costa, A.B., et al., *3'-nucleotidase/nuclease activity allows Leishmania parasites to escape killing by neutrophil extracellular traps.* Infection and immunity, 2014. **82**(4): p. 1732-1740.
35. Guimarães-Costa, A.B., et al., *Neutrophil extracellular traps reprogram IL-4/GM-CSF-induced monocyte differentiation to anti-inflammatory macrophages.* Frontiers in immunology, 2017. **8**: p. 523.
36. Ritter, U., F. Frischknecht, and G. van Zandbergen, *Are neutrophils important host cells for Leishmania parasites?* Trends in parasitology, 2009. **25**(11): p. 505-510.
37. van Zandbergen, G., et al., *Cutting edge: neutrophil granulocyte serves as a vector for Leishmania entry into macrophages.* The Journal of Immunology, 2004. **173**(11): p. 6521-6525.
38. Ribeiro-Gomes, F.L., et al., *Efficient capture of infected neutrophils by dendritic cells in the skin inhibits the early anti-leishmania response.* PLoS pathogens, 2012. **8**(2).
39. Beattie, L. and P.M. Kaye, *Leishmania–host interactions: what has imaging taught us?* Cellular microbiology, 2011. **13**(11): p. 1659-1667.
40. Goundry, A., et al., *Inhibitor of serine peptidase 2 enhances Leishmania major survival in the skin through control of monocytes and monocyte-derived cells.* The FASEB Journal, 2018. **32**(3): p. 1315-1327.

41. Bates, P.A., *Transmission of Leishmania metacyclic promastigotes by phlebotomine sand flies.* International journal for parasitology, 2007. **37**(10): p. 1097-1106.
42. Shio, M.T., et al., *Host cell signalling and leishmania mechanisms of evasion.* Journal of tropical medicine, 2012. **2012**.
43. Sacks, D. and C. Anderson, *Re-examination of the immunosuppressive mechanisms mediating non-cure of Leishmania infection in mice.* Immunological reviews, 2004. **201**(1): p. 225-238.
44. Vinet, A.F., et al., *The Leishmania donovani lipophosphoglycan excludes the vesicular proton-ATPase from phagosomes by impairing the recruitment of synaptotagmin V.* PLoS pathogens, 2009. **5**(10): p. e1000628.
45. Bhattacharyya, S., et al., *Selective impairment of protein kinase C isotypes in murine macrophage by Leismania donovani.* Molecular and cellular biochemistry, 2001. **216**(1): p. 47-57.
46. Guler, R., et al., *PKCδ regulates IL-12p40/p70 production by macrophages and dendritic cells, driving a type 1 healer phenotype in cutaneous leishmaniasis.* European journal of immunology, 2011. **41**(3): p. 706-715.
47. Privé, C. and A. Descoteaux, *Leishmania donovani promastigotes evade the activation of mitogen-activated protein kinases p38, c-Jun N-terminal kinase, and extracellular signal-regulated kinase-1/2 during infection of naive macrophages.* European journal of immunology, 2000. **30**(8): p. 2235-2244.
48. Forget, G., et al., *Role of host protein tyrosine phosphatase SHP-1 in Leishmania donovani-induced inhibition of nitric oxide production.* Infection and immunity, 2006. **74**(11): p. 6272-6279.
49. Gomez, M.A., et al., *Leishmania GP63 alters host signaling through cleavage-activated protein tyrosine phosphatases.* Science signaling, 2009. **2**(90): p. ra58-ra58.
50. Hallé, M., et al., *The Leishmania surface protease GP63 cleaves multiple intracellular proteins and actively participates in p38 mitogen-activated protein kinase inactivation.* Journal of Biological Chemistry, 2009. **284**(11): p. 6893-6908.
51. Olivier, M., et al., *Modulation of interferon-γ-induced macrophage activation by phosphotyrosine phosphatases inhibition: effect on murine leishmaniasis progression.* Journal of Biological Chemistry, 1998. **273**(22): p. 13944-13949.
52. Matte, C., et al., *Peroxovanadium-mediated protection against murine leishmaniasis: role of the modulation of nitric oxide.* European journal of immunology, 2000. **30**(9): p. 2555-2564.
53. Fukao, T., et al., *PI3K-mediated negative feedback regulation of IL-12 production in DCs.* Nature immunology, 2002. **3**(9): p. 875-881.
54. Pereira, R.M., et al., *Novel role for the double-stranded RNA-activated protein kinase PKR: modulation of macrophage infection by the protozoan parasite Leishmania.* The FASEB Journal, 2010. **24**(2): p. 617-626.
55. Faria, M.S., et al., *Role of protein kinase R in the killing of Leishmania major by macrophages in response to neutrophil elastase and TLR4 via TNFα and IFNβ.* The FASEB Journal, 2014. **28**(7): p. 3050-3063.
56. Rawlings, J.S., K.M. Rosler, and D.A. Harrison, *The JAK/STAT signaling pathway.* Journal of cell science, 2004. **117**(8): p. 1281-1283.
57. Forget, G., D.J. Gregory, and M. Olivier, *Proteasome-mediated degradation of STAT1α following infection of macrophages with Leishmania donovani.* Journal of Biological Chemistry, 2005. **280**(34): p. 30542-30549.
58. Fernández-Figueroa, E.A., et al., *Down-regulation of TLR and JAK/STAT pathway genes is associated with diffuse cutaneous leishmaniasis: a gene expression analysis in NK cells from patients infected with Leishmania mexicana.* PLoS neglected tropical diseases, 2016. **10**(3): p. e0004570.

59. Matte, C. and A. Descoteaux, *Leishmania donovani amastigotes impair gamma interferon-induced STAT1α nuclear translocation by blocking the interaction between STAT1α and importin-α5.* Infection and immunity, 2010. **78**(9): p. 3736-3743.
60. Franco, L.H., S.M. Beverley, and D.S. Zamboni, *Innate immune activation and subversion of mammalian functions by Leishmania lipophosphoglycan.* Journal of parasitology research, 2012. **2012**.
61. Gupta, G., S. Oghumu, and A.R. Satoskar, *Mechanisms of immune evasion in leishmaniasis.* Advances in applied microbiology, 2013. **82**: p. 155-184.
62. Forestier, C.-L., Q. Gao, and G.-J. Boons, *Leishmania lipophosphoglycan: how to establish structure-activity relationships for this highly complex and multifunctional glycoconjugate?* Frontiers in cellular and infection microbiology, 2015. **4**: p. 193.
63. Anversa, L., et al., *Human leishmaniasis in Brazil: a general review.* Revista da Associação Médica Brasileira, 2018. **64**: p. 281-289.
64. Živanović, V., et al., *Chemical mapping of leishmania infection in live cells by SERS microscopy.* Analytical chemistry, 2018. **90**(13): p. 8154-8161.
65. Chawla, M. and R.A. Vishwakarma, *Alkylacylglycerolipid domain of GPI molecules of Leishmania is responsible for inhibition of PKC-mediated c-fos expression.* Journal of lipid research, 2003. **44**(3): p. 594-600.
66. Isnard, A., M.T. Shio, and M. Olivier, *Impact of Leishmania metalloprotease GP63 on macrophage signaling.* Frontiers in cellular and infection microbiology, 2012. **2**: p. 72.
67. Shao, S., et al., *Complement evasion: an effective strategy that parasites utilize to survive in the host.* Frontiers in microbiology, 2019. **10**: p. 532.
68. Olivier, M., et al., *Leishmania virulence factors: focus on the metalloprotease GP63.* Microbes and infection, 2012. **14**(15): p. 1377-1389.
69. Podinovskaia, M. and A. Descoteaux, *Leishmania and the macrophage: a multifaceted interaction.* Future microbiology, 2015. **10**(1): p. 111-129.
70. Jaramillo, M., et al., *Leishmania repression of host translation through mTOR cleavage is required for parasite survival and infection.* Cell host & microbe, 2011. **9**(4): p. 331-341.
71. Elmahallawy, E.K. and A.A. Alkhaldi, *Insights into Leishmania Molecules and Their Potential Contribution to the Virulence of the Parasite.* Veterinary Sciences, 2021. **8**(2): p. 33.
72. Atayde, Vanessa D., et al., *Exosome Secretion by the Parasitic Protozoan Leishmania within the Sand Fly Midgut.* Cell Reports, 2015. **13**(5): p. 957-967.
73. Chargaff, E. and R. West, *The biological significance of the thromboplastic protein of blood.* J Biol Chem, 1946. **166**(1): p. 189-197.
74. Wolf, P., *The nature and significance of platelet products in human plasma.* British journal of haematology, 1967. **13**(3): p. 269-288.
75. De Broe, M.E., et al., *Spontaneous shedding of plasma membrane fragments by human cells in vivo and in vitro.* Clinica Chimica Acta, 1977. **81**(3): p. 237-245.
76. Taylor, D.D., H.D. Homesley, and G.J. Doellgast, *Binding of specific peroxidase-labeled antibody to placental-type phosphatase on tumor-derived membrane fragments.* Cancer Research, 1980. **40**(11): p. 4064-4069.
77. Harding, C. and P. Stahl, *Transferrin recycling in reticulocytes: pH and iron are important determinants of ligand binding and processing.* Biochemical and biophysical research communications, 1983. **113**(2): p. 650-658.
78. Pan, B.-T. and R.M. Johnstone, *Fate of the transferrin receptor during maturation of sheep reticulocytes in vitro: selective externalization of the receptor.* Cell, 1983. **33**(3): p. 967-978.

79. Harding, C., J. Heuser, and P. Stahl, *Receptor-mediated endocytosis of transferrin and recycling of the transferrin receptor in rat reticulocytes.* The Journal of cell biology, 1983. **97**(2): p. 329-339.
80. Raposo, G., et al., *B lymphocytes secrete antigen-presenting vesicles.* The Journal of experimental medicine, 1996. **183**(3): p. 1161-1172.
81. Valadi, H., et al., *Exosome-mediated transfer of mRNAs and microRNAs is a novel mechanism of genetic exchange between cells.* Nature cell biology, 2007. **9**(6): p. 654-659.
82. Raposo, G. and P.D. Stahl, *Extracellular vesicles: a new communication paradigm?* Nature Reviews Molecular Cell Biology, 2019. **20**(9): p. 509-510.
83. Gould, S.J. and G. Raposo, *As we wait: coping with an imperfect nomenclature for extracellular vesicles.* Journal of extracellular vesicles, 2013. **2**(1): p. 20389.
84. Cocucci, E. and J. Meldolesi, *Ectosomes and exosomes: shedding the confusion between extracellular vesicles.* Trends in cell biology, 2015. **25**(6): p. 364-372.
85. Mathivanan, S., H. Ji, and R.J. Simpson, *Exosomes: extracellular organelles important in intercellular communication.* Journal of proteomics, 2010. **73**(10): p. 1907-1920.
86. Akers, J.C., et al., *Biogenesis of extracellular vesicles (EV): exosomes, microvesicles, retrovirus-like vesicles, and apoptotic bodies.* Journal of neuro-oncology, 2013. **113**(1): p. 1-11.
87. Crescitelli, R., et al., *Distinct RNA profiles in subpopulations of extracellular vesicles: apoptotic bodies, microvesicles and exosomes.* Journal of extracellular vesicles, 2013. **2**(1): p. 20677.
88. Simpson, R.J. and S. Mathivanan, *Extracellular microvesicles: the need for internationally recognised nomenclature and stringent purification criteria.* 2012.
89. Abels, E.R. and X.O. Breakefield, *Introduction to extracellular vesicles: biogenesis, RNA cargo selection, content, release, and uptake*. 2016, Springer.
90. Takahashi, A., et al., *Exosomes maintain cellular homeostasis by excreting harmful DNA from cells.* Nature communications, 2017. **8**: p. 15287.
91. Kosaka, N., et al., *Secretory mechanisms and intercellular transfer of microRNAs in living cells.* Journal of Biological Chemistry, 2010. **285**(23): p. 17442-17452.
92. Nolte, E., et al., *Extracellular vesicles and viruses: Are they close relatives?* Proceedings of the National Academy of Sciences, 2016. **113**(33): p. 9155-9161.
93. Sanjuán, R., *Collective infectious units in viruses.* Trends in microbiology, 2017. **25**(5): p. 402-412.
94. Singh, P.P., et al., *Exosomes isolated from mycobacteria-infected mice or cultured macrophages can recruit and activate immune cells in vitro and in vivo.* The Journal of Immunology, 2012. **189**(2): p. 777-785.
95. Mantel, P.-Y., et al., *Malaria-infected erythrocyte-derived microvesicles mediate cellular communication within the parasite population and with the host immune system.* Cell host & microbe, 2013. **13**(5): p. 521-534.
96. Szempruch, A.J., et al., *Extracellular vesicles from Trypanosoma brucei mediate virulence factor transfer and cause host anemia.* Cell, 2016. **164**(1-2): p. 246-257.
97. Silverman, J.M., et al., *Proteomic analysis of the secretome of Leishmania donovani.* Genome biology, 2008. **9**(2): p. R35.
98. Silverman, J.M., et al., *An exosome-based secretion pathway is responsible for protein export from Leishmania and communication with macrophages.* Journal of Cell Science, 2010. **123**(6): p. 842-852.
99. Hassani, K., et al., *Temperature-induced protein secretion by Leishmania mexicana modulates macrophage signalling and function.* PloS one, 2011. **6**(5): p. e18724-e18724.
100. Castelli, G., et al., *Exosome secretion by Leishmania infantum modulate the chemotactic behavior and cytokinic expression creating an environment permissive for early infection.* Experimental Parasitology, 2019. **198**: p. 39-45.

101. Gómez, M.A. and M. Olivier, *Proteases and phosphatases during Leishmania-macrophage interaction: paving the road for pathogenesis.* Virulence, 2010. **1**(4): p. 314-318.
102. Leitherer, S., et al., *Characterization of the Protein Tyrosine Phosphatase LmPRL-1 Secreted by Leishmania major via the Exosome Pathway.* Infection and Immunity, 2017. **85**(8): p. e00084-17.
103. Atayde, V.D., et al., *Exploitation of the Leishmania exosomal pathway by Leishmania RNA virus 1.* Nat Microbiol, 2019. **4**(4): p. 714-723.
104. Takeuchi, O. and S. Akira, *Pattern recognition receptors and inflammation.* Cell, 2010. **140**(6): p. 805-820.
105. Chen, K., et al., *Regulation of inflammation by members of the formyl-peptide receptor family.* Journal of Autoimmunity, 2017. **85**: p. 64-77.
106. Cattaneo, F., M. Parisi, and R. Ammendola, *Distinct signaling cascades elicited by different formyl peptide receptor 2 (FPR2) agonists.* International journal of molecular sciences, 2013. **14**(4): p. 7193-7230.
107. He, H.-Q. and R.D. Ye, *The formyl peptide receptors: diversity of ligands and mechanism for recognition.* Molecules, 2017. **22**(3): p. 455.
108. Li, L., et al., *New development in studies of formyl-peptide receptors: critical roles in host defense.* Journal of leukocyte biology, 2016. **99**(3): p. 425-435.
109. Cattaneo, F., et al., *Cell-surface receptors transactivation mediated by g protein-coupled receptors.* International journal of molecular sciences, 2014. **15**(11): p. 19700-19728.
110. Iaccio, A., et al., *FPRL1-mediated induction of superoxide in LL-37-stimulated IMR90 human fibroblast.* Archives of Biochemistry and Biophysics, 2009. **481**(1): p. 94-100.
111. Richard, D.Y., et al., *International Union of Basic and Clinical Pharmacology. LXXIII. Nomenclature for the formyl peptide receptor (FPR) family.* Pharmacological reviews, 2009. **61**(2): p. 119-161.
112. Venkatakrishnan, A.J., et al., *Molecular signatures of G-protein-coupled receptors.* Nature, 2013. **494**(7436): p. 185-194.
113. Nawaz, M.I., et al., *d-Peptide analogues of Boc-Phe-Leu-Phe-Leu-Phe-COOH induce neovascularization via endothelial N-formyl peptide receptor 3.* Angiogenesis, 2020. **23**(3): p. 357-369.
114. He, H.-Q. and R.D. Ye, *The Formyl Peptide Receptors: Diversity of Ligands and Mechanism for Recognition.* Molecules (Basel, Switzerland), 2017. **22**(3): p. 455.
115. Nathan, C. and A. Ding, *Nonresolving inflammation.* Cell, 2010. **140**(6): p. 871-882.
116. Sodin-Semrl, S., et al., *Opposing regulation of interleukin-8 and NF-kB responses by lipoxin A4 and serum amyloid a via the common lipoxin a receptor.* International journal of immunopathology and pharmacology, 2004. **17**(2): p. 145-155.
117. Gerke, V. and S.E. Moss, *Annexins: from structure to function.* Physiological reviews, 2002. **82**(2): p. 331-371.
118. Gavins, F.N.E. and M.J. Hickey, *Annexin A1 and the regulation of innate and adaptive immunity.* Frontiers in immunology, 2012. **3**: p. 354.
119. Solito, E., et al., *Post-translational modification plays an essential role in the translocation of annexin A1 from the cytoplasm to the cell surface.* The FASEB journal, 2006. **20**(9): p. 1498-1500.
120. Perretti, M., et al., *Endogenous lipid-and peptide-derived anti-inflammatory pathways generated with glucocorticoid and aspirin treatment activate the lipoxin A 4 receptor.* Nature medicine, 2002. **8**(11): p. 1296-1302.
121. Ernst, S., et al., *An annexin 1 N-terminal peptide activates leukocytes by triggering different members of the formyl peptide receptor family.* The Journal of Immunology, 2004. **172**(12): p. 7669-7676.

122. Frey, O., et al., *The role of regulatory T cells in antigen-induced arthritis: aggravation of arthritis after depletion and amelioration after transfer of CD4+ CD25+ T cells.* Arthritis Res Ther, 2005. **7**(2): p. 1-11.
123. Yang, Y.H., et al., *Modulation of inflammation and response to dexamethasone by Annexin 1 in antigen-induced arthritis.* Arthritis & Rheumatism, 2004. **50**(3): p. 976-984.
124. Solito, E., et al., *A novel calcium-dependent proapoptotic effect of annexin 1 on human neutrophils.* The FASEB journal, 2003. **17**(11): p. 1-27.
125. Scannell, M., et al., *Annexin-1 and peptide derivatives are released by apoptotic cells and stimulate phagocytosis of apoptotic neutrophils by macrophages.* The Journal of Immunology, 2007. **178**(7): p. 4595-4605.
126. Nathan, C., *Neutrophils and immunity: challenges and opportunities.* Nature reviews immunology, 2006. **6**(3): p. 173-182.
127. Headland, S.E. and L.V. Norling. *The resolution of inflammation: Principles and challenges*. in *Seminars in immunology*. 2015. Elsevier.
128. Subramanian, P., et al., *Regulation of tissue infiltration by neutrophils: role of integrin α3β1 and other factors.* Current opinion in hematology, 2016. **23**(1): p. 36.
129. Lim, L.H., et al., *Promoting detachment of neutrophils adherent to murine postcapillary venules to control inflammation: effect of lipocortin 1.* Proceedings of the National Academy of Sciences, 1998. **95**(24): p. 14535-14539.
130. ZOUKI, C., S. OUELLET, and J.G. FILEP, *The anti-inflammatory peptides, antiflammins, regulate the expression of adhesion molecules on human leukocytes and prevent neutrophil adhesion to endothelial cells.* The FASEB Journal, 2000. **14**(3): p. 572-580.
131. Blume, K.E., et al., *Cleavage of annexin A1 by ADAM10 during secondary necrosis generates a monocytic "find-me" signal.* The Journal of Immunology, 2012. **188**(1): p. 135-145.
132. Arur, S., et al., *Annexin I is an endogenous ligand that mediates apoptotic cell engulfment.* Developmental cell, 2003. **4**(4): p. 587-598.
133. Poon, I.K., et al., *Apoptotic cell clearance: basic biology and therapeutic potential.* Nature Reviews Immunology, 2014. **14**(3): p. 166-180.
134. Maderna, P. and C. Godson, *Phagocytosis of apoptotic cells and the resolution of inflammation.* Biochimica et Biophysica Acta (BBA)-Molecular Basis of Disease, 2003. **1639**(3): p. 141-151.
135. Soehnlein, O., L. Lindbom, and C. Weber, *Mechanisms underlying neutrophil-mediated monocyte recruitment.* Blood, The Journal of the American Society of Hematology, 2009. **114**(21): p. 4613-4623.
136. McArthur, S., et al., *Definition of a novel pathway centered on lysophosphatidic acid to recruit monocytes during the resolution phase of tissue inflammation.* The Journal of Immunology, 2015. **195**(3): p. 1139-1151.
137. Maderna, P., et al., *Modulation of phagocytosis of apoptotic neutrophils by supernatant from dexamethasone-treated macrophages and annexin-derived peptide Ac2–26.* The Journal of Immunology, 2005. **174**(6): p. 3727-3733.
138. Yona, S., et al., *Impaired phagocytic mechanism in annexin 1 null macrophages.* British journal of pharmacology, 2006. **148**(4): p. 469-477.
139. Cooray, S.N., et al., *Ligand-specific conformational change of the G-protein–coupled receptor ALX/FPR2 determines proresolving functional responses.* Proceedings of the National Academy of Sciences, 2013. **110**(45): p. 18232-18237.
140. Vanessa, K.H.Q., et al., *Absence of Annexin A1 impairs host adaptive immunity against Mycobacterium tuberculosis in vivo.* Immunobiology, 2015. **220**(5): p. 614-623.

141. Tzelepis, F., et al., *Annexin1 regulates DC efferocytosis and cross-presentation during Mycobacterium tuberculosis infection.* The Journal of clinical investigation, 2015. **125**(2): p. 752-768.
142. Machado, M.G., et al., *The Annexin A1/FPR2 pathway controls the inflammatory response and bacterial dissemination in experimental pneumococcal pneumonia.* The FASEB Journal, 2020. **34**(2): p. 2749-2764.
143. Damazo, A.S., et al., *Critical protective role for annexin 1 gene expression in the endotoxemic murine microcirculation.* The American journal of pathology, 2005. **166**(6): p. 1607-1617.
144. Hiramoto, H., et al., *Annexin A1 negatively regulates viral RNA replication of hepatitis C virus.* Acta Medica Okayama, 2015. **69**(2): p. 71-78.
145. Arora, S., et al., *Influenza A virus enhances its propagation through the modulation of Annexin-A1 dependent endosomal trafficking and apoptosis.* Cell Death & Differentiation, 2016. **23**(7): p. 1243-1256.
146. Ampomah, P.B., et al., *Formyl peptide receptor 2 is regulated by RNA mimics and viruses through an IFN-β-STAT3-dependent pathway.* The FASEB Journal, 2018. **32**(3): p. 1468-1478.
147. Alessi, M.-C., et al., *FPR2: A novel promising target for the treatment of influenza.* Frontiers in microbiology, 2017. **8**: p. 1719.
148. de Oliveira Cardoso, M.F., et al., *Annexin A1 peptide is able to induce an anti-parasitic effect in human placental explants infected by Toxoplasma gondii.* Microbial pathogenesis, 2018. **123**: p. 153-161.
149. Forget, G., et al., *Role of host phosphotyrosine phosphatase SHP-1 in the development of murine leishmaniasis.* European journal of immunology, 2001. **31**(11): p. 3185-3196.
150. Roy, G., et al., *Episomal and stable expression of the luciferase reporter gene for quantifying Leishmania spp. infections in macrophages and in animal models.* Molecular and biochemical parasitology, 2000. **110**(2): p. 195-206.
151. Da Silva, R. and D. Sacks, *Metacyclogenesis is a major determinant of Leishmania promastigote virulence and attenuation.* Infection and immunity, 1987. **55**(11): p. 2802-2806.
152. Soo, C.Y., et al., *Nanoparticle tracking analysis monitors microvesicle and exosome secretion from immune cells.* Immunology, 2012. **136**(2): p. 192-197.
153. Ridnour, L.A., et al., *A spectrophotometric method for the direct detection and quantitation of nitric oxide, nitrite, and nitrate in cell culture media.* Anal Biochem, 2000. **281**(2): p. 223-9.
154. Chen, E.Y., et al., *Enrichr: interactive and collaborative HTML5 gene list enrichment analysis tool.* BMC bioinformatics, 2013. **14**(1): p. 1-14.
155. Mi, H. and P. Thomas, *PANTHER pathway: an ontology-based pathway database coupled with data analysis tools*, in *Protein Networks and Pathway Analysis*. 2009, Springer. p. 123-140.
156. Szklarczyk, D., et al., *The STRING database in 2021: customizable protein–protein networks, and functional characterization of user-uploaded gene/measurement sets.* Nucleic acids research, 2021. **49**(D1): p. D605-D612.
157. Clarke, D.J.B., et al., *eXpression2Kinases (X2K) Web: linking expression signatures to upstream cell signaling networks.* Nucleic acids research, 2018. **46**(W1): p. W171-W179.
158. Panaro, M., et al., *Nitric oxide production by Leishmania-infected macrophages and modulation by prostaglandin E 2.* Clinical and experimental medicine, 2001. **1**(3): p. 137-143.
159. Matte, C. and M. Olivier, *Leishmania-induced cellular recruitment during the early inflammatory response: modulation of proinflammatory mediators.* The journal of infectious diseases, 2002. **185**(5): p. 673-681.
160. Scott, P. and F.O. Novais, *Cutaneous leishmaniasis: immune responses in protection and pathogenesis.* Nature Reviews Immunology, 2016. **16**(9): p. 581-592.

161. Wei, F., et al., *Role of the lipoxin A4 receptor in the development of neutrophil extracellular traps in Leishmania infantum infection.* Parasites & Vectors, 2019. **12**(1): p. 275.
162. Wenzel, A. and G. Van Zandbergen, *Lipoxin A4 receptor dependent leishmania infection: Brief definite report.* Autoimmunity, 2009. **42**(4): p. 331-333.
163. Plagge, M. and T. Laskay, *Early production of the neutrophil-derived lipid mediators LTB4 and LXA4 is modulated by intracellular infection with Leishmania major.* BioMed research international, 2017. **2017**.
164. Oliveira, L.G., et al., *Annexin A1 is involved in the resolution of inflammatory responses during Leishmania braziliensis infection.* The Journal of Immunology, 2017. **198**(8): p. 3227-3236.
165. Filardy, A.A., et al., *Infection with Leishmania major induces a cellular stress response in macrophages.* PLoS One, 2014. **9**(1): p. e85715.
166. Rabhi, I., et al., *Transcriptomic signature of Leishmania infected mice macrophages: a metabolic point of view.* 2012.
167. Louzir, H., et al., *Immunologic determinants of disease evolution in localized cutaneous leishmaniasis due to Leishmania major.* Journal of Infectious Diseases, 1998. **177**(6): p. 1687-1695.
168. Moskowitz, N.H., D.R. Brown, and S.L. Reiner, *Efficient immunity against Leishmania major in the absence of interleukin-6.* Infection and immunity, 1997. **65**(6): p. 2448-2450.
169. Liew, F.Y., X.Q. Wei, and L. Proudfoot, *Cytokines and nitric oxide as effector molecules against parasitic infections.* Philosophical Transactions of the Royal Society of London. Series B: Biological Sciences, 1997. **352**(1359): p. 1311-1315.
170. Voronov, E., et al., *IL-1-induced inflammation promotes development of leishmaniasis in susceptible BALB/c mice.* International immunology, 2010. **22**(4): p. 245-257.
171. Gonzalez-Lombana, C., et al., *IL-17 mediates immunopathology in the absence of IL-10 following Leishmania major infection.* PLoS pathogens, 2013. **9**(3): p. e1003243.
172. Shio, M.T., et al., *PKC/ROS-mediated NLRP3 inflammasome activation is attenuated by Leishmania zinc-metalloprotease during infection.* PLoS neglected tropical diseases, 2015. **9**(6): p. e0003868.
173. Kim, S.D., et al., *The agonists of formyl peptide receptors prevent development of severe sepsis after microbial infection.* The Journal of Immunology, 2010. **185**(7): p. 4302-4310.
174. Kim, S.D., et al., *The immune-stimulating peptide WKYMVm has therapeutic effects against ulcerative colitis.* Experimental & molecular medicine, 2013. **45**(9): p. e40-e40.
175. Kang, H.K., et al., *The synthetic peptide Trp-Lys-Tyr-Met-Val-D-Met inhibits human monocyte-derived dendritic cell maturation via formyl peptide receptor and formyl peptide receptor-like 2.* The Journal of Immunology, 2005. **175**(2): p. 685-692.
176. Souza, D.G., et al., *The required role of endogenously produced lipoxin A4 and annexin-1 for the production of IL-10 and inflammatory hyporesponsiveness in mice.* The Journal of Immunology, 2007. **179**(12): p. 8533-8543.
177. Kane, M.M. and D.M. Mosser, *The role of IL-10 in promoting disease progression in leishmaniasis.* The Journal of Immunology, 2001. **166**(2): p. 1141-1147.
178. Gantt, K.R., et al., *Oxidative responses of human and murine macrophages during phagocytosis of Leishmania chagasi.* The Journal of Immunology, 2001. **167**(2): p. 893-901.
179. Horewicz, V.V., et al., *FPR2/ALX activation reverses LPS-induced vascular hyporeactivity in aorta and increases survival in a pneumosepsis model.* European journal of pharmacology, 2015. **746**: p. 267-273.
180. Carlsen, E., et al., *Permissive and protective roles for neutrophils in leishmaniasis.* Clinical & Experimental Immunology, 2015. **182**(2): p. 109-118.

181. Park, H., et al., *A point mutation in the murine Hem1 gene reveals an essential role for Hematopoietic protein 1 in lymphopoiesis and innate immunity.* The Journal of experimental medicine, 2008. **205**(12): p. 2899-2913.
182. Stahnke, S., et al., *Loss of Hem1 disrupts macrophage function and impacts migration, phagocytosis, and integrin-mediated adhesion.* Current Biology, 2021. **31**(10): p. 2051-2064.e8.
183. Ostermann, G., et al., *JAM-1 is a ligand of the β2 integrin LFA-1 involved in transendothelial migration of leukocytes.* Nature immunology, 2002. **3**(2): p. 151-158.
184. Kristóf, E., et al., *Novel role of ICAM3 and LFA-1 in the clearance of apoptotic neutrophils by human macrophages.* Apoptosis, 2013. **18**(10): p. 1235-1251.
185. May, R.C. and L.M. Machesky, *Phagocytosis and the actin cytoskeleton.* Journal of cell science, 2001. **114**(6): p. 1061-1077.
186. Schlam, D., et al., *Phosphoinositide 3-kinase enables phagocytosis of large particles by terminating actin assembly through Rac/Cdc42 GTPase-activating proteins.* Nature Communications, 2015. **6**(1): p. 8623.
187. Wang, S., et al., *S100A8/A9 in Inflammation.* Frontiers in Immunology, 2018. **9**.
188. McGeachy, M.J., et al., *TGF-β and IL-6 drive the production of IL-17 and IL-10 by T cells and restrain TH-17 cell–mediated pathology.* Nature immunology, 2007. **8**(12): p. 1390-1397.
189. Lin, Y., et al., *Notch signaling modulates macrophage polarization and phagocytosis through direct suppression of signal regulatory protein α expression.* Frontiers in immunology, 2018. **9**: p. 1744.
190. Wu, J., et al., *Lipoxin A4 regulates lipopolysaccharide-induced BV2 microglial activation and differentiation via the Notch signaling pathway.* Frontiers in cellular neuroscience, 2019. **13**: p. 19.
191. Li, Q.-Q., et al., *Lipoxin A4 regulates microglial M1/M2 polarization after cerebral ischemia-reperfusion injury via the Notch signaling pathway.* Experimental Neurology, 2021. **339**: p. 113645.
192. Malumbres, M., *Cyclin-dependent kinases.* Genome biology, 2014. **15**(6): p. 1-10.
193. Sarkar, A., et al., *Infection of neutrophil granulocytes with Leishmania major activates ERK 1/2 and modulates multiple apoptotic pathways to inhibit apoptosis.* Medical Microbiology and Immunology, 2013. **202**(1): p. 25-35.
194. Parsa, K.V.L., et al., *The tyrosine kinase Syk promotes phagocytosis of Francisella through the activation of Erk.* Molecular immunology, 2008. **45**(10): p. 3012-3021.
195. Petropoulos, M., et al., *Hydrogen peroxide signals E. coli phagocytosis by human polymorphonuclear cells; up-stream and down-stream pathway.* Redox Biology, 2015. **6**: p. 100-105.